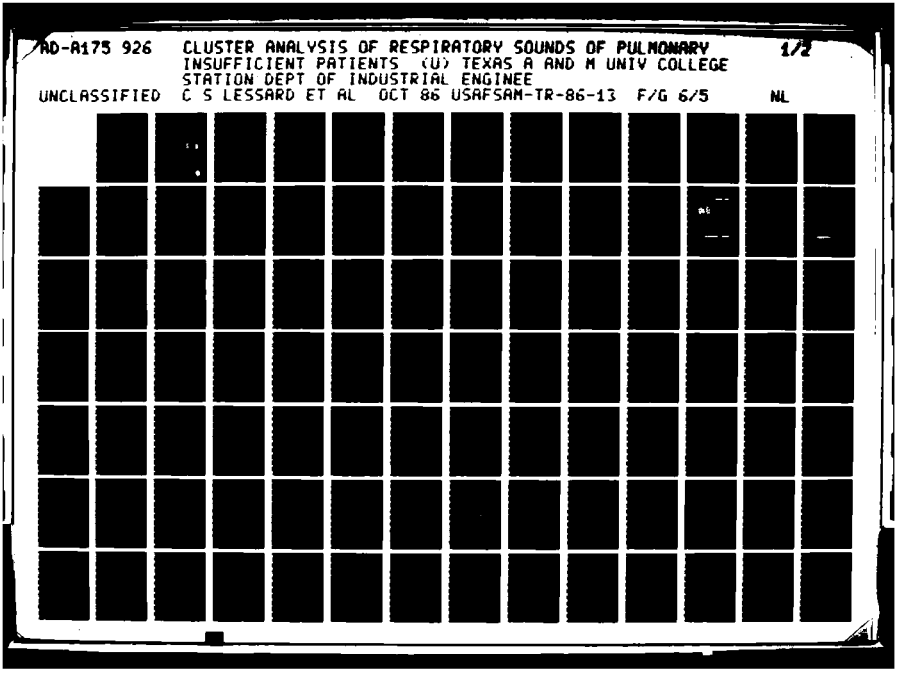
AD-A175 926 CLUSTER ANALYSIS OF RESPIRATORY SOUNDS OF PULMONARY INSUFFICIENT PATIENTS (U) TEXAS A AND M UNIV COLLEGE STATION DEPT OF INDUSTRIAL ENGINEE
1/2
UNCLASSIFIED C S LESSARD ET AL OCT 86 USAFSAM-TR-86-13 F/G 6/5
NL

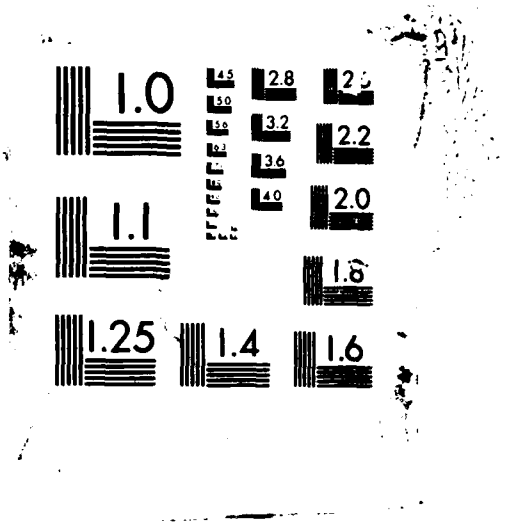
1.0
1.1
1.25
1.4
1.6
2.8
3.2
3.6
4.0
2.2
2.0
1.8

USAFSAM-TR-86-13

AD-A175 926

CLUSTER ANALYSIS OF RESPIRATORY SOUNDS OF PULMONARY INSUFFICIENT PATIENTS AND NORMAL SUBJECTS

Charles S. Lessard, Ph.D., P.E.
Brenda Ann Wolf, M.S.
Wing Chan Wong, M.S.

Bioengineering Program
Industrial Engineering Department
Texas A&M University
College Station, TX 77843

October 1986

Final Report for Period 1 June 1985 - 30 August 1985

Approved for public release; distribution is unlimited.

Prepared for

USAF SCHOOL OF AEROSPACE MEDICINE
Aerospace Medical Division (AFSC)
Brooks Air Force Base, TX 78235-5301

UNCLASSIFIED
SECURITY CLASSIFICATION OF THIS PAGE

ADA175926

REPORT DOCUMENTATION PAGE

1a. REPORT SECURITY CLASSIFICATION: Unclassified	1b. RESTRICTIVE MARKINGS
2a. SECURITY CLASSIFICATION AUTHORITY	3. DISTRIBUTION / AVAILABILITY OF REPORT: Approved for public release; distribution is unlimited.
2b. DECLASSIFICATION / DOWNGRADING SCHEDULE	
4. PERFORMING ORGANIZATION REPORT NUMBER(S)	5. MONITORING ORGANIZATION REPORT NUMBER(S): USAFSAM-TR-86-13
6a. NAME OF PERFORMING ORGANIZATION: Bioengineering Program, Industrial Engineering Dept. / 6b. OFFICE SYMBOL (If applicable)	7a. NAME OF MONITORING ORGANIZATION: USAF School of Aerospace Medicine (VNC)
6c. ADDRESS (City, State, and ZIP Code): Texas A&M University, College Station, Texas 77843	7b. ADDRESS (City, State, and ZIP Code): Aerospace Medical Division (AFSC), Brooks Air Force Base, Texas 78235-5301
8a. NAME OF FUNDING / SPONSORING ORGANIZATION / 8b. OFFICE SYMBOL (If applicable)	9. PROCUREMENT INSTRUMENT IDENTIFICATION NUMBER: F33615-83-D-0602-10
8c. ADDRESS (City, State, and ZIP Code)	10. SOURCE OF FUNDING NUMBERS

PROGRAM ELEMENT NO.	PROJECT NO.	TASK NO.	WORK UNIT ACCESSION NO.
62202F	2729	02	20

11. TITLE (Include Security Classification)
Cluster Analysis of Respiratory Sounds of Pulmonary Insufficient Patients and Normal Subjects

12. PERSONAL AUTHOR(S)
Lessard, Charles S.; Wolf, Brenda Ann; Wong, Wing Chan

13a. TYPE OF REPORT	13b. TIME COVERED	14. DATE OF REPORT (Year, Month, Day)	15. PAGE COUNT
Final Report	FROM Jun 85 TO Aug 85	1986, October	131

16. SUPPLEMENTARY NOTATION

17. COSATI CODES			18. SUBJECT TERMS (Continue on reverse if necessary and identify by block number)
FIELD	GROUP	SUB-GROUP	Cluster analysis; Expiratory cluster analysis; Inspiratory cluster analysis; Respiratory sound detection; Expiratory flow rate; Inspiratory flow rate; Power spectra.
06	05		

19. ABSTRACT (Continue on reverse if necessary and identify by block number)

Respiration is one of the physiological functions of concern when a patient is under examination or treatment. A clinical relationship between respiratory sounds and gross respiratory pathology was established in the nineteenth century. Auscultation of respiratory sounds, however, is very subjective. Due to the subjectiveness, there are varying degrees of acceptance of respiratory sounds as a clinical sign. To alleviate the problem, various researchers have studied respiratory sounds to explore and develop automated methods for analysis and diagnosis of pulmonary diseases.

Our objective is to determine whether respiratory sound data of normal volunteers and pulmonary insufficiency subjects reveals groupings or clusters of the data. Cluster analysis of the analyzed data is done to achieve this objective. The three indices of the power spectra analysis of

20. DISTRIBUTION / AVAILABILITY OF ABSTRACT	21. ABSTRACT SECURITY CLASSIFICATION
☒ UNCLASSIFIED/UNLIMITED ☐ SAME AS RPT. ☐ OTIC USERS	Unclassified

22a. NAME OF RESPONSIBLE INDIVIDUAL	22b. TELEPHONE (Include Area Code)	22c. OFFICE SYMBOL
YASU TAI CHEN, M.S.	(512) 536-2921	USAFSAM/VNC

DD FORM 1473, 84 MAR — 83 APR edition may be used until exhausted. All other editions are obsolete.

SECURITY CLASSIFICATION OF THIS PAGE
UNCLASSIFIED

19. ABSTRACT (Continued)

the respiratory sound data (MPF, FPK, FMAX) and the mean flow-rate data are the variables used in the cluster analysis. The MPF refers to the mean frequency of the power spectra, FPK is the frequency of the maximum power, and FMAX refers to the highest frequency at which the power in the spectrum equals or is less than 10% of the maximum power.

Results indicate that clustering the data according to the indices MPF and FMAX appears to cluster the data into 3 groups. However, some combinations appear to show 3 clusters; others appear to show 4 clusters, and some do not reveal any distinct clusters at all. In summary, from the cluster plots, we conclude that the data may be clustered into 3 or 4 groups.

TABLE OF CONTENTS

List of Figures

CLUSTER ANALYSIS OF RESPIRATORY SOUNDS OF PULMONARY INSUFFICIENT PATIENTS AND NORMAL SUBJECTS

INTRODUCTION

Respiration is one of the physiological functions of concern when a patient is under examination or treatment. A clinical relationship between respiratory sounds and gross respiratory pathology was established in the nineteenth century. Auscultation of respiratory sounds, however, is very subjective. Due to the subjectiveness, there are varying degrees of acceptance of respiratory sounds as a clinical sign. To alleviate the problem, various researchers have studied respiratory sounds to explore and develop automated methods for analysis and diagnosis of pulmonary diseases.

Our objective is to determine whether respiratory sound data of normal volunteers and pulmonary insufficiency subjects reveals groupings or clusters of the data. Patient data was obtained from the USAF School of Aerospace Medicine, Brooks Air Force Base, Texas. The study is a "blind" study since the classification (normal/pulmonary insufficiency) of the subjects was not revealed.

Background

The process of respiration is of vital importance to life and includes the following mechanistic events: (1) pulmonary ventilation, the inflow and outflow of air between the atmosphere and the lung alveoli, (2) diffusion of oxygen and carbon dioxide between the alveoli and the blood, and (3) transportation of oxygen in the blood, principally in combination with hemoglobin, to the tissue capillaries where it is released for use by the cells according to their metabolic needs [19].

The foundations of respiratory medicine were laid at the beginning of the nineteenth century when Laennec established the clinical relationship between respiratory sound and gross pulmonary pathology by the use of the early stethoscope [22]. Auscultation in respiratory medicine, however, has advanced slowly since Laennec established auscultation of lung sounds as a means of diagnosing the condition of the lungs.

The slow progress is due to: (1) a variety of human factor problems, (2) the limitations of the instrumentation, (3) the lack of total understanding of the mechanism of production of respiratory sounds, and (4) the lack of understanding of the origin of the source of the sounds.

Human Factor Problems

Respiratory sounds heard through a stethoscope can be roughly classified into two major types. The first major type of respiratory sounds are normal respiratory sounds. These sounds are both inspiratory and expiratory sounds heard as the air moves in and out of the chest during

normal breathing. There are two types of normal respiratory sounds. Tracheal or bronchial respiratory sounds are heard by placing the stethoscope over the trachea and listening as the patient breathes in and out with the mouth open. The sound is described as "tubular" and is similar to the sound that arises when air is blown through a tube. The second major type of respiratory sound is called vesicular. The term "vesicular" in Latin refers to little vessels. This description refers to the sound that is heard over the majority of the chest of normal persons during normal breathing. The analogy used is the sound heard by the rustle of wind in the trees [11].

The term "adventitious" is used to describe sounds not expected in the normal chest. To complicate matters, the terminology of adventitious sounds is not standard. The clinician attempts to describe the quality of sounds by adjectives that convey an idea of relative intensity and pitch. Different clinicians use the same term to describe dissimilar sounds [3,11].

Adventitious sounds are divided into those believed to have a bronchopulmonary origin and those thought to be due to pleural disease. Those of bronchopulmonary origin are further subdivided into "continuous" and "discontinuous". Sounds that last for more than a tiny fraction of the respiratory cycle are referred to as continuous. Rales, the discontinuous sounds, are further subdivided into fine, medium, and coarse. A variety of adjectives appear in the medical literature to classify these sounds further. Examples of these adjectives include dry, wet, moist, bubbling, crepitant, subcrepitant, and consonnating. The terminology is subjective in its interpretation depending greatly on the hearing and experience of the clinician [3,5,14,15,27-29].

Another problem in chest auscultation is that so much information exists that it is difficult either to record it properly or to remember the observed details. By listening over a single site in the chest, it is possible to observe the intensity of both inspiration and expiration. It is also possible to grade these on a scale that may reflect normality or abnormality of the site. The clinician may also be able to record the presence or absence of various adventitious sounds and their relationship to the respiratory cycle. The duration of inspiration with respect to expiration may also be noted. If the clinician listens to one or more sites, as is common in routine chest auscultation, then there is a possibility that information may be lost due to various factors such as interruptions in the physical examination, lack of accurate record keeping, or the clarity of the clinician's initial observations [27].

The diversity of the terms used to describe respiratory sounds, together with the nonuniformity of their usage by clinicians, poses difficulties in the use of respiratory sounds as a precise indicator of the condition of the respiratory system.

Limitations of Instrumentation

The binaural stethoscope appeared towards the middle of the nineteenth century and became popular mainly because it excludes extraneous noise [17,26]. The choice of the best chest piece remained controversial until physicians agreed that both the diaphragm and the bell were necessary for auscultation of the heart; they are combined in most stethoscopes now in use.

The stethoscope transmits the range of frequencies which includes frequencies of heart and lung sounds. By varying the pressure between the chest piece and the skin, the intensities of certain frequencies are increased while others are decreased. Low pitched heart sounds are heard best with the bell resting lightly on the skin, while firm pressure of the bell or diaphragm increases the intensity of higher frequencies and suppresses unwanted low pitched sounds.

Respiratory sounds contain a wide range of frequencies. To compare relative frequency intensities within a particular sound spectrum, the measuring instrument should not contribute variations in intensity. The conventional stethoscope exhibits this limitation [13,27].

Sound evaluation is further complicated by the nonlinearity of the human auditory system. The ear is capable of distinguishing small differences in pitch. As the intensity of the sound increases, the sensitivity of the ear to intensity variations decreases logarithmically. The ears' perception of intensity falls off at both ends of the frequency spectrum [13]. The frequencies of sound that a young person can hear differ from the frequencies of sound that an older person can hear. The range falls between 30 and 20 thousand cycles per second (cps) for a young person and 50 to 8 thousand cps in old age [18]. The ear is unable to distinguish short sound bursts. A burst shorter than 3 ms will be heard only as a click regardless of the frequency [15].

Electronic instruments can be designed to exhibit a flat frequency response over the range of respiratory sound spectrum and thus overcome some of the instrumentation shortcomings. The major obstacles, however, in the acceptance and advancement of using respiratory sounds as a major clinical tool in pulmonary medicine are the lack of complete understanding of: (1) the mechanism of production of respiratory sounds, and (2) the sources from which respiratory sounds are generated.

Mechanisms and Source of Respiratory Sounds

Numerous theories exist on the source of respiratory sounds and the mechanisms by which they are produced. In 1884, Bullar [2] performed an experiment with an exteriorized lung of a calf. The left lung was enclosed in an air-tight, fluid-filled chamber with glass sides, and the right lung remained outside the thorax in a collapsed state. The pressure surrounding the left lung was lowered, thus simulating inspiration in the left lung. During the simulated inspiration, a bronchial breathing sound was heard

over the right lung. Bullar then plugged the trachea and forced air out of the left lung into the right lung and noted that a vesicular inspiratory murmur was heard over the right lung. He also showed that without air flow no sounds were heard. Bullar's conclusion was that air currents that passed over the main bronchus of the outside lung generated bronchial sounds and air that passed from narrower to wider passages inside the lung generated expiratory sounds.

Bushnell [4] claimed that the sounds of expiration originated in the larynx, and that the sounds of inspiration originated partly in the larynx and partly in the alveoli.

Martini and Muller [24] believed that the bronchial network of the lungs was responsible for the generation of respiratory sounds. They showed that each generation of bronchus up to the generation with inner caliber of 3 mm had its own specific frequency of vibration. During respiration the bronchi would vibrate at their specific frequency. These vibrations acted on the lung tissues and on the chest wall.

Forgacs et al. [14] performed an experiment on asthmatic and chronic bronchitic patients. Measurements were taken on these patients while breathing both air and a mixture of 79% helium and 21% oxygen. They found that the respiratory sound intensity of the patients was lower while breathing the mixture as opposed to breathing air. The respiratory sounds were silenced by the helium mixture because flow is less turbulent in gases of low density.

At very low inspiratory flow rates the flow of air in the trachea and bronchi is laminar and presumably silent. At higher flow rates turbulence sets in and some of the kinetic energy of flow is then converted into heat and sound. In engineering problems the transition from laminar to turbulent flow is predictable by the Reynolds number, calculated from the density and viscosity of the gas, the dimensions of the pipe, and the flow velocity. This prediction, however, is less reliable when applied to a complicated system of branching pipes like the bronchial tree. Forgacs et al. [14] concluded that respiratory sounds were generated in the turbulent zone of the bronchial tree.

Calculations based on the Reynolds number and experimental observations of gas flow in models of the bronchi suggest that flow is turbulent in the trachea and the first few generations of the bronchi, and laminar in the peripheral bronchi where the Reynolds number is less than one. Between these two regions there lies an intermediate zone, extending from the segmental bronchi to the fifteenth generation of the airways, where the laminar flow pattern is disrupted by vortices [8,16,21,33,34].

Hardin and Patterson [20] claimed that the production of respiratory sounds was primarily by vortices and that turbulence played only a minor role. When a stream of gas emerging from a slit or a circular orifice enters a wider channel, a shearing force arises at the boundary between the jet and the surrounding fluid. The circular motion set up by this force generates whirlpools or vortices, shed alternately from opposite sides of

the jet. Similar vortices are produced where a curvature or angle in the pipe forces flow to change directions abruptly. The gas stream separates into layers that move forward at different velocities. The slower streams are turned into circular motion by the shearing force of the high velocity streamlines flowing alongside. This motion creates vortices, usually in pairs, whirling in opposite directions. Like turbulence, vortex formation begins when the Reynolds number reaches a critical value. Above this number the rate of formation of vortices depends on flow velocity alone. The distance between vortices carried downstream by the flow of gas varies at random, so that the resulting sound is a noise with a wide frequency spectrum [16].

The source of production of the "vesicular" (normal) respiratory sound has been a matter of debate for more than 100 years. Bullar [2] proposed that the production of the inspiratory component was attributed to the alveoli. Bushnell [4] and Bates [1], however, proposed that the production of the inspiratory component was attributed to the larynx. Forgacs [14] stated that the airways in between the larynx and alveoli were the source of production of the inspiratory component.

Recent studies [23,31,32] indicate that the inspiratory vesicular sound is produced within the lung, near the area auscultated, although the exact site of production is not established.

The origin of the expiratory component of the vesicular sound is more obscure. We frequently reasoned that this sound is generated either at the glottis, as a result of passage of air through partially adducted vocal cords, or within the larger airways, as a result of convergence of air streams [12,25,35].

Since Laennec's [22] time it has been known that pulmonary pathology can cause a change in respiratory sound. Differences exist between normal and pathological respiratory sounds. In 1976, Grassi et al. [17] used the technique of phonopneumography to analyze respiratory sounds. Phonopneumography is defined as the technique of detecting and analyzing the sounds that are produced in the bronchopulmonary area during respiration. The apparatus Grassi et al. used was intended to provide a graphic recording of the level of the sounds the clinician perceives through the stethoscope during auscultation. The phonopneumographic records revealed that inspiration was louder than expiration in the healthy subjects. Wherever the ratio between inspiratory and expiratory peak amplitudes was found to be highly modified, either because inspiration was much louder than normal, or because an inversion of the ratio occurred with an expiratory sound louder than inspiratory, the finding was always accompanied by pathological alteration of the pulmonary zone.

Chowdhury and Majumder [7] conducted an experiment using digital spectral analysis of respiratory sounds for the purpose of determining the clinical relationship between the frequency spectrum and the conditions of the lungs in pulmonary diagnosis. Their study included 6 normal subjects and 6 tuberculosis patients with fibrosis. The recordings of respiratory sounds were made in a quiet room with the subject in the supine position

and the microphone placed on the right lung base. The Fast Fourier Transform algorithm of Cooley and Tukey was used to obtain the normalized autospectrum of 0.25 s time segments of respiratory sound. Their analysis indicates a maximum amplitude of about 250 Hz for subjects without pathological lung history, with rapid decrease in amplitude as the frequency increases and approaches 1000 Hz. In the case of the tubercular lung, a downward frequency shift of amplitude peak and the presence of higher frequency components were observed.

Charbonneau et al. [6] developed an index which they used to discriminate between asthmatics and normal subjects. They calculated the average spectrum for inspiration and expiration and referred to this as a histogram. Four parameters for both expiratory and inspiratory histograms were calculated and the sum of the parameters was used as an index to discriminate between asthmatics and normal subjects. The parameters were: the bandwidth (taken at half of the peak amplitude), the integral over the range 60-1260 Hz, the highest significant frequency (taken to be 10% of the amplitude of the peak frequency), and the weighted mean frequency of each mean spectra. Their study included 11 normal and 10 asthmatic subjects.

Problems with Sound Intensity Recorded from Chest Wall

The correlation of respiratory sound intensity and the distribution of pulmonary ventilation was first studied by Leblanc et al. [23]. From their study they concluded that the intensity of respiratory sounds varied with lung volume, flow rate, body orientation, and the site of the recording. O'Donnell and Kraman [30] and Dosani and Kraman [9] conducted studies to investigate the intensity patterns of lung sound on the chest wall. They concluded that there was a considerable intersubject and intrasubject variability in amplitude of the inspiratory vesicular sound heard on the chest wall, and that the variability was due to factors other than the distribution of ventilation and chest wall thickness. These variations happen even with normal subjects without any diseases of the lung. They believed that the other factors included the site of production of these sounds and their transmission through the airways and lung tissue. Dosani and Kraman [9] pointed out that the chest wall thickness may not have a predominant effect on the intensity. Their results showed that sound intensity at the lateral wall was similar to sound at positions near the spine where the thickness of the chest wall is greater.

Rationale for Trachea as Site of Respiratory Sound Detection

The variability of acoustic properties of the chest wall account for the variability of sound intensity as measured at the chest wall [6,10,18,31]. Previous research indicates that respiratory sounds measured at the trachea undergo very little filtering [6,10,18]. Charbonneau [6] stated that the sound level is higher at the trachea than at any other point of the chest or back and the localization of the point is more precise. Therefore, recordings of the respiratory sound here were obtained from the area of the trachea.

EXPERIMENTAL PROCEDURES

Air Force Experimental Procedures

Data were obtained from the USAF School of Aerospace Medicine under USAF contract F36615-83-D-0602, Academic Research in Biotechnology, Task 001, sponsored by the USAF School of Aerospace Medicine, Brooks AFB, Texas. The data were collected by USAF personnel at Wilford Hall USAF Medical Center on patients with pulmonary insufficiency and on normal volunteers. The experimental procedure used by the U.S. Air Force for data collection was as follows:

The patient was instrumented with a pulmonary flowmeter that was comprised of two Fleisch pneumotachometers with a Rudolph valve between them and connected to a mouthpiece. One pneumotachometer was used to transduce the inspiratory flow rate and the other one was used to transduce the expiratory flow rate. The pneumotachometer devices had pressure taps that were connected to Validyne pressure transducers. An electronic stethoscope was held at the anterior cervical triangle for the detection of respiratory sounds. The patient breathed through the flowmeter exclusively. This method was accomplished by using a nose clip to prevent nose breathing. A minimum of 5 min of recording time for each patient was collected to allow the patient to become accustomed to the apparatus. This procedure was done to establish a normal breathing pattern. The respiratory sounds and the flow rate were transduced and recorded on an FM analog tape recorder.

Experimental Procedure for Data Analysis

The magnetic tapes were provided under contract to Texas A&M University, Bioengineering Department for data analysis. Since the classification (normal/pulmonary insufficiency) of the subject, number of subjects, and location of each subject in relation to the time code was not revealed by the U.S. Air Force, the study was a "blind study".

The equipment used in the analysis of the magnetic tapes consisted of the following components:

1. Ampex 2200 FM analog tape recorder
2. Datum Time Code Generator/Reader Model 9300
3. 20-Hz, 1800-Hz low-pass filters
4. 100-Hz high-pass filter
5. A/D Multiprogrammer (HP 6942A)
6. Tektronix 5A22N Differential Amplifier
7. Tektronix 5111A Storage Oscilloscope
8. Tektronix 2236 100-MHz Storage Oscilloscope

A block diagram which illustrates the logical arrangement of the equipment used for analysis of inspiratory and expiratory data is shown in Figure 1.

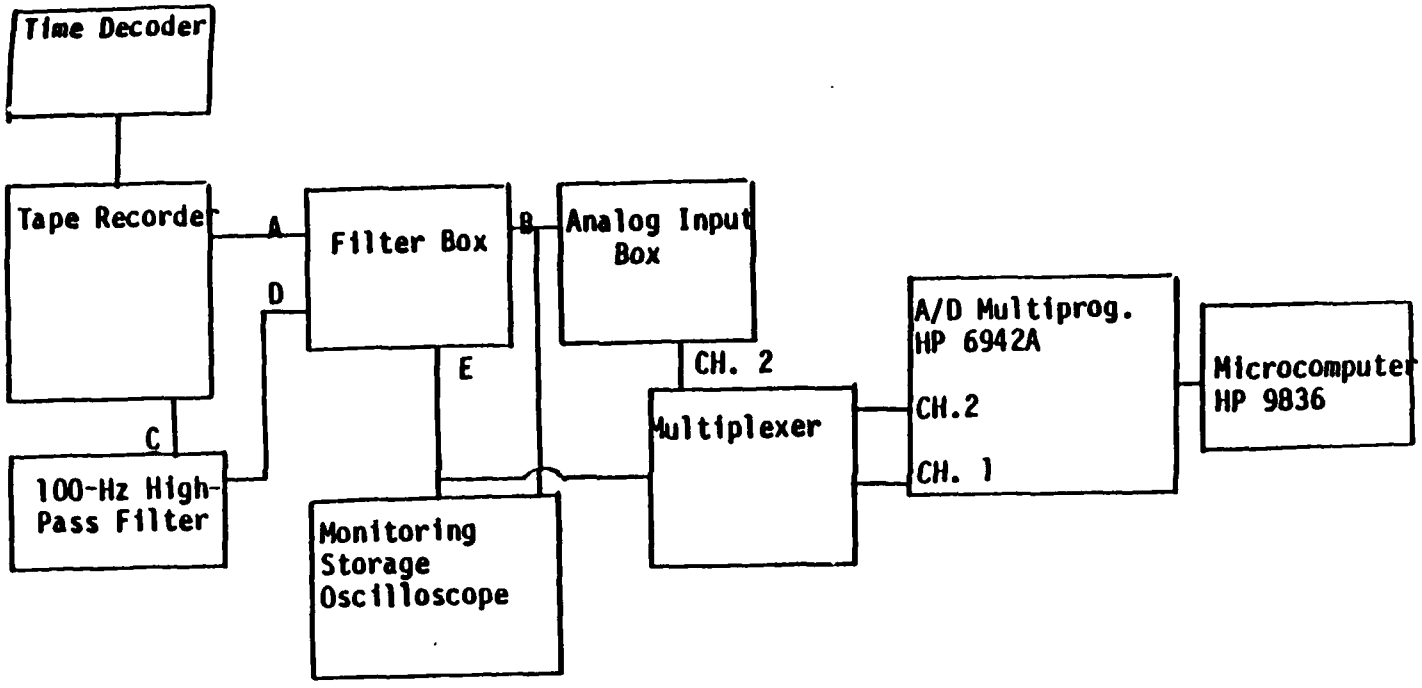

A= 20-Hz input
B= 20-Hz output
C= 100-Hz input
D= 1800-Hz input
E= 1800-Hz output

Figure 1. Logical arrangement of equipment setup.

Inspiratory Data Analysis

As shown in Figure 1, the respiratory sound signal and the inspiratory flow-rate signal were monitored simultaneously on an oscilloscope. The magnetic tape speed was 3-3/4 in./s. Recordings were made with standard IRIG intermediate band record/reproduce amplifiers with a cutoff frequency (3 db) at 19 kHz and a signal-to-noise ratio of 35 db. Channel 10 of the FM recorder was connected to the time decoder to display the recorded time. The time decoder was monitored until a valid time code was displayed, indicating a subject's data were recorded on Channel 2 (inspiratory flow data) and on Channel 4 (respiratory sound data) of the magnetic tape. Then, the time code and signals were simultaneously monitored and the total length of the subject's inspiratory data was recorded. The total length of time was assumed to be the time between the beginning of a time code and the time when the time code cleared. Then, the time of each inspiratory breath was also recorded. A calibration procedure was performed on the inspiratory flow-rate signal to calculate the gain that was used. For a specific inspiratory breath the signal on the magnetic tape was viewed on an oscilloscope and the voltage of the signal was recorded. The signal from the output of the 20-Hz filter for the same inspiratory breath was viewed on another oscilloscope simultaneously and the voltage of the signal was recorded. The gain was calculated by the ratio of the voltage recorded from the output of the 20-Hz filter to the voltage recorded directly off the magnetic tape. The value of the gain was necessary in determining the correct inspiratory flow rate. This procedure was done prior to inspiratory data collection for each new subject.

The inspiratory flow-rate signal was taken from Channel 2 of the FM recorder and fed into the 20-Hz low-pass filter. The output of the filter was fed into the oscilloscope for monitoring and the analog input box for manual triggering. The output of the analog input box was then fed into Channel 2 of the analog-to-digital (A/D) converter.

The inspiratory sound signal was taken from Channel 4 of the FM recorder and fed into a 100-Hz high-pass filter followed by a 1800-Hz low-pass filter. The output of the filter was fed into the oscilloscope for monitoring and into Channel 1 of the A/D converter. After calibration of the flow data and random selection of four breaths, data collection began.

The HP-9836 desktop microcomputer was programmed to monitor the inspiratory flow rate in the A/D channel and begin data collection when the flow rate reached a predetermined level. The level was determined by viewing the signal on the oscilloscope. Data collection was handled by the multiplexed A/D channel at the sampling rate of 8192 samples/second. By choosing a sampling rate of 8192 samples/second, the result was to sample each analog channel (respiratory sound and flow rate) at 4096 samples/second. The program was modified to be interactive; therefore, it allowed for versatility in the processing of recorded data with large variabilities. The program prompted the operator for changes of the flow-rate trigger level, the duration of data collection, the number of repetitions, the data file name, the data file structure, and the sampling

rate. The program also had additional flexibility allowing the operator to decide whether or not he/she wanted to save the collected data.

The voltage level at which the A/D converter started collecting data was displayed on the screen. If the level was acceptable with the trigger level that was set (within 0.2 V), then the data were saved and stored on the diskette. The data file names used were the respective time codes of the breaths collected. This procedure continued until four inspiratory breaths of each subject had been collected, digitized, and stored on diskettes for further signal processing.

Expiratory Data Analysis

A block diagram which illustrates the logical arrangement of the equipment used for analysis of expiratory data is shown in Figure 1. As shown in the figure, both the expiratory flow rate signal and the expiratory sound signal were monitored simultaneously on an oscilloscope. The same procedure for locating the inspiratory data was used to locate expiratory data.

A calibration procedure was then performed on the expiratory flow-rate signal to calculate the gain that was used. For a specific expiratory breath, the signal off the magnetic tape was viewed on an oscilloscope and the voltage of the signal was recorded. The signal from the output of the 20-Hz filter for the same expiratory breath was viewed on an oscilloscope and the voltage of the signal was recorded. The gain was calculated by the ratio of the voltage recorded from the output of the 20-Hz filter to the voltage recorded directly off the magnetic tape. The value of the gain was necessary in determining the correct expiratory flow rate. This procedure was done prior to expiratory data collection for each new subject.

The expiratory flow-rate signal was taken from Channel 3 of the FM recorder and fed into the differential amplifier of the oscilloscope. The differential amplifier was used to balance the DC offset by adjusting the DC step attenuation balance and the position knob. The filter setting was DC. This step was needed because the expiratory flow transducer that was used had a 1.4 V DC offset. The output of the oscilloscope was fed into the input of the 20-Hz filter, and the output of the 20-Hz filter was fed into both the oscilloscope for monitoring and the analog input box for manual triggering. The output of the analog input box was then fed into Channel 2 of the A/D converter. The respiratory sound signal was taken from Channel 4 of the FM recorder and fed into a 100-Hz high-pass filter followed by a 1800-Hz low-pass filter. The output of the filter was fed into the oscilloscope for monitoring and into Channel 1 of the A/D converter.

The same procedure of expiratory data collection employing the HP-9836 microcomputer and A/D converter as noted for the inspiratory data collection was used. This procedure continued until four expiratory breaths of each subject had been collected, digitized, and stored on diskettes for further signal processing.

QUANTITATIVE ANALYSIS

The Fourier series is used to represent arbitrary periodic functions by an infinite series of sinusoids of harmonically related frequencies to study the time domain responses in networks. The Fourier series expressed as a linear combination of harmonically related complex exponentials can be written in the form:

$$x(t) = \int a_k e^{-jk\omega_o t}\, dt \qquad (1)$$

$$a_k = 1/T_o \int x(t) e^{-jk\omega_o t}\, dt \qquad (2)$$

where $k = 1, 2, \ldots, \infty$.

Equation (1) is often referred to as the synthesis equation and equation (2) as the analysis equation. The coefficients, a_k, are often called the Fourier series coefficients or the spectral coefficients of $x(t)$. These complex coefficients measure the portion of the signal $x(t)$ that is at each harmonic of the fundamental component. The fundamental frequency is defined as ω_o, and the fundamental period is $T_o = 2\pi/\omega_o$.

The Fourier series method, however, has limitations in analyzing linear systems for the following reasons: 1) The Fourier series can be used for inputs which are periodic; however, most inputs in practice are nonperiodic. 2) The method applies only to systems that are stable. A stable system is a system whose natural response decays in time.

The first limitation can be overcome since we can represent the nonperiodic input in terms of exponential components. A method of accomplishing this function is the Fourier Transform. For instance, consider the nonperiodic function $f(t)$ in Figure 2 which we would like to represent in terms of exponential components. To do this, we constructed a periodic function $f_T(t)$ in Figure 2 with a period T, where the function $f(t)$ is repeated every T seconds. The period, T, is considered large enough so there is not any overlap between pulse shapes of $f(t)$. The new function is a periodic function and can be represented with an exponential Fourier series as follows:

$$f_T(t) = \Sigma F_n e^{jn\omega_o t} \qquad (3)$$

$$\text{where } \omega_o = 2\pi/T, \qquad (4)$$

$$\text{and } F_n = 1/T \; \Sigma \; f_T(t) e^{-jn\omega_o t} \qquad (5)$$

The next process is to evaluate the function as the period increases to infinity. As T becomes infinite, the pulses repeat after an infinite interval. Therefore, $f_T(t)$ and $f(t)$ are identical in the limit, and the Fourier series representing the periodic function $f_T(t)$ will also represent $f(t)$.

In the limit, as T approaches infinity, ω approaches zero. Therefore, ω_o can be denoted as $\delta\omega$. Then: $T = 2\pi/\omega_o = 2\pi/\delta\omega_o$ and,

$$TF_n = \Sigma f_T(t) e^{-jn\delta\omega t} \tag{6}$$

TF_n is a function of $jn\delta\omega$, so let $TF = F(jn\delta\omega)$. Equation (3) becomes:

$$f_T(t) = \Sigma F_n e^{jn\omega_o t} \tag{7}$$

$$= \Sigma [F(jn\delta\omega)/T] e^{(jn\delta\omega)t} \tag{8}$$

$$= \Sigma \{ [F(jn\delta\omega)/2\pi] \delta\omega \} \; e^{(jn\delta\omega)t} \tag{9}$$

In the limit, as T approaches infinity, $\delta\omega$ approaches zero, and $f_T(t)$ approaches f(t). Then:

$$f(t) = \text{Lim} \;\; f_T(t) = [\text{Lim} \;\; 1/2\pi \; F(jn\delta\omega) \; e^{jn\delta\omega t} \delta\omega] \tag{10}$$

is by definition:

$$f(t) = 1/2\pi \int F(j\omega) e^{j\omega t} \, d\omega \tag{11}$$

Equation (5) is known as the inverse Fourier transform. Recall equation (5):

$$F_n = 1/T \int f_T(t) e^{-jn\omega_o t} \, dt \tag{12}$$

$$= F(jn\delta\omega)/T \tag{13}$$

then

$$F(j\omega) = \text{Lim} \int f_T(t) e^{-jn\delta\omega t} dt \tag{14}$$

$$F(j\omega) = \int f(t) e^{-j\omega t} \, dt \tag{15}$$

Equation (15) is known as the direct Fourier transform. The result is that

$$F(j\omega) = \int f(t) e^{-j\omega t} \, dt \tag{16}$$

is the representation of the nonperiodic function f(t) in terms of exponential functions. The amplitude of the component of any frequency ω is proportional to $F(j\omega)$. In analogy with the terminology used for the Fourier series coefficient of a periodic signal, the transform $F(j\omega)$ of an aperiodic signal f(t) is commonly referred to as the spectrum of f(t), as it provides us with the information concerning how f(t) is composed of sinusoidal signals at different frequencies.

Figure 3 illustrates the steps discussed in the following section. The signal was conditioned by the use of the analog filters previously discussed in the experimental procedures. The 100-Hz high-pass filter and the 1800-Hz low-pass filter were thus acting together as a band-pass filter. The respiratory sound data and flow data were digitized, separated using the separation program, and stored on diskettes for the FFT analysis. The respiratory sound signal was digitized at a rate of 4096 samples/second. The sampling rate was chosen to avoid "aliasing" of the spectra. The literature indicates that the highest frequency of normal respiratory sound is about 1500 Hz, and this may be higher for abnormal

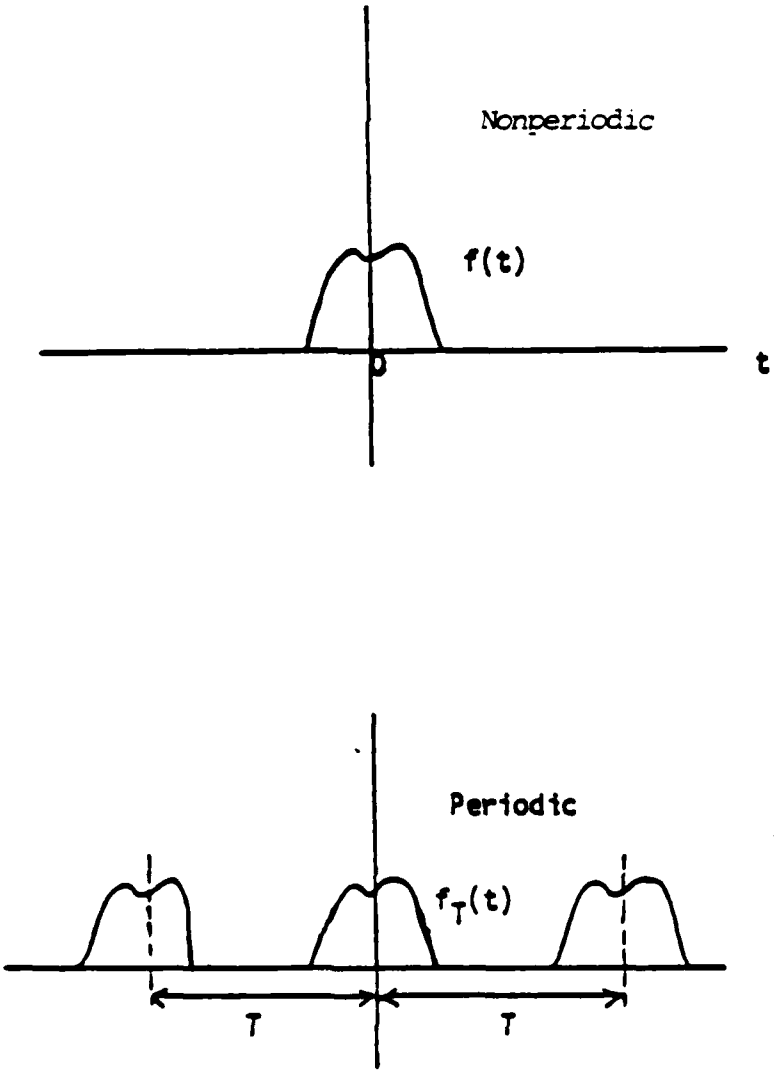

Figure 2. Aperiodic function.

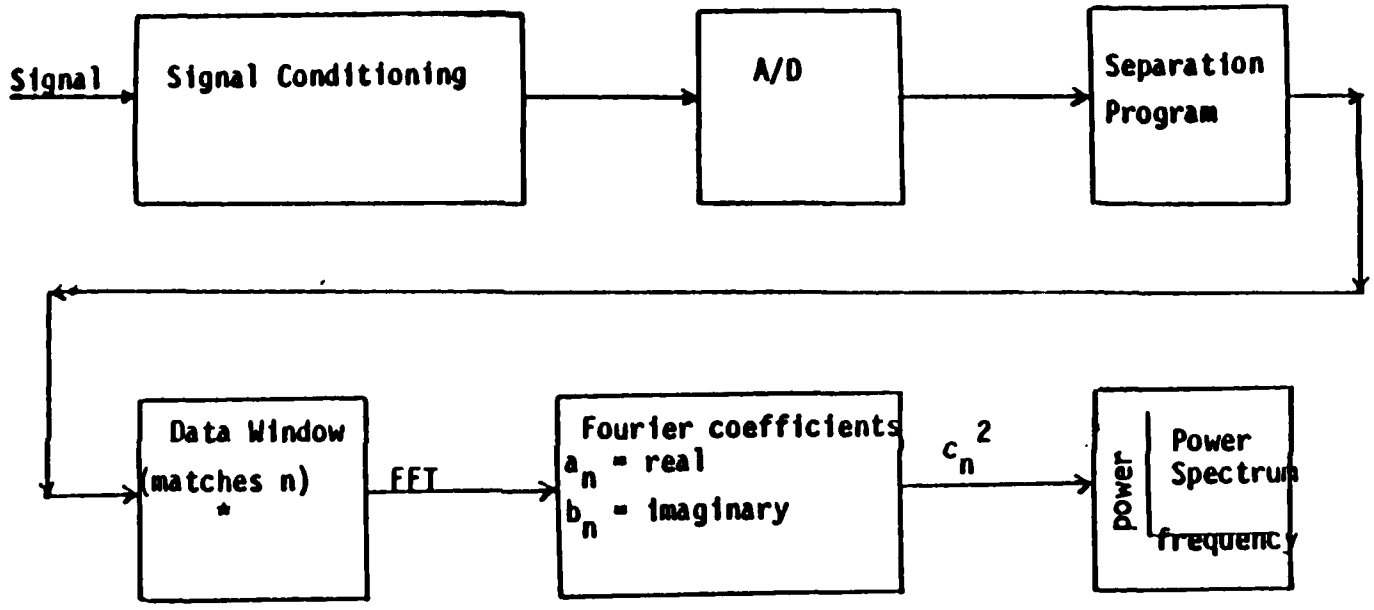

* n=(sampling frequency)(total length of time of data collection) 4096(1/4)=1024

Figure 3. Logical flow of data analysis.

subjects. The Nyquist sampling criteria require that the Nyquist frequency be at least twice the highest frequency of interest of the signal being sampled. The first 1024 samples, which correspond to 0.25 s of real time data, were transformed by the Cooley-Tukey Fast Fourier Transform (FFT) algorithm.

When only a finite segment of the signal is observed, the process is equivalent to multiplying the signal by a rectangular window function. In the frequency domain, this multiplication becomes a convolution between the desired spectrum and that of the window. As a result, the frequency spectrum is distorted, and the spectral components "leak" away from their time frequencies and are distributed over the total spectrum [34]. A rectangular window function is not accurate in describing the signal and therefore produces signal discontinuities at the boundaries. The Fourier transform will add all harmonics to simulate the fast rising edge of the window, and this is inaccurate in representing the signal. A suitable window function needs to be chosen to minimize the "spectral leakage". The window chosen was a 10% cosine tapered window. This window forces the first data point to zero, and the rising edge of the window is a cosine function. The equations for the cosine taper are:

$$0.5(1-\cos(10*\pi*I/N)) \quad \text{for } 0 \le I \le N/10 \tag{17}$$

$$1 \quad \text{for } N/10 < I < N*9/10 \tag{18}$$

and

$$0.5(1-\cos(10*\pi*I/N)) \quad \text{for } N*9/10 \le I \le N \tag{19}$$

where pi=3.1415926, I is the index, and N is the number of samples being used for the FFT calculation (in this case 1024).

Calculation of Parameters

Three indices of measure were calculated from the power spectrum. These parameters were the mean frequency of the power spectrum (MPF), the frequency of the maximum power (FPK), and the highest frequency at which the power in the spectrum equals or is less than 10% of the maximum power (FMAX). The rationale behind selection of these parameters is as follows:

(1) In descriptive statistics, the mean (MPF) corresponds to the central tendency of the distribution.

(2) The peak value (FPK) or the mode of a distribution corresponds to the most frequent occurrence of an event, in this case the power within the respiratory sound spectrum.

(3) The highest frequency (FMAX) at which the power in the spectrum becomes 10% of the peak power corresponds to a rough bandwidth from DC to the frequency at which the power contents remain 10 db below maximum power in the spectrum. This parameter may also be used as an indicator of the correctness in the selection of the Nyquist sampling frequency. Also, Charbonneau et al. [6] used the FMAX parameter as

part of a linear function to discriminate normal from asthmatic patients.

The mean frequency of the power spectra was calculated from the equation:

$$MPF = \Sigma(C_i^2 * F_i)/\Sigma C_i^2 \quad (20)$$

where i is the index 0, 1, 2,....., N-1. F_i is the frequency at index i, and C_i is the Fourier coefficient at index i. The coefficient C_i is computed from the FFT:

$$C_i = (a_i^2 + b_i^2)^{1/2} \quad (21)$$

where a_i is the real component of the Fourier coefficient at index i, and b_i is the imaginary component of the Fourier coefficient at index i.

The next parameter calculated by the program is the frequency of the maximum power of the power spectrum. A sorting routine is used to locate the maximum power and the index at which the maximum power occurred. The peak frequency then becomes

$$FP = I * FR \quad (22)$$

where I is the index 0,2,...,N-1, and FR is the frequency resolution. The frequency resolution (FR) is calculated from the period or window length in time, that is:

$$FR = 1/(0.25 \text{ sec}) = 4 \text{ Hz} \quad (23)$$

The final parameter, the highest frequency at 10% of the maximum power (FMAX), is calculated in a manner similar to the calculation of the frequency of the maximum power. Again, a sorting routine is used to find the index at which the power becomes 10% of the maximum power. Then the frequency is calculated from the index.

As previously mentioned, a FFT was performed on the respiratory sound data and power spectra plots were obtained. Several plots of the power spectra for both expiration and inspiration have been included for illustration. As shown on the following figures, the percentage of maximum power was plotted on the vertical axis and the frequency was plotted on the horizontal axis. The plots show the power spectra analysis of each 0.25 s for the entire length of time specified during data collection. The time interval varied between 1.5 s to 2.5 s.

Inspiratory and Expiratory Power Spectra Plots

Figure 4 illustrates a plot of the power spectra analysis of the inspiration from one subject. This plot appears to indicate a bimodal pattern of the power spectra. The breath sounds for this specific time interval are depicted in the upper right-hand corner. Figure 5 illustrates

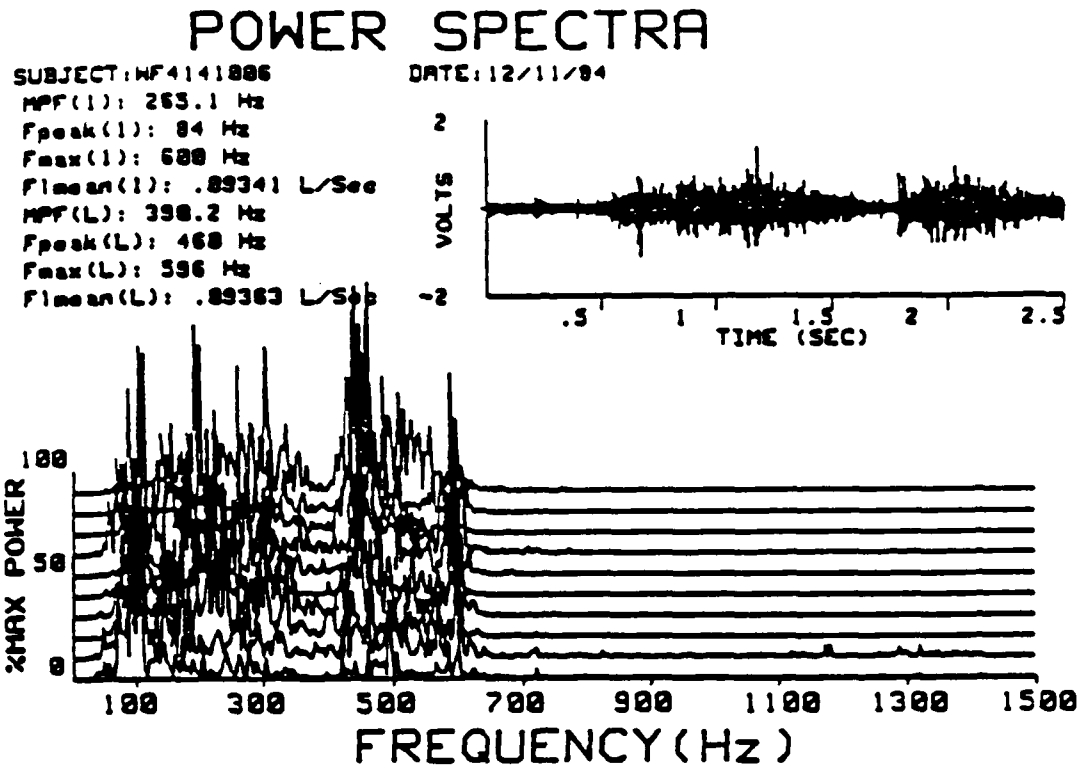

Figure 4. Power spectra plot of inspiratory sound (4141006).

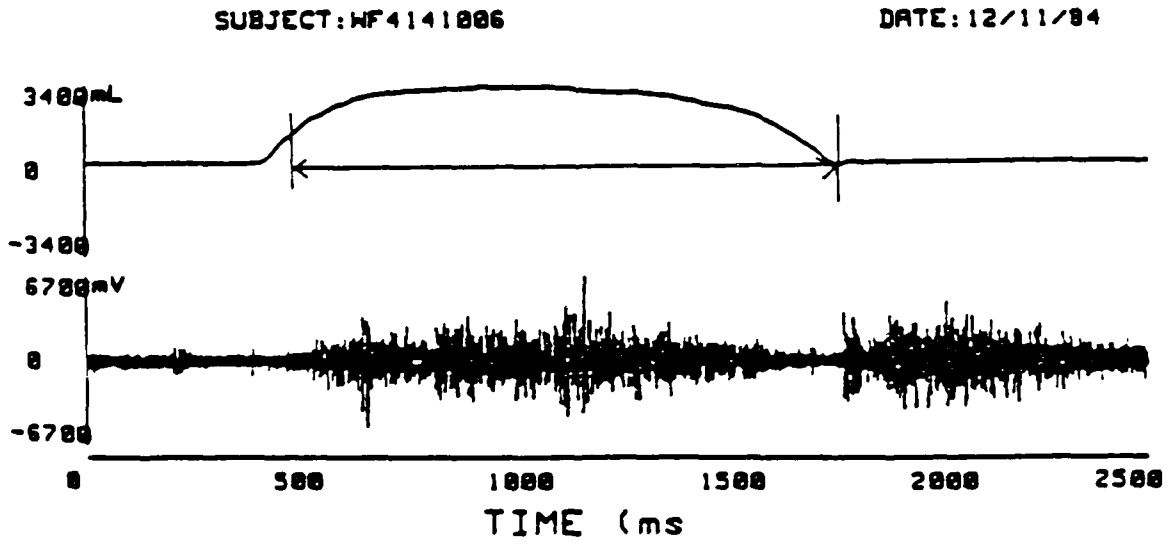

Figure 5. Plot of flow rate and inspiratory sound (4141006).

a plot of both the respiratory sound data and the inspiratory flow rate. A plot of this type was done for every inspiratory and expiratory respiratory sound analyzed. The purpose was to determine the 0.25 intervals of the power spectra that correspond to either inspiration or expiration. Since Figure 4 was the power spectra analysis of an inspiratory breath, Figure 5 was used to determine which 0.25 s intervals corresponded to the inspiratory respiratory sounds. Intervals 3 through 7 corresponded to the inspiratory respiratory sounds; therefore, the indices of the power spectra for these 5 intervals were tabulated for use in the cluster analysis of the data. This procedure was followed for every respiratory sound (expiration, inspiration) that was analyzed to ensure that the indices of the power spectra analysis for expiration and inspiration were kept separate for the cluster analysis of the data.

A plot of expiratory sound power spectra is included for illustration. Figure 6 illustrates a possible bimodal pattern of the power spectra for the expiration cycle of this particular subject. Figure 7 illustrates the expiratory cycle and the intervals chosen for the cluster analysis. We noted that the expiratory respiratory sounds appear to be more forceful at the start of the cycle and then taper off. These plots illustrate a variety in the power spectra which may indicate a difference of breathing patterns and/or a difference in subjects. The bimodal patterns of the power spectra, illustrated in some of the figures, indicate that the type of analysis chosen may need modifications to handle this type of power spectra arrangement.

CLUSTER ANALYSIS

The previously mentioned quantitative analysis of the data resulted in three parameters of the power spectra for each 0.25 s observation. These parameters are MPF, FPK, and PMAX. Expiratory and inspiratory data can be found in Appendix E. Since the study is a blind study, the best way to approach the test of the hypothesis is by cluster analysis.

Cluster analysis is used when the classification of the observations is not known. The objective of cluster analysis is to determine whether or not the data fall into separate clusters or groups. The very concept of "cluster" is a subjective matter. One ordinarily thinks of a cluster as a set of objects which are all close together. Examples may include a sunburst or a group of people at a party. A set of objects arranged along a straight line would not be described as a cluster in the ordinary connotation of the word.

Statisical Analysis System (SAS) is a computer software system for data analysis. A SAS data set contains not only the data values, but also such information as variable names, labels, and formats.

The procedure used for cluster analysis was the FASTCLUS procedure. FASTCLUS performs a cluster analysis on the basis of Euclidean distances computed from one or more quantitative variables. The analysis is a

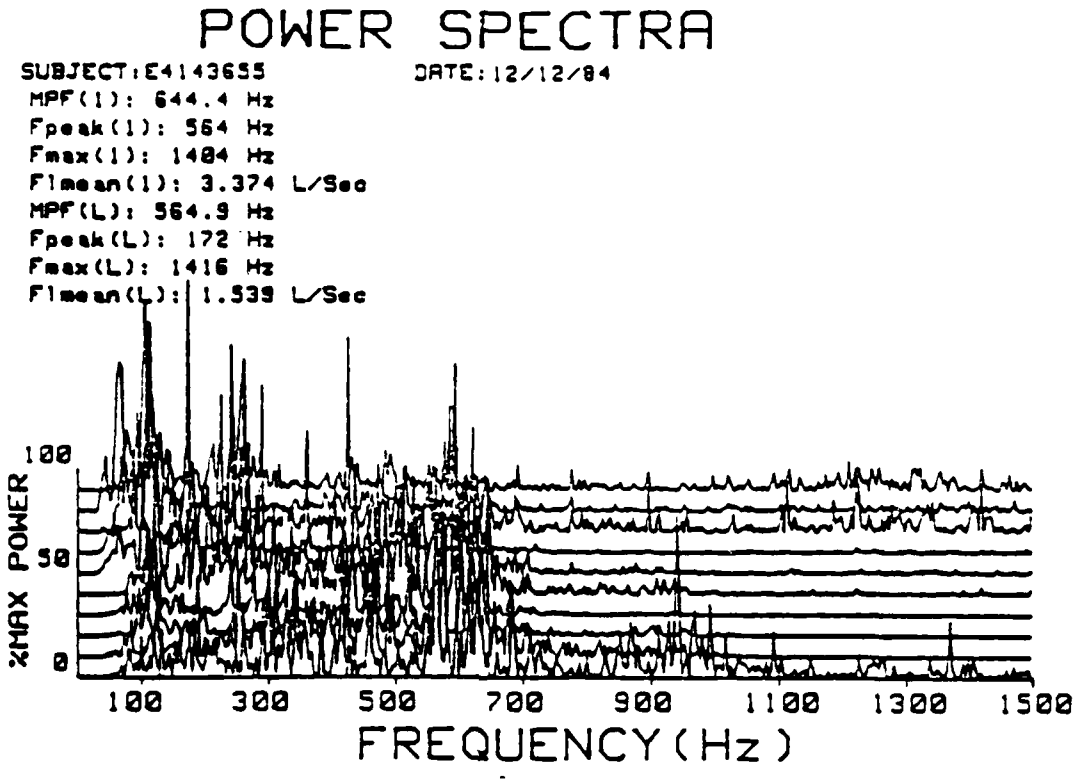

Figure 6. Power spectra plot of expiratory sound (4143655).

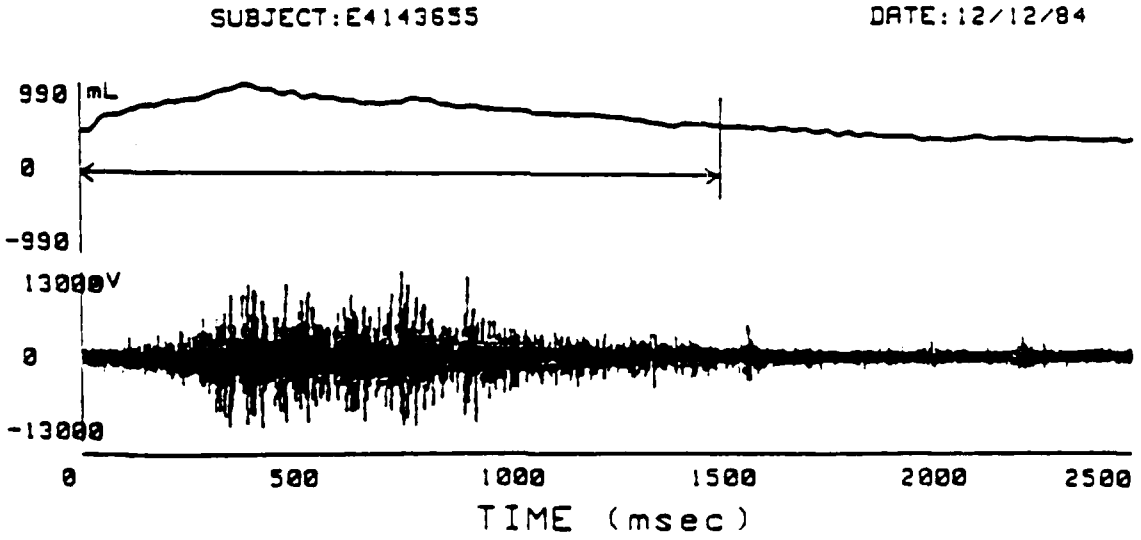

Figure 7. Plot of flow rate and expiratory sound (4143655).

disjoint cluster analysis, meaning that every observation belongs to one and only one cluster. FASTCLUS is intended for use with large data sets (about 100 to 100,000 observations), and uses a method that is sometimes referred to as the nearest centroid sorting. FASTCLUS is an iterative algorithm for minimizing the sum of squared distances from the cluster means. Clusters are formed such that all the Euclidean distances between observations in the same cluster are less than all Euclidean distances between observations in different clusters. The Euclidean distance between two points $P_1(x_1,y_1)$ and $P_2(x_2,y_2)$ can be written as:

$$d^2 = (x_2-x_1)^2+(y_2-y_1)^2 \qquad (24)$$

where x and y are the coordinates of the points.

FASTCLUS always selects the first complete (no missing values) observation as the first seed. A seed refers to the mean of a cluster. The number of seeds selected corresponds to the number of clusters specified in the procedure statement. The next complete observation that is separated from the first seed by at least the RADIUS becomes the second seed, and so forth until the desired number of seeds are chosen. The default value of zero was used for RADIUS. RADIUS establishes the minimum distance criterion for selecting new seeds. Two tests are made to see if an observation can qualify as a new seed. First, an old seed is replaced if the distance between the two closest seeds is less than the distance from the observation to the nearest seed. The seed that is chosen to be replaced is selected from the two seeds that are closest to each other, and it is the seed that is also closest to the observation. If this test fails, a second test is performed. The observation will replace the nearest seed if the smallest distance from the observation to all seeds other than the nearest one is greater than the shortest distance from the nearest seed to all other seeds. If this test also fails, FASTCLUS goes on to the next observation. Each observation is assigned to the nearest seed to form temporary clusters. The seeds are then replaced by the means of the temporary clusters and the process is repeated until no further changes occur in the clusters.

RESULTS AND DISCUSSION

The SAS FASTCLUS program was used to obtain clusters of 10, 5, 4, 3, and 2 groups from the respiratory spectral data. In all, 14 cases with 5 selections of groupings resulted in 70 cases-groups being analyzed. Cases 1 through 6 are two-dimensional plots of paired variables (i.e., MPF vs. FLOW, FPK vs. FLOW, etc.) during expiration. Table 1 summarizes the cases for both inspiratory and expiratory data. Cases 8 through 13 are the two-variable cluster plots during inspiration. Cases 7 and 14 present three-dimensional cluster.

Table 1. SUMMARY OF CLUSTER ANALYSES OF INSPIRATORY AND EXPIRATORY DATA.

Mode	Case	Cluster variables	Max. cluster
Expiration	1	MPF*FLOW	10,5,4,3,2
Expiration	2	FPK*FLOW	10,5,4,3,2
Expiration	3	FMAX*FLOW	10,5,4,3,2
Expiration	4	MPF*FPK	10,5,4,3,2
Expiration	5	FPK*FMAX	10,5,4,3,2
Expiration	6	FPK*FMAX	10,5,4,3,2
Expiration	7	MPF*FPK*FMAX	
Inspiration	8	MPF*FLOW	10,5,4,3,2
Inspiration	9	FPK*FLOW	10,5,4,3,2
Inspiration	10	FMAX*FLOW	10,5,4,3,2
Inspiration	11	MPF*FPK	10,5,4,3,2
Inspiration	12	MPF*FMAX	10,5,4,3,2
Inspiration	13	FPK*FMAX	10,5,4,3,2
Inspiration	14	MPF*FPK*FLOW	

FLOW is respiratory flow-rate in liters per second.

Expiratory Cluster Analysis

Figures 8 and 9 illustrate cluster attempts for Case 1 with 10 groups and 5 groups respectively. The numbers on the figure represent the cluster group to which the data point is assigned. From inspection, no distinguishable clusters appear in Figures 8 or 9. Figure 10 illustrates the clustering of Case 1 data into 4 groups. Boundaries between the groups appear at values of the mean frequency at 260, 480, and 750 Hz. Figure 11 represents clustering of Case 1 data into 3 groups. The boundaries appear at values of the mean frequency at 310 and 640 Hz. The boundary between groups 2 and 3 is not well defined, with some data points overlapping in the 2 cluster groups. Figure 12 shows clustering of Case 1 data into 2 groups. The rationale for the 2 groups is to have 1 cluster group represent normal subjects and the other group represent abnormal subjects with pulmonary insufficiency. The boundary between the 2 groups appears to be at a mean frequency of 510 Hz. Group 2 is not a clearly defined cluster group. From Figure 12, it appears that 2 groups are not enough to cluster the expiratory data by the variables MPF and FLOW.

Clustering the data by the variable MPF and FLOW does not appear to separate the data into distinguishable clusters. The 3 clusters in Figure 11 appear to have a sharper boundary drawn between clusters than the other combinations tried; however, it does not appear to be 3 distinct clusters.

In all the two-dimensional clusters cases, clustering into 10 or 5 groups results in 3 distinct cluster groupings. This result indicates that trying to cluster into more than 4 groups is too many. Also, clustering into 2 groups indicates the number of groups selected are not enough. Therefore, in the discussion that follows only clustering of the data into 4 and 3 groups will be presented.

Figure 13 presents clustering into 4 groups for Case 2. The figure seems to indicate 3 separate groups. The data points in groups 1 and 2 appear to belong into a single group. Figure 14 illustrates clustering of Case 2 data into 3 groups. The boundaries between groups appear at mean frequency values of 820 and 380 Hz. In summary, separating the data into clusters by the variables FPK and FLOW (Case 2) appears to show 3 separate clusters.

Case 3 is an attempt to cluster the data by the variables FMAX and FLOW. From this point on, plots for 10 and 5 groups may be found in Appendixes A and B, respectively, since in all cases these clusters seem to intermingle, indicating that the number of clusters chosen is too high. Likewise, cluster plots for 2 groups may be found in Appendix C, since in all cases there appear to be more than 2 groups. Thus, in the interest of brevity, only cluster plots of 4 and 3 groups will be presented and discussed. Figure 15 illustrates the clustering of 4 groups. Two cluster groups are above a FMAX value of 900. The other two boundaries may be drawn at FMAX values of 425 and 1225. Figure 16 is a plot of 3 group clusters. Thus, separating the data by variables FMAX and FLOW appears to cluster the data into 3 groups. In Case 4 the data are clustered by the variables MPF and FPK. Figure 17 is a plot of 4 clusters for the variables

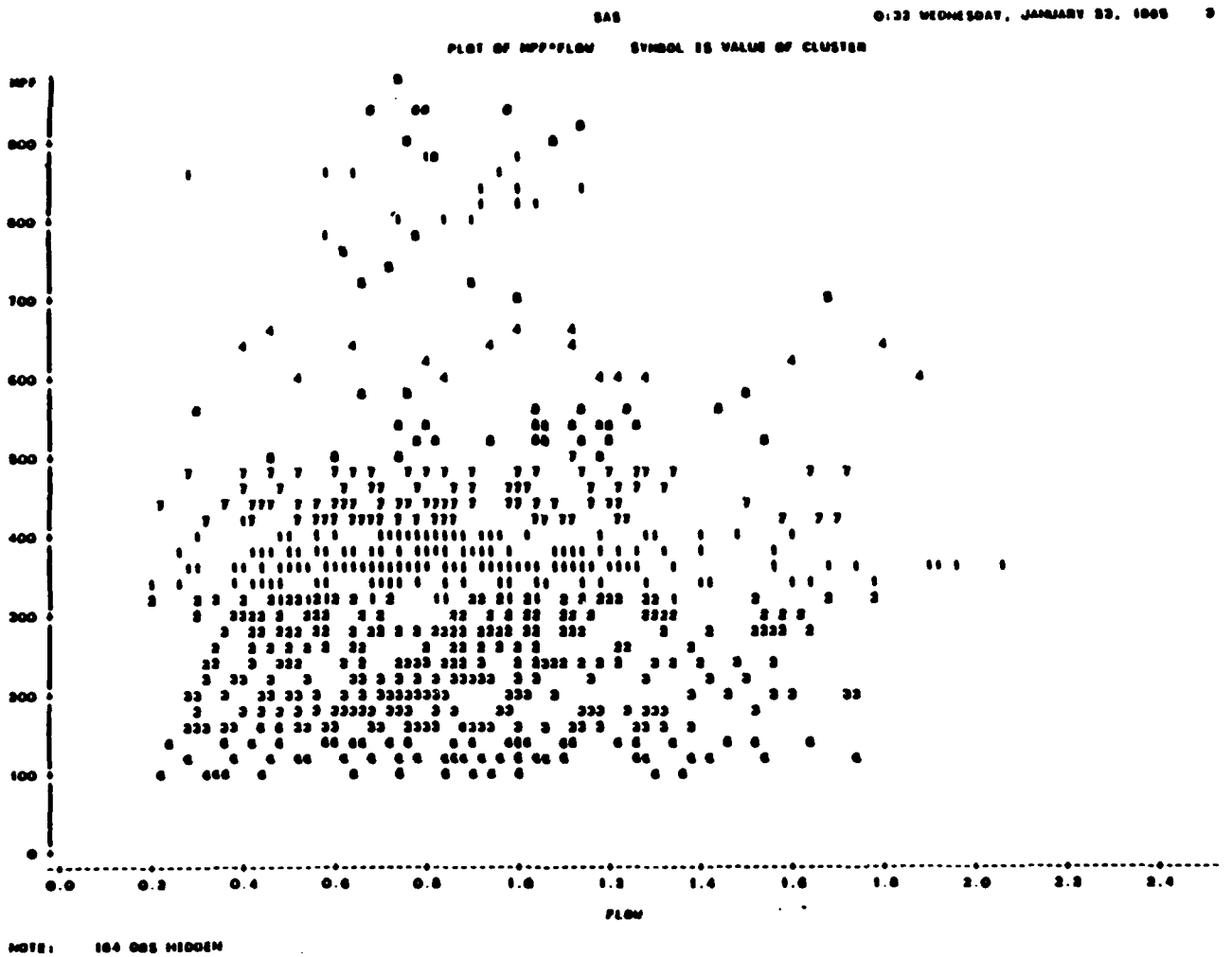

Figure 8. Cluster plot of Case 1, expiration, with 10 cluster groups (Maxc=10).

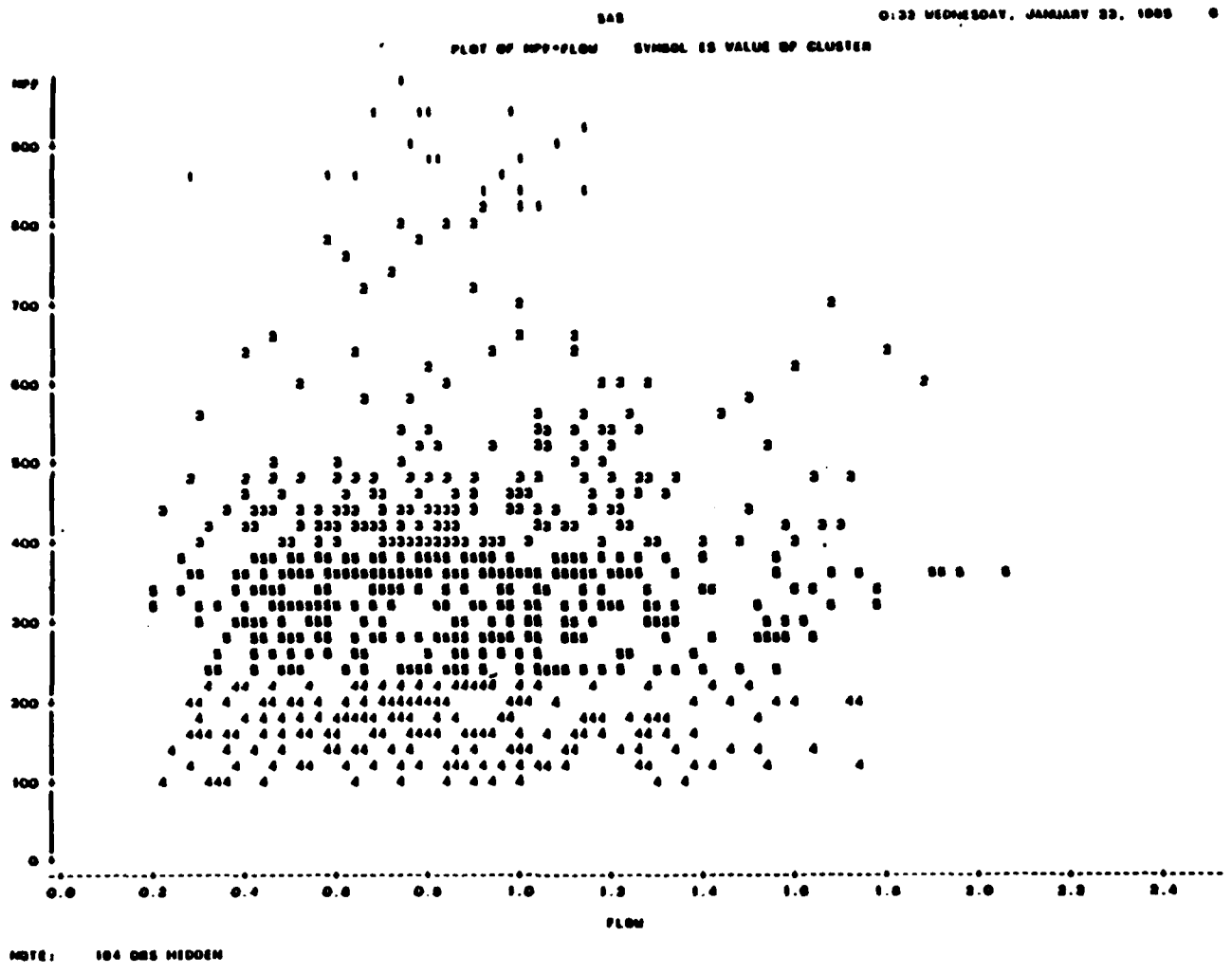

Figure 9. Cluster plot of Case 1, expiration, with 5 cluster groups (Maxc=5).

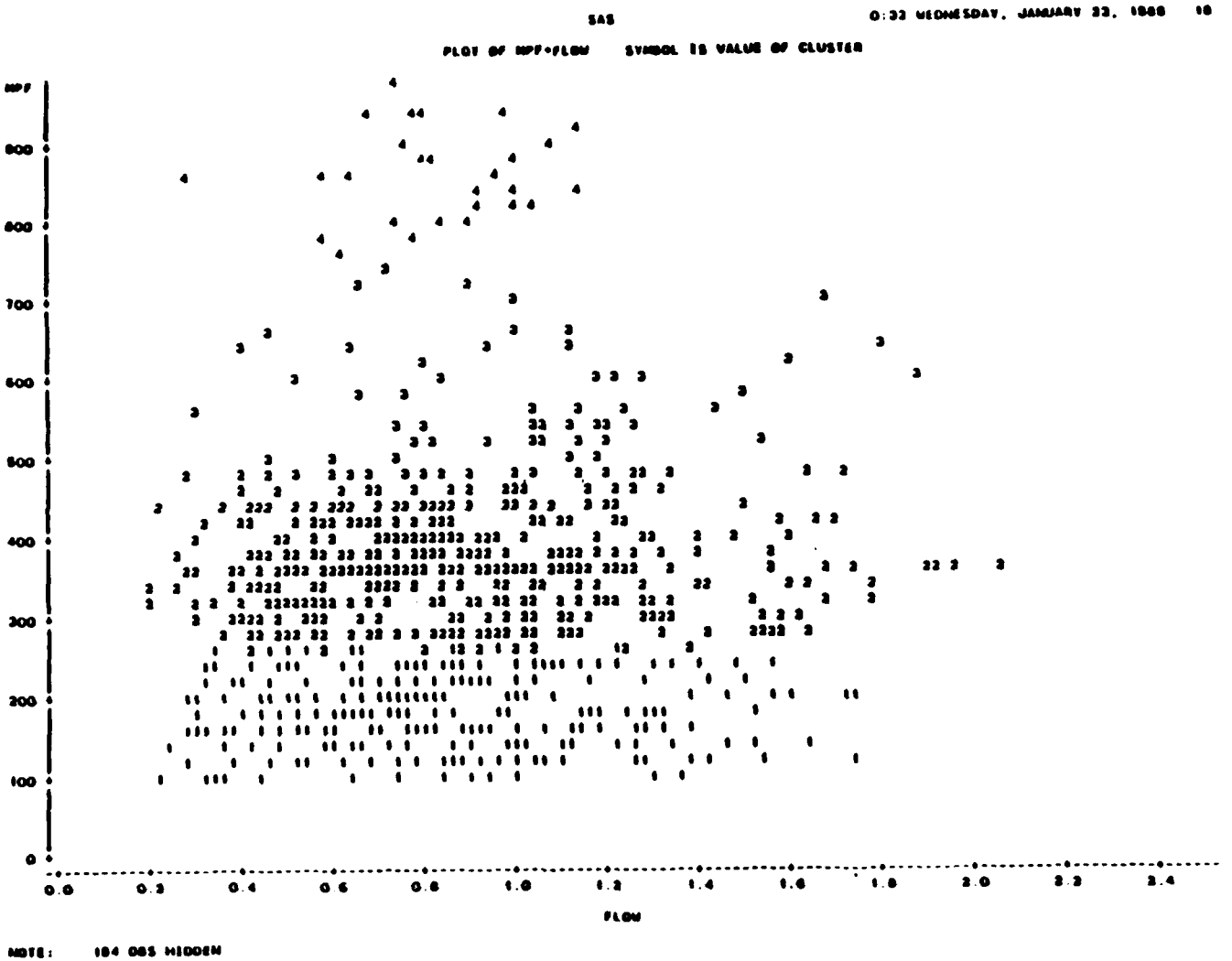

Figure 10. Cluster plot of Case 1, expiration, with 4 cluster groups (Maxc=4).

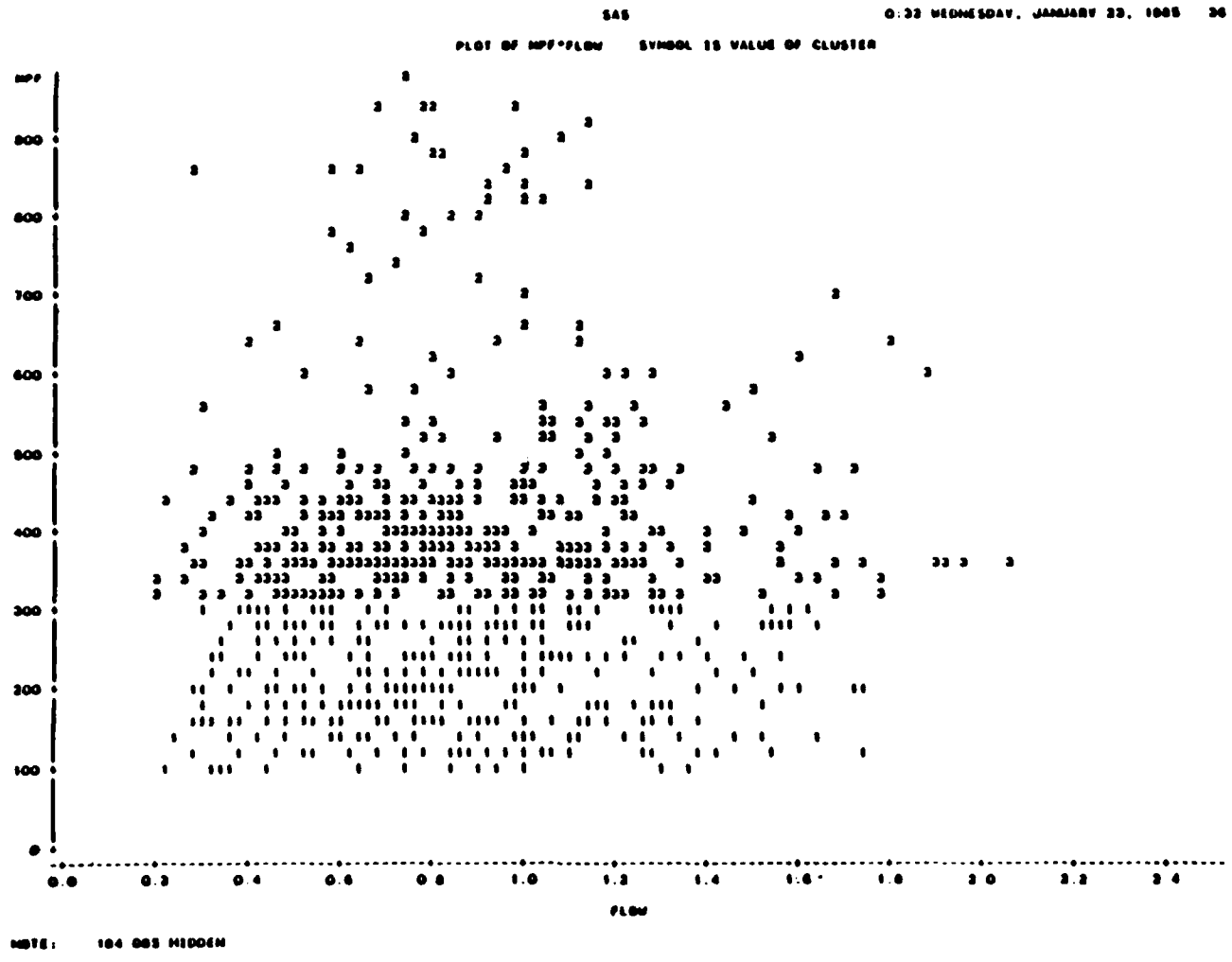

Figure 11. Cluster plot of Case 1, expiration, with 3 cluster groups (Maxc=3).

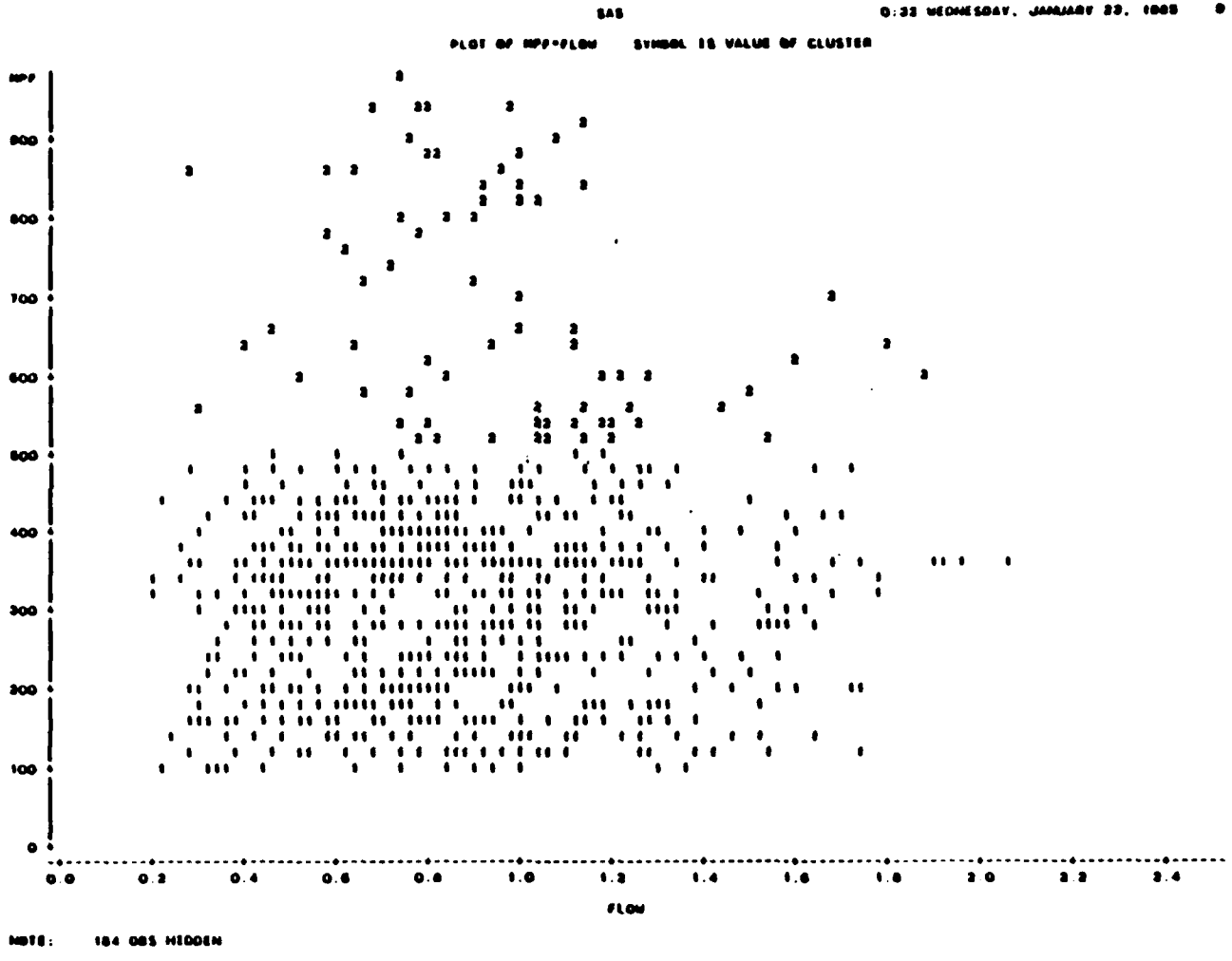

Figure 12. Cluster plot of Case 1, expiration, with 2 cluster groups (Maxc=2).

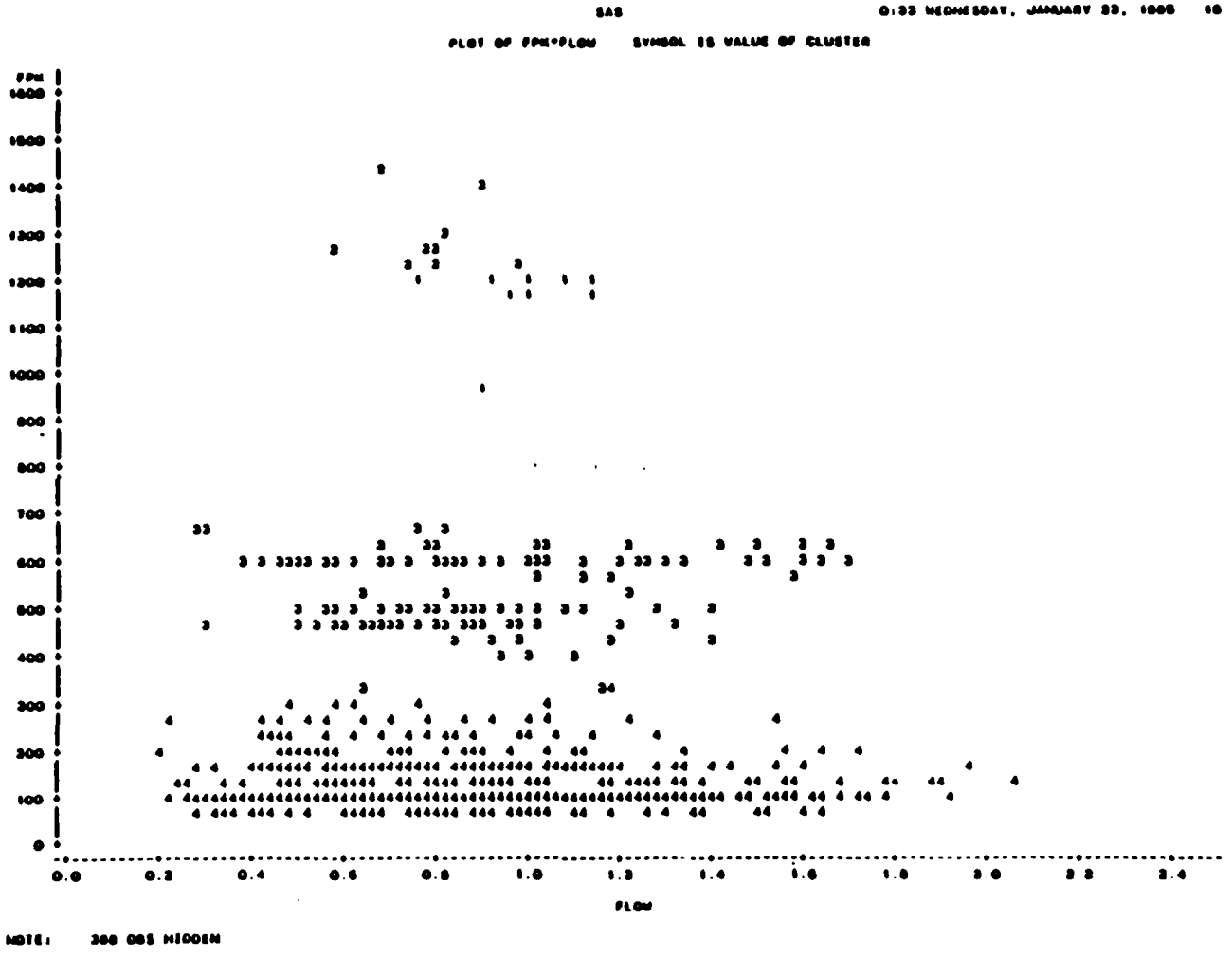

Figure 13. Cluster plot of Case 2, expiration, with 4 cluster groups (Maxc=4).

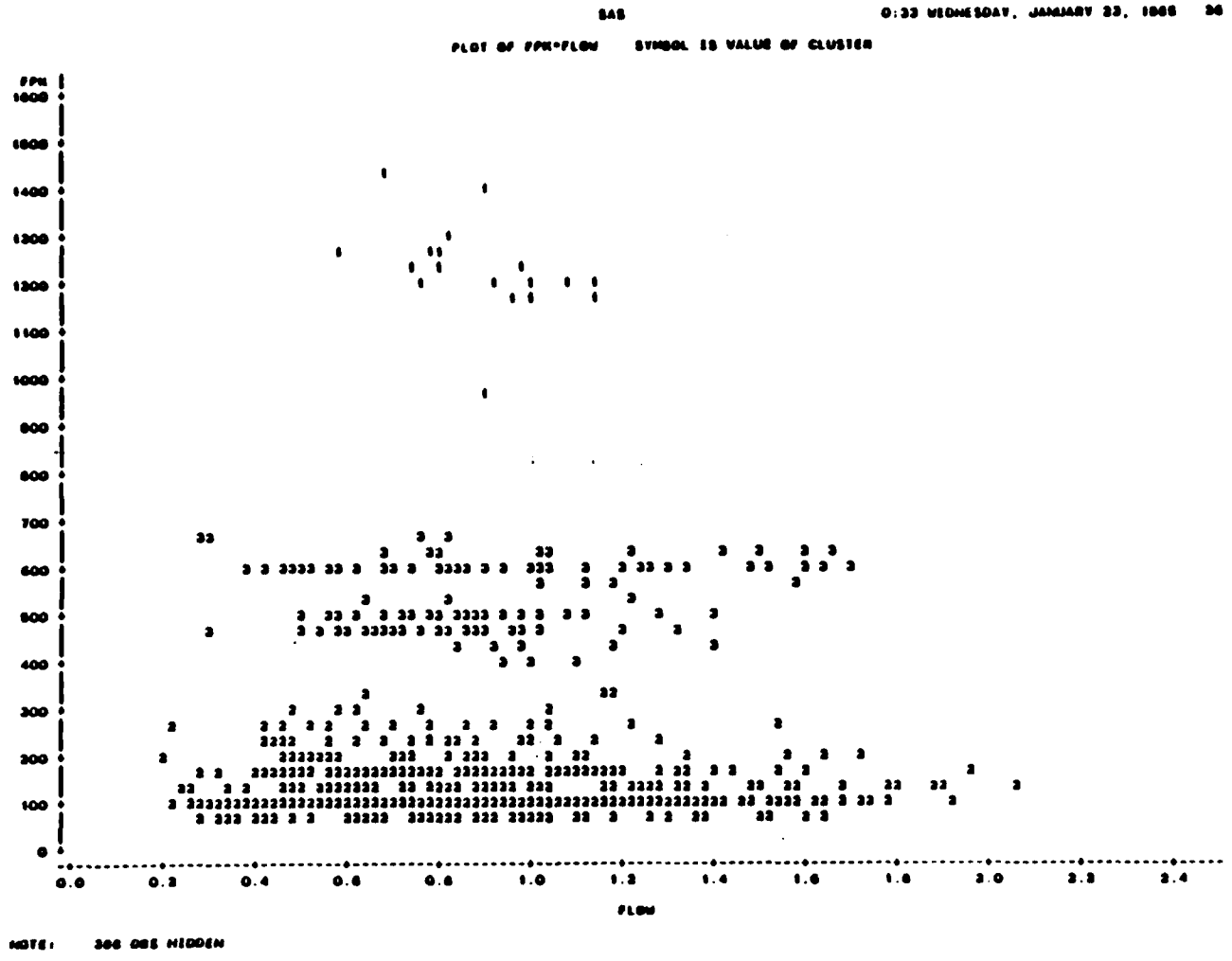

Figure 14. Cluster plot of Case 2, expiration, with 3 cluster groups (Maxc=3).

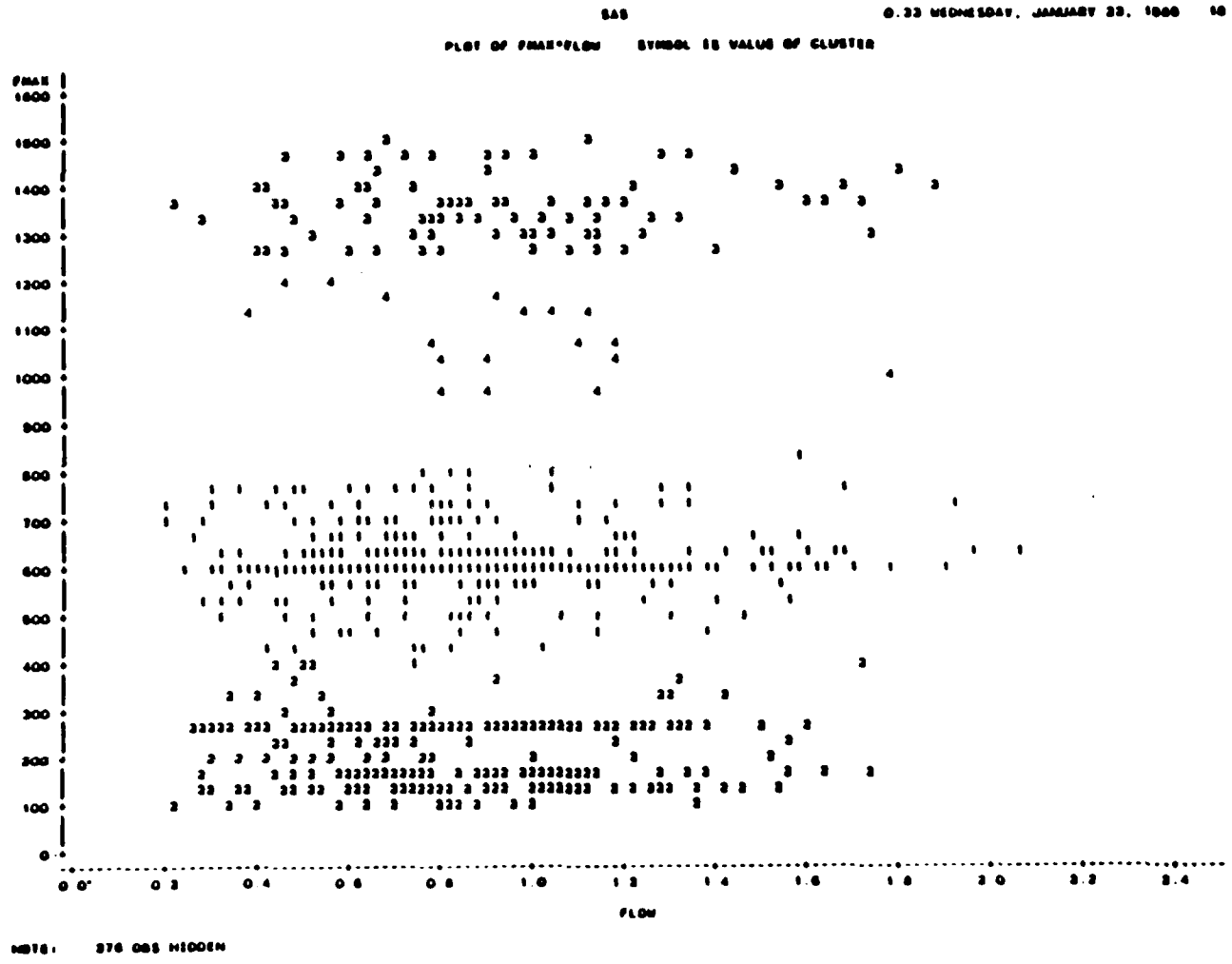

Figure 15. Cluster plot of Case 3, expiration, with 4 cluster groups (Maxc=4).

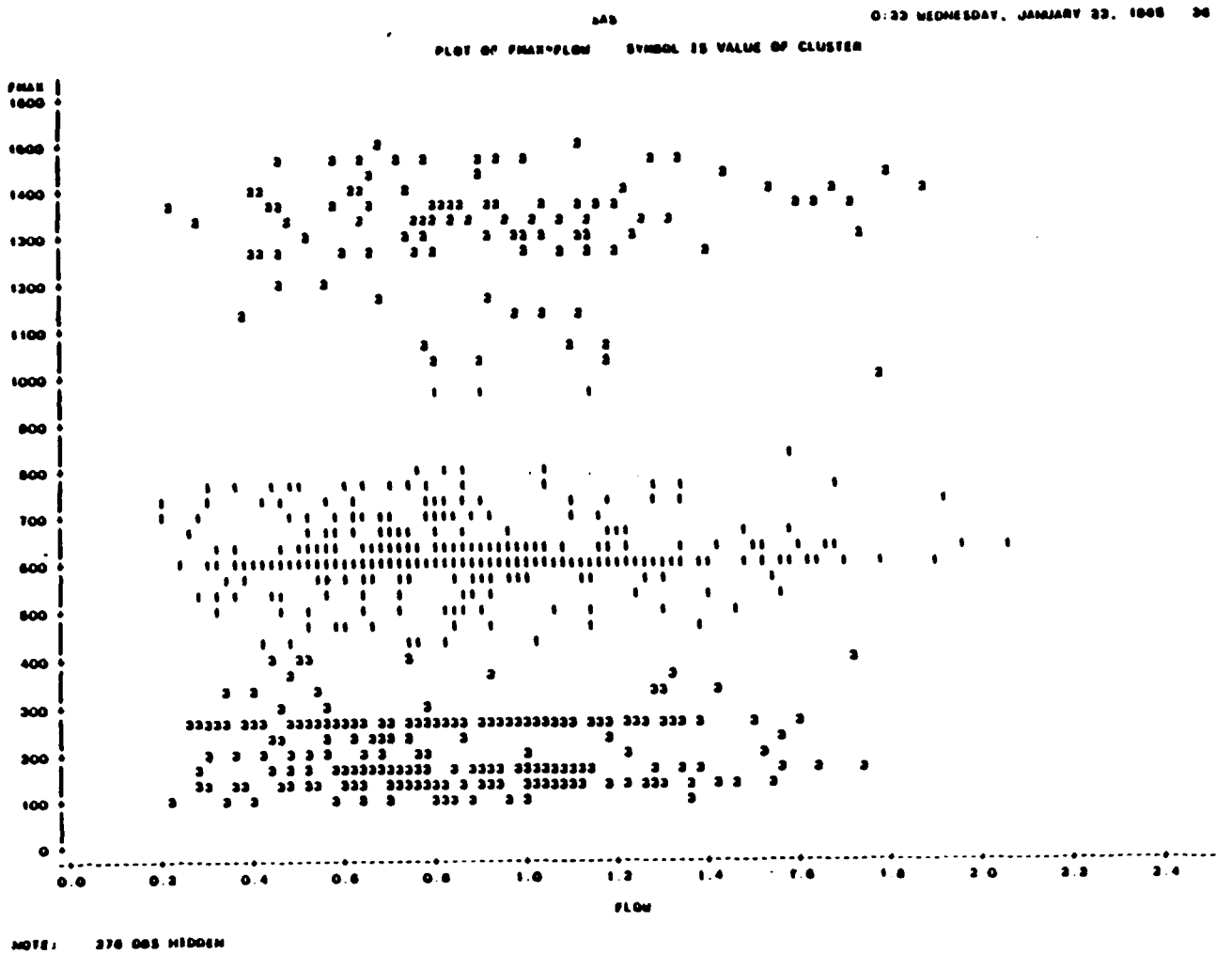

Figure 16. Cluster plot of Case 3, expiration, with 3 cluster groups (Maxc=3).

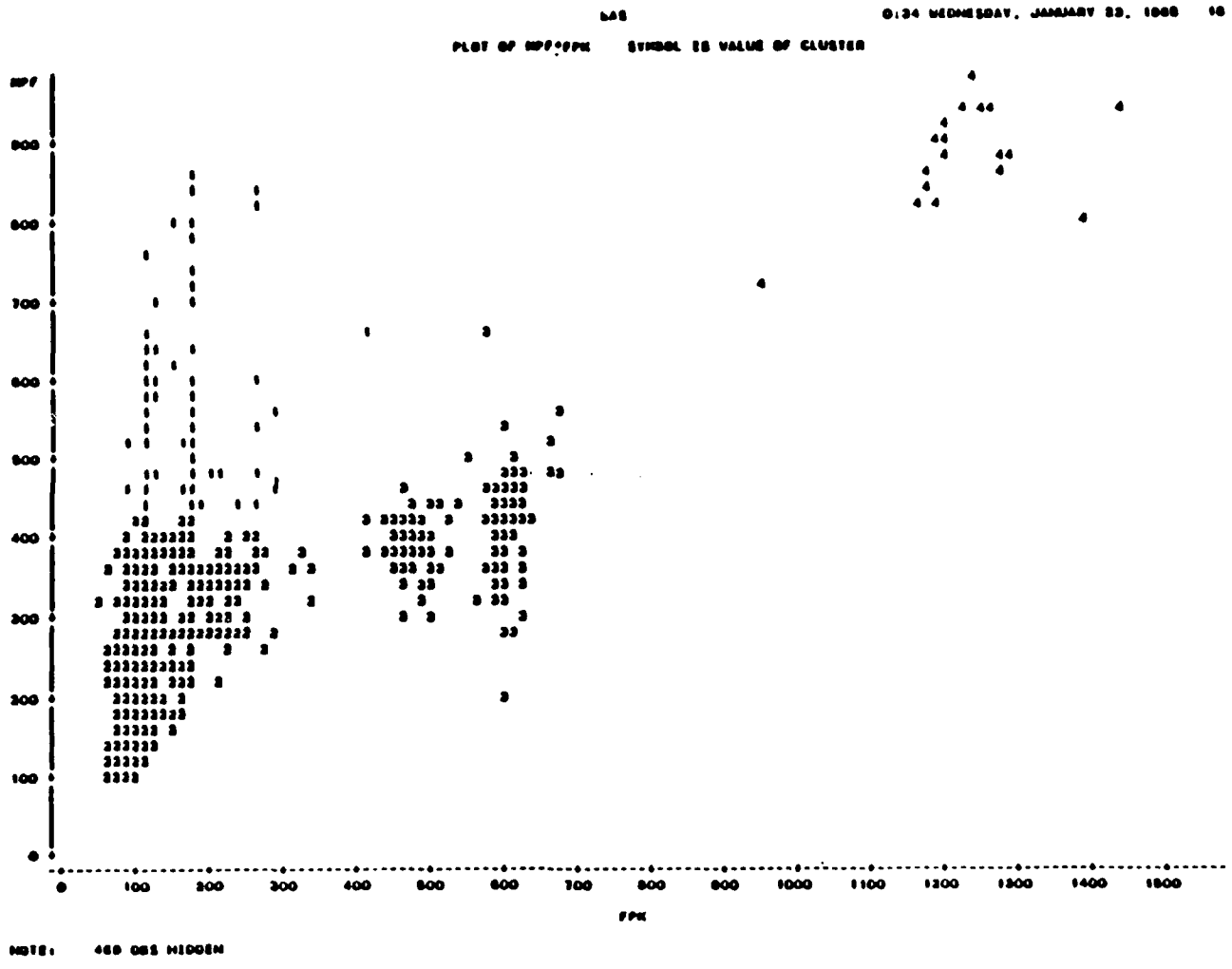

Figure 17. Cluster plot of Case 4, expiration, with 4 cluster groups (Maxc=4).

MPF and FPK. This figure appears to indicate 4 separate cluster groups. Clusters 2 and 3 appear to be dense and distinctly separate from each other. Cluster 4 is separate from the other 3 clusters, with a very high value for MPF and FPK. Cluster 1 appears to be dense with respect to FPK; however, it is not as dense of a cluster as are 2 and 3. The boundaries for the 4 separate clustersare as follows:

Cluster 1	440	MPF	860	88	FPK	413
Cluster 2	100	MPF	420	50	FPK	338
Cluster 3	200	MPF	600	325	FPK	775
Cluster 4	720	MPF	980	950	FPK	1450

Figure 18 is a plot of MPF vs. FPK for 3 cluster groups. Cluster 1 appears to be at least 2 separate clusters. Thus, separating the data by the variables MPF vs. FPK appears to cluster the data into 4 groups.

Case 5 clusters the data by the variables MPF and FMAX. Figure 19 is a plot of MPF vs. FMAX for a maximum of 4 clusters. This plot shows 4 clusters with boundaries with some overlapping data points near the boundaries.

Cluster 1	640	MPF	980	1050	FMAX	1500
Cluster 2	100	MPF	580	100	FMAX	413
Cluster 3	100	MPF	560	388	FMAX	838
Cluster 4	320	MPF	640	950	FMAX	1475

Figure 20 is a cluster plot of MPF vs. FMAX for clusters of 3 groups. From this plot it appears as if the data is clustered into 3 groups along the FMAX scale. Thus, separating the data by both variables MPF and FMAX appears to cluster the data into 4 groups.

In Case 6 the data is clustered by variables FPK and FMAX. Figure 21 is a plot of FPK vs. FMAX for a maximum cluster of 4. This plot shows 4 cluster groups with boundaries as follows:

Cluster 1	967	FPK	1433	1050	FMAX	1488
Cluster 2	67	FPK	300	100	FMAX	675
Cluster 3	67	FPK	667	550	FMAX	975
Cluster 4	67	FPK	567	975	FMAX	1488

Figure 22 shows the cluster plot of FPK vs. FMAX for 3 cluster groups. This plot appears to cluster the data along the FMAX scale with the boundary at FMAX equal to a value of 900. Cluster group 2 in Figure 22

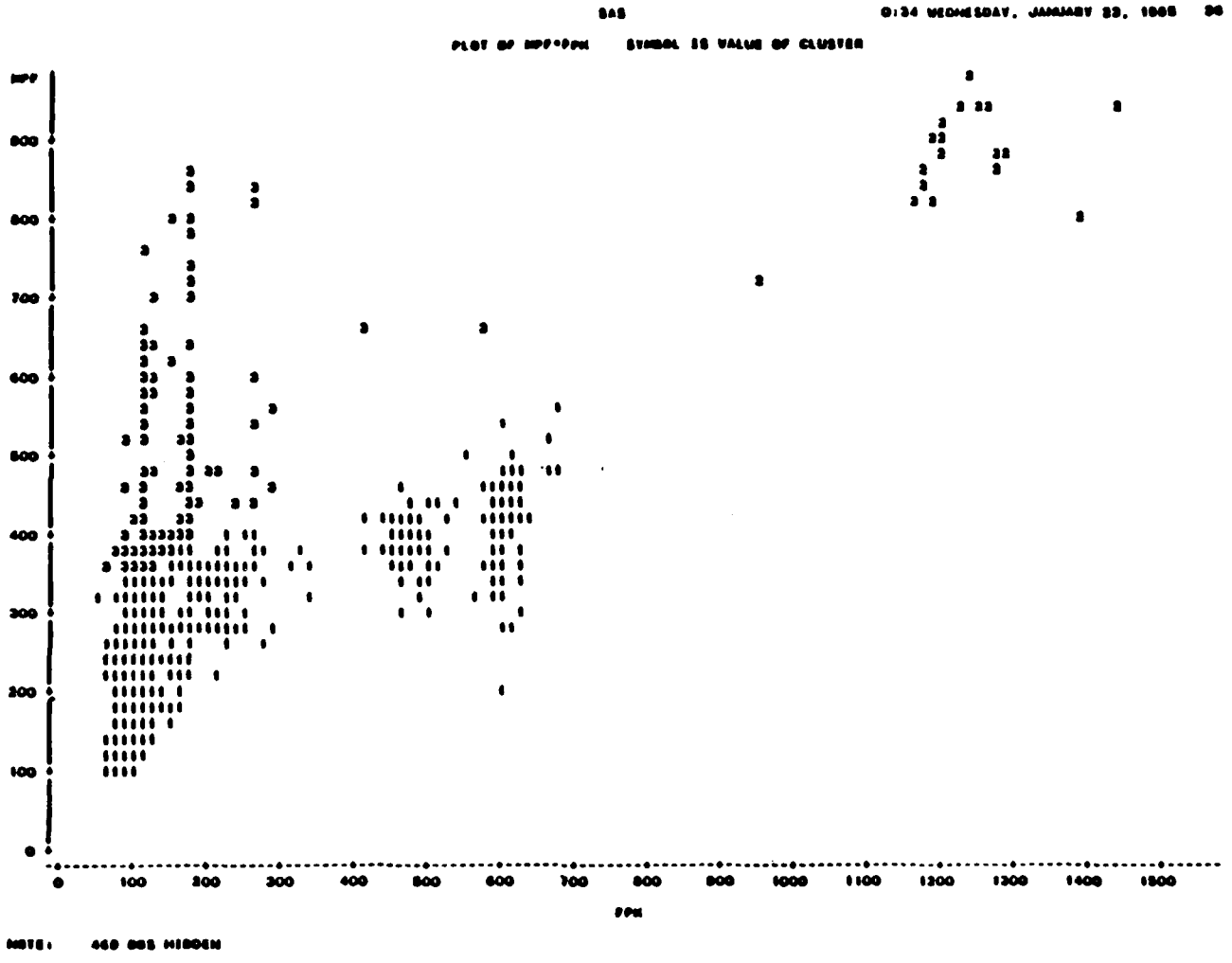

Figure 18. Cluster plot of Case 4, expiration, with 3 cluster groups (Maxc=3).

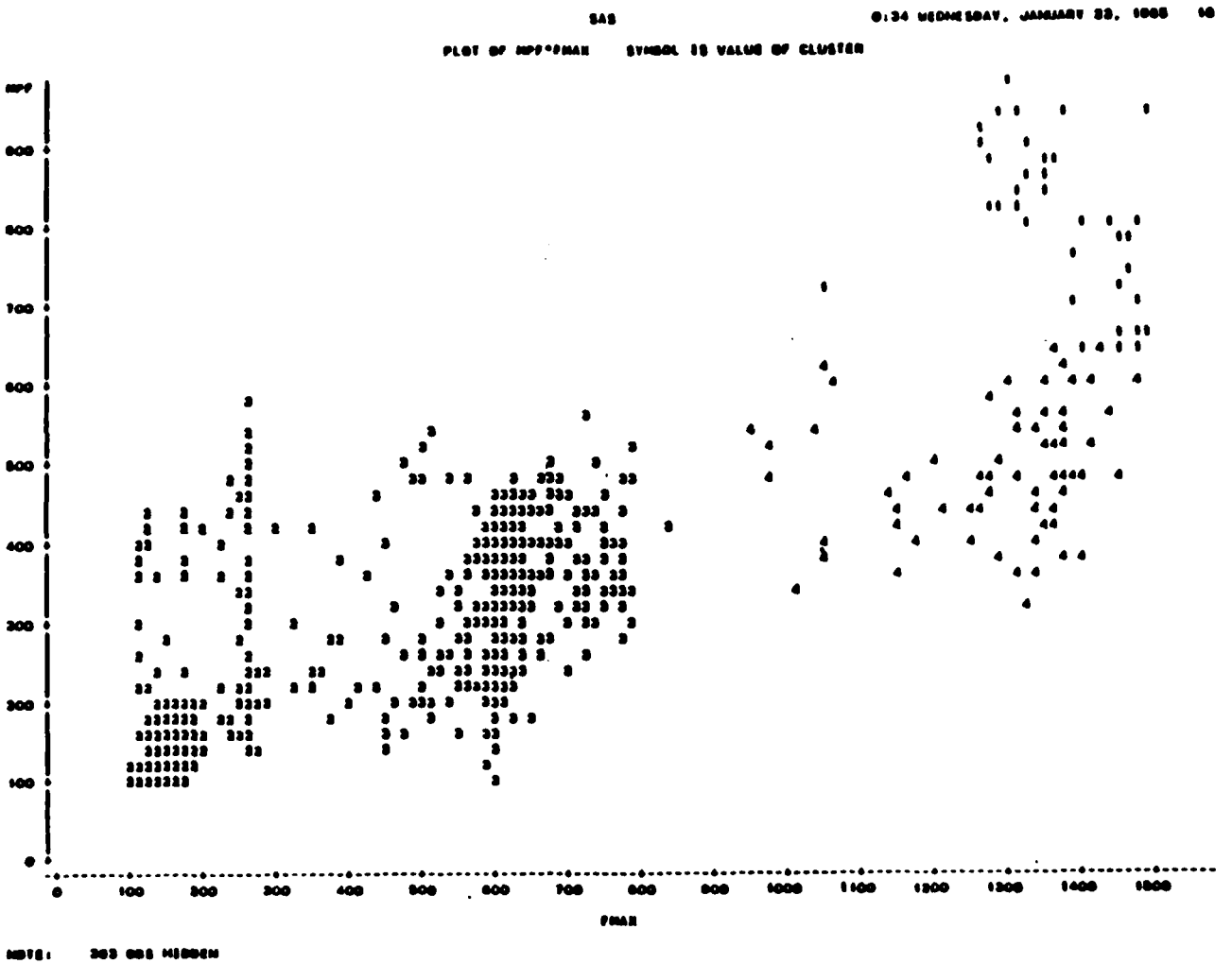

Figure 19. Cluster plot of Case 5, expiration, with 4 cluster groups (Maxc=4).

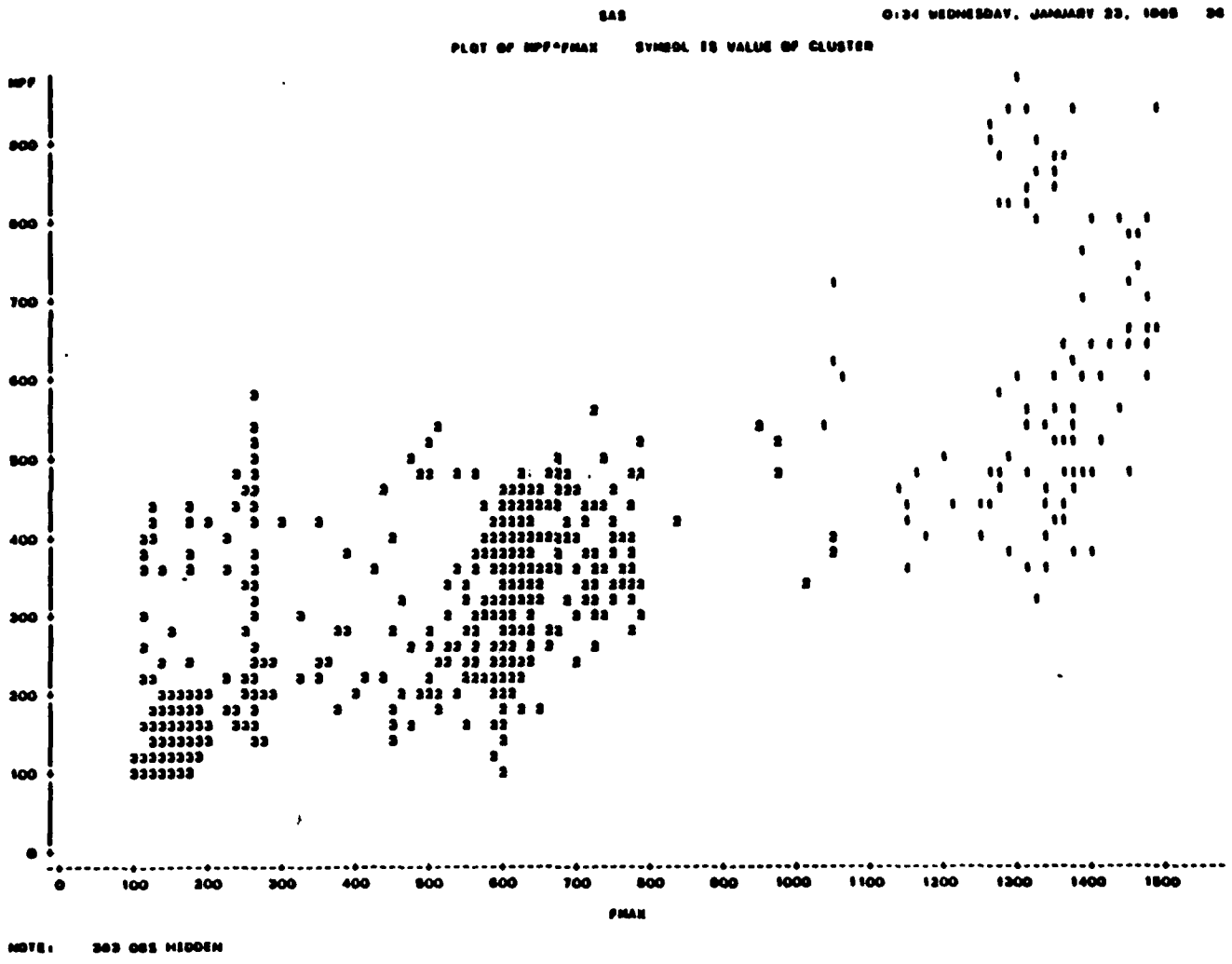

Figure 20. Cluster plot of Case 5, expiration, with 3 cluster groups (Maxc=3).

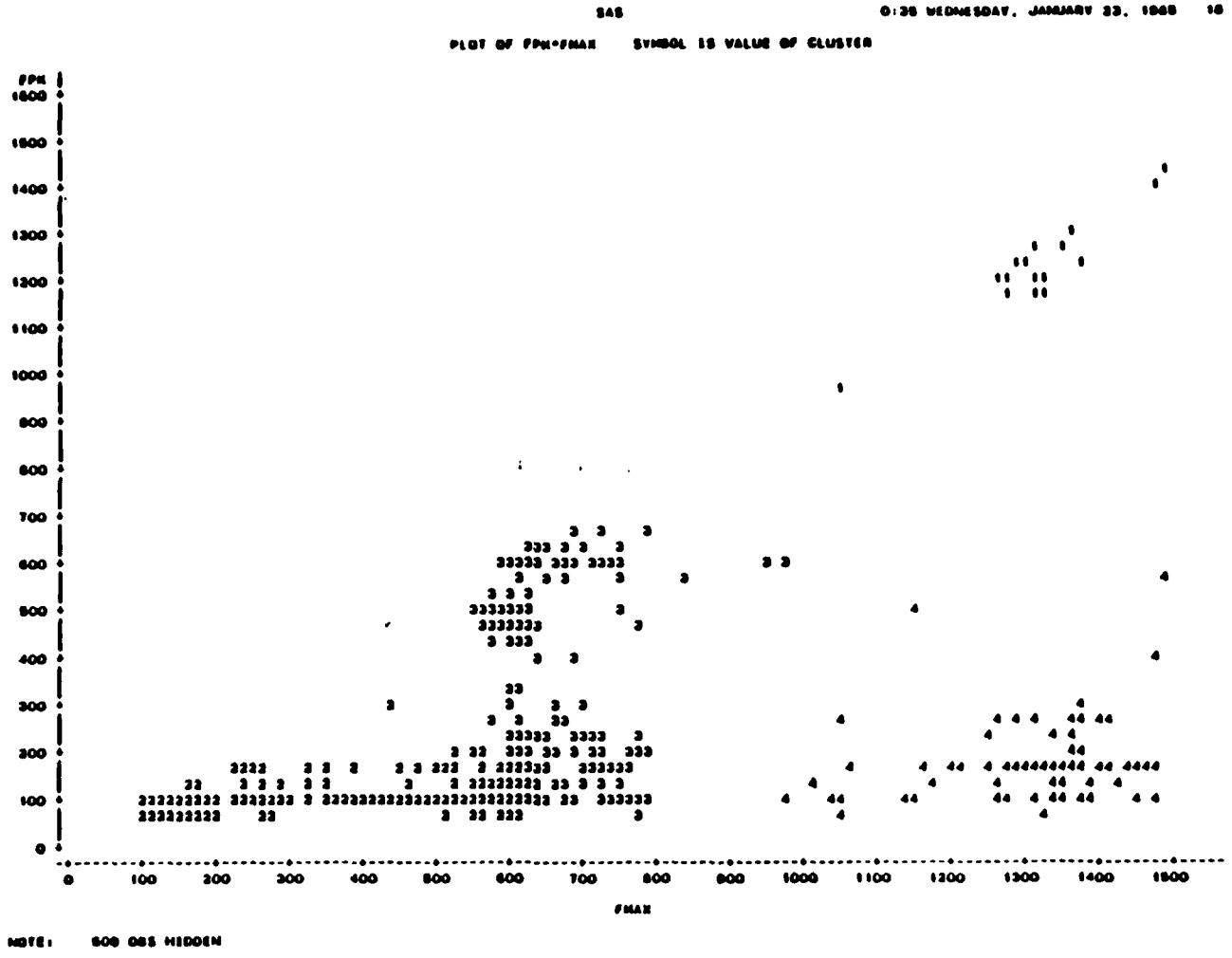

Figure 21. Cluster plot of Case 6, expiration, with 4 cluster groups (Maxc=4).

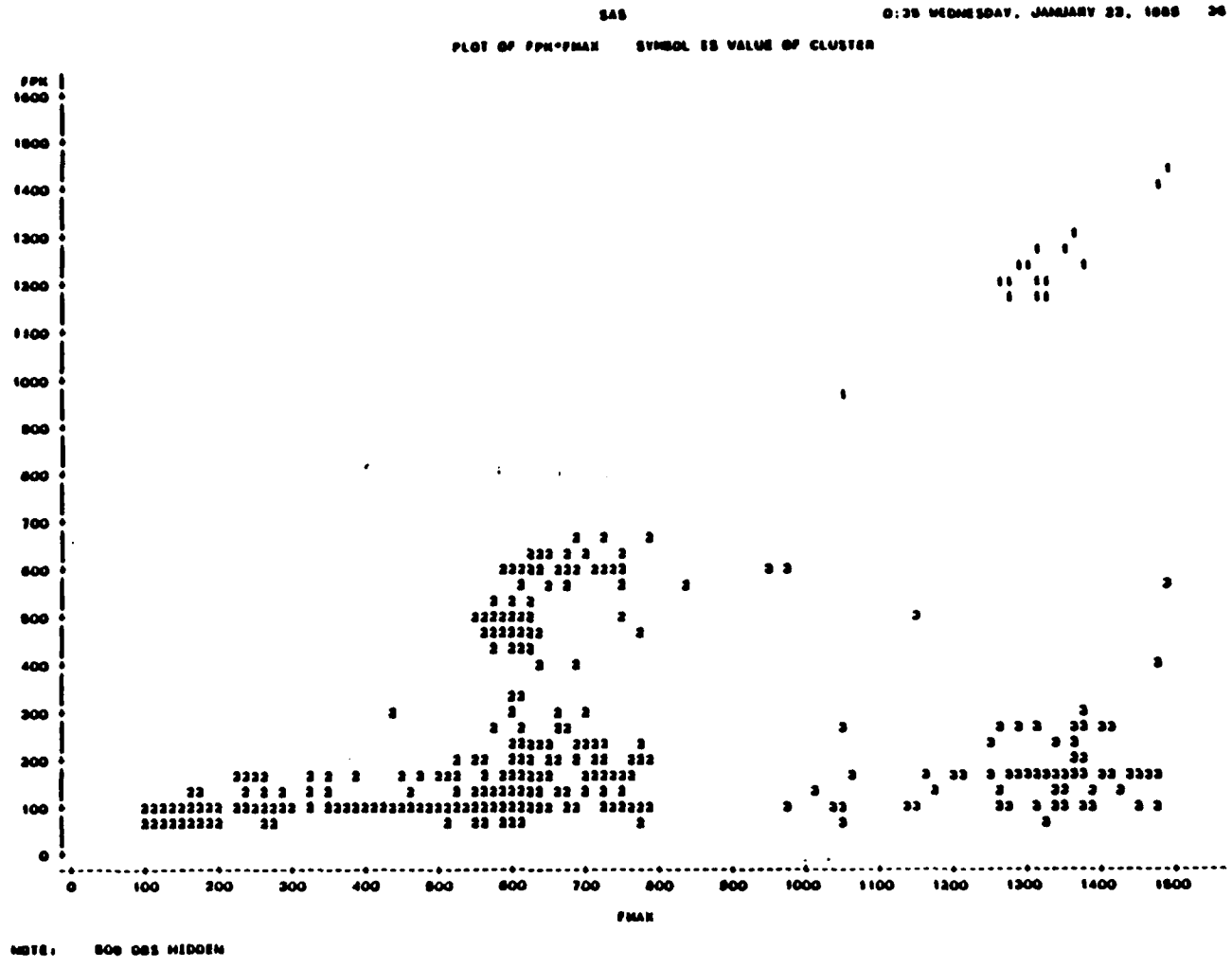

Figure 22. Cluster plot of Case 6, expiration, with 3 cluster groups (Maxc=3).

appears to be 2 cluster groups, instead of 1 as shown. Thus, separating the data by both variables FPK and FMAX appears to cluster the data into 4 groups. As noted, the previous 6 cases studied are not consistent in the number of cluster groupings which are apparent. Some combinations of parameters appear to indicate 3 cluster groups while other combinations appear to show 4 clusters. Some combinations do not reveal any distinct clusters at all.

Case 7 is an attempt to give a clearer indication of the relationship among the 3 indices of the power spectra (MPF, FPK and FMAX) by a three-dimensional cluster plot.

An IBM XT microcomputer and graphics printer were used to construct three-dimensional plots of the USAF data and data from a previous study by Wong [36]. Wong's study was a power spectral analysis of respiratory sounds at the trachea of normal young men. Since USAF data contained normal subjects and pulmonary insufficiency patients, Wong's population of subjects was used as a comparison.

A scale was chosen according to the maximum value of the 3 parameters of the power spectra of the USAF data. This scale was used for both the USAF data plots and for the normal subjects of Wong's study. A grid pattern was set up and the data was entered at the intersection of the grid lines. The plots are an approximation of a three-dimensional view. Three various angles were used to obtain a clear picture of the relationship between the parameters:

Figure	Viewing Angle	Table Angle
23	85°	5°
24	45°	5°
25	5°	5°

A boundary was drawn around the points in the three-dimensional plot of normal subjects. The individual plots of normal subjects and USAF data for the angles noted before are found in Appendix D. A plot of the normal subjects superimposed onto the plot of the USAF data is included for discussion. The normal subjects of Wong's study are surrounded by the boundary. In Figure 23, the normal subjects appear to be at an angle from the vertical, while other data points appear to follow more of a vertical line. Figure 24 does not appear to show any distinction among the data points. Figure 25 appears to show 3 groups. The normals are centrally clustered and there are data points clustered both to the right of the normals and some to the lower left of the cluster.

Figures 23 and 25 show an appearance of a possible clustering of the data into separate groups. The indication of these plots is that just 1 or 2 parameters is probably not enough to be able to distinctly separate the data into groups.

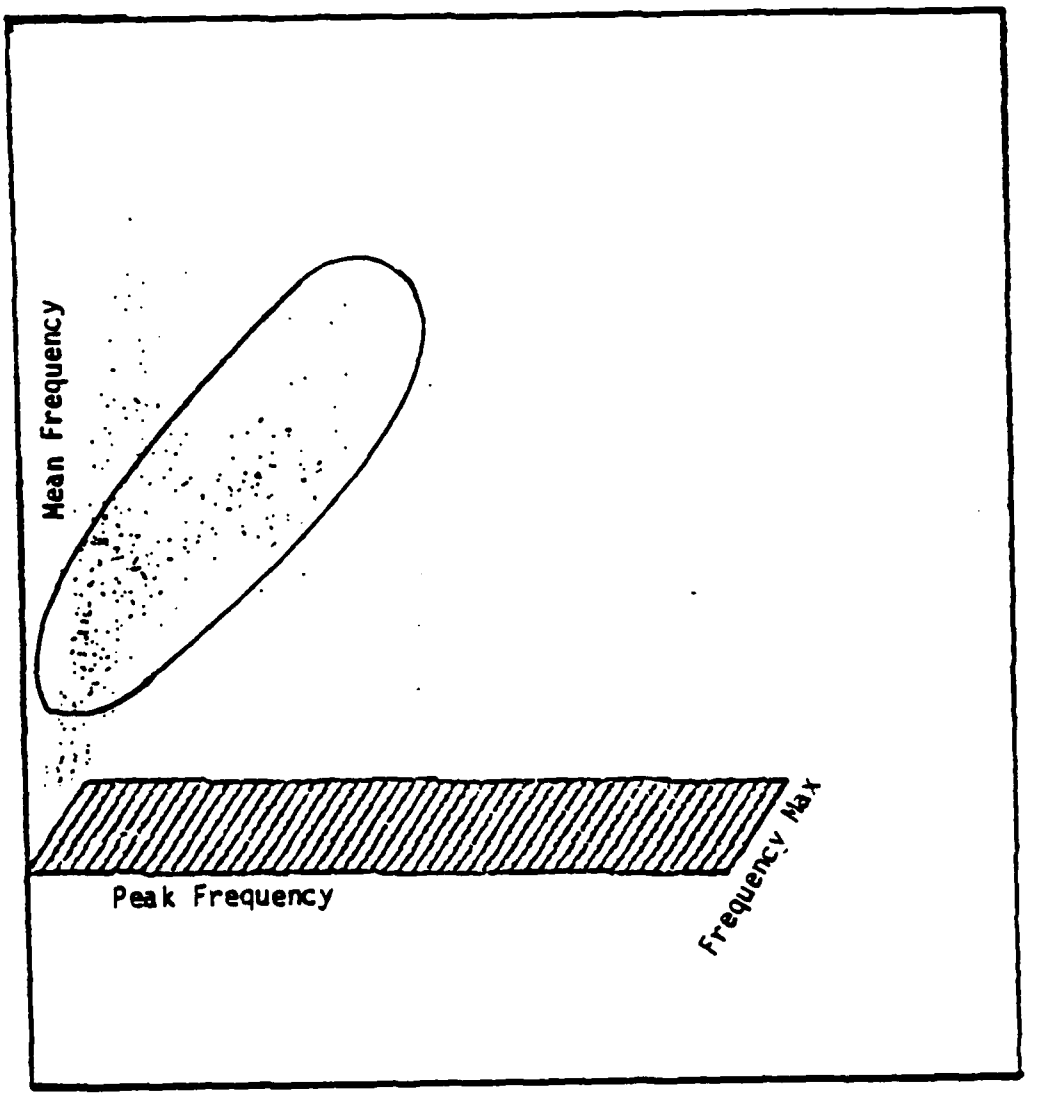

Figure 23. 3-D plot of Case 7, expiration, rotation = 85° and tilt = 5°.

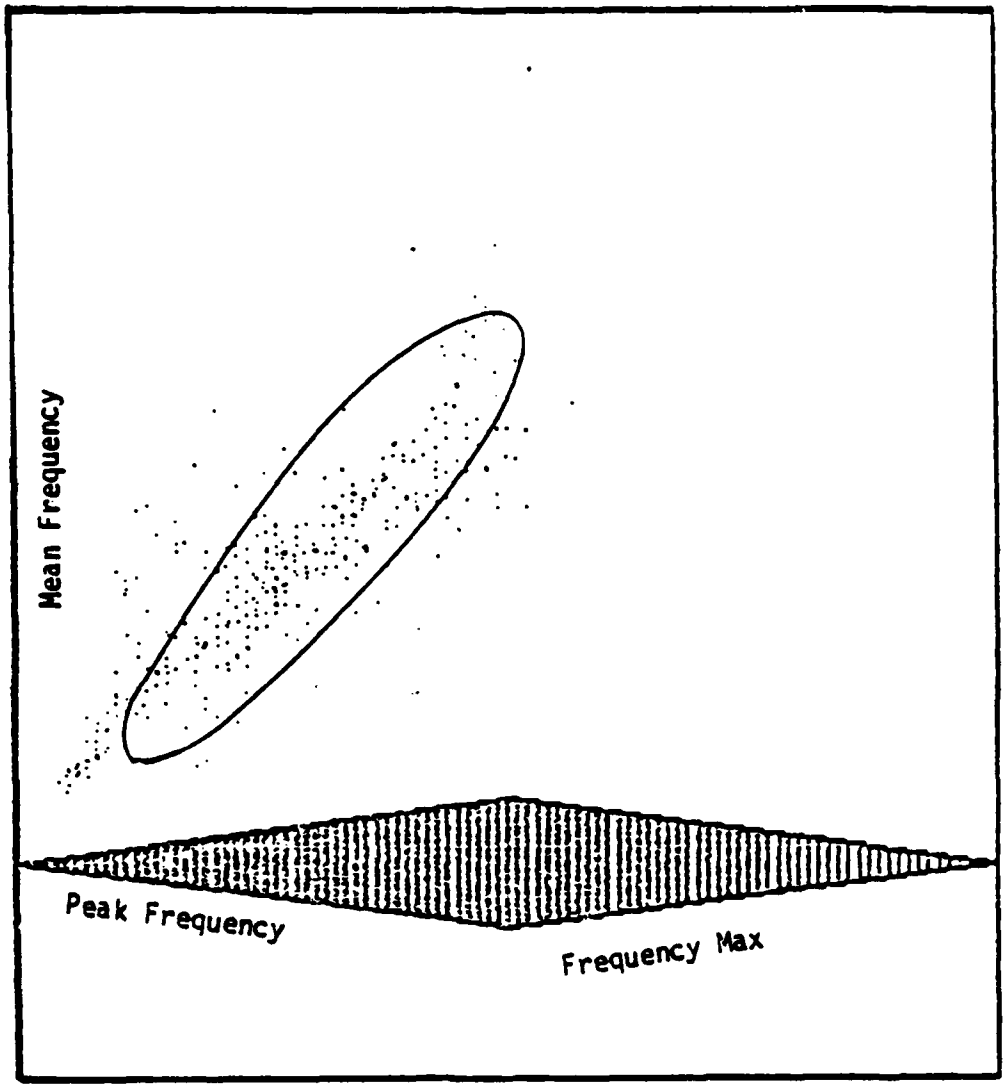

Figure 24. 3-D plot of Case 7, expiration, rotation = 45° and tilt = 5°.

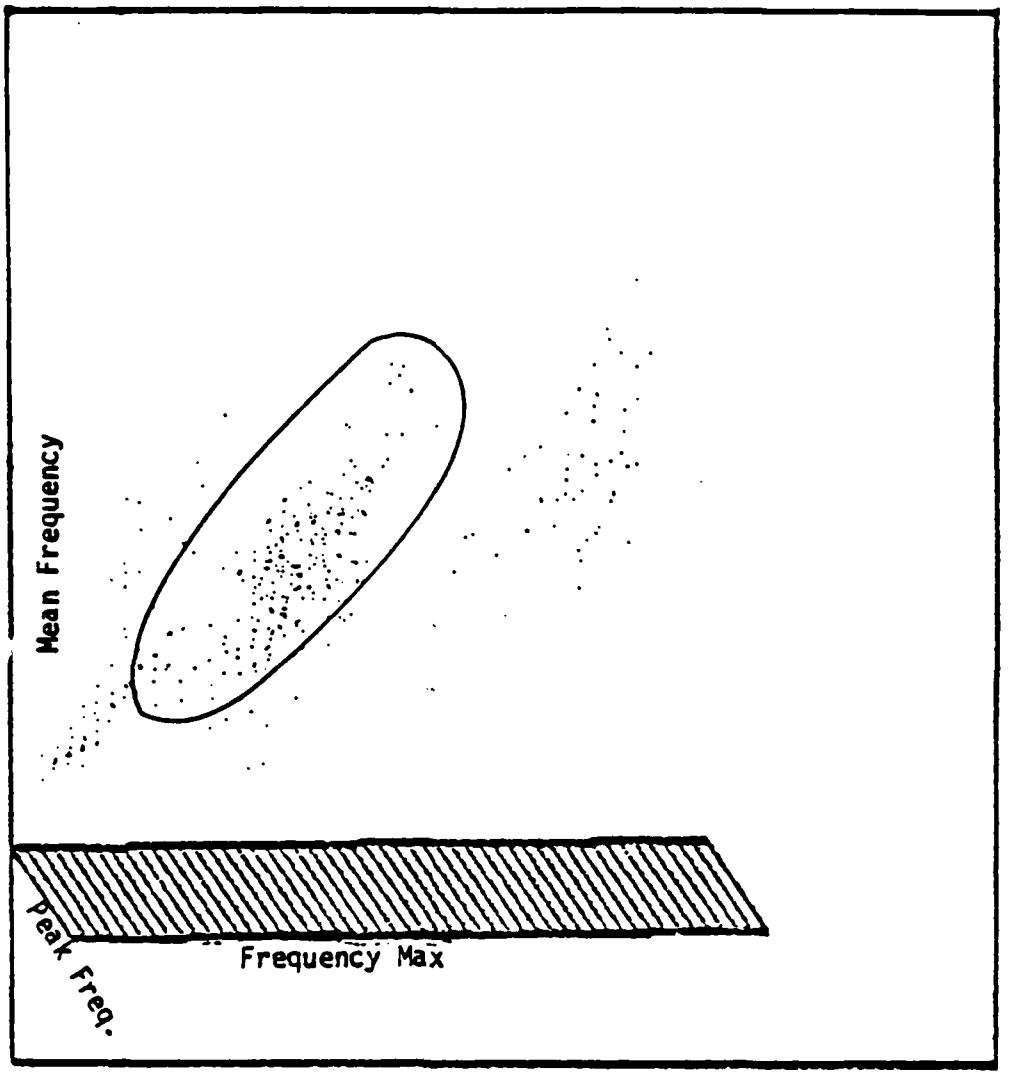

Figure 25. 3-D plot of Case 7, expiration, rotation = 5° and tilt = 5°.

Inspiratory Cluster Analysis

The remaining part of the discussion deals with cases 8 through 14 which are the combinations of variables used to cluster the inspiratory data in various number of grouping. The number cluster groups used in the program are 10, 5, 4, 3, and 2. As previously discussed with the expiratory data, clustering of the data into 10 and 5 groups appears to be too large. The plots either reveal no distinguishable cluster groups or there are only a few members in a cluster group. Therefore, the number of cluster groups (i.e., 10 and 5 groups) are not the optimum number for the data being analyzed. Plots of the 10 and 5 cluster groups for the cases 8 through 14 are found in Appendixes A and B respectively. Discussion of these results has been omitted in the interest of brevity.

Case 8 is a plot of MPF vs. FLOW. Figure 26 illustrates clustering into 4 cluster groups. The boundaries between the clusters are not distinct and the plot does not show separate distinct groupings. For example, cluster 2 is a very scattered group with some of the 2's found very close to the 4th cluster. Cluster 3 is relatively dense with a mean flow value less than 1.8 l/s; however, the plot shows the cluster also including data with very high mean flow values. The boundaries appear to be oriented horizontally with the main emphasis on the MPF parameter. For this case, clusters of the data are not well defined.

Figure 27 illustrates the attempt to make 3 clusters. The boundaries in this plot also appear to be oriented horizontally with the main emphasis on the MPF parameter. The boundaries, however, have intermingling data points and the plot does not show 3 distinct clusters.

Figure 28 illustrates clustering of the inspiratory data into 2 groups. The boundary is drawn at a MPF of 550, with anything above the value being defined as cluster 2 and anything below the value being defined as cluster 1. The boundary is not well defined with intermingling of data points, and the clusters are not 2 clearly separate groups. Clustering the data by the variables MPF and FLOW does not appear to separate the data into distinguishable clusters. This agrees with the result of using the variables MPF and FLOW to cluster the expiratory data.

Case 9 clusters the data by the variables FPK and FLOW. Figure 29 illustrates clustering of the data into 4 groups. The data appear to separate into 3 groups instead of 4. Clusters 2 and 3 appear to belong together and be separate from the other 2 clusters. Figure 30 is a plot of FPK vs. FLOW for 3 cluster groups. This plotting appears to be a better cluster than the plot of 4 clusters. The boundaries drawn between the 3 clusters are at FPK values of 350 and 950. In Figure 31, it appears as if there are 3 cluster groups with cluster group 1 actually being 2 separate groups clustering into 2 groups. Clustering the data by the variables FPK and FLOW appears to separate the data into 3 separate clusters. This grouping agrees with the number of clusters found for FPK and FLOW in expiratory data.

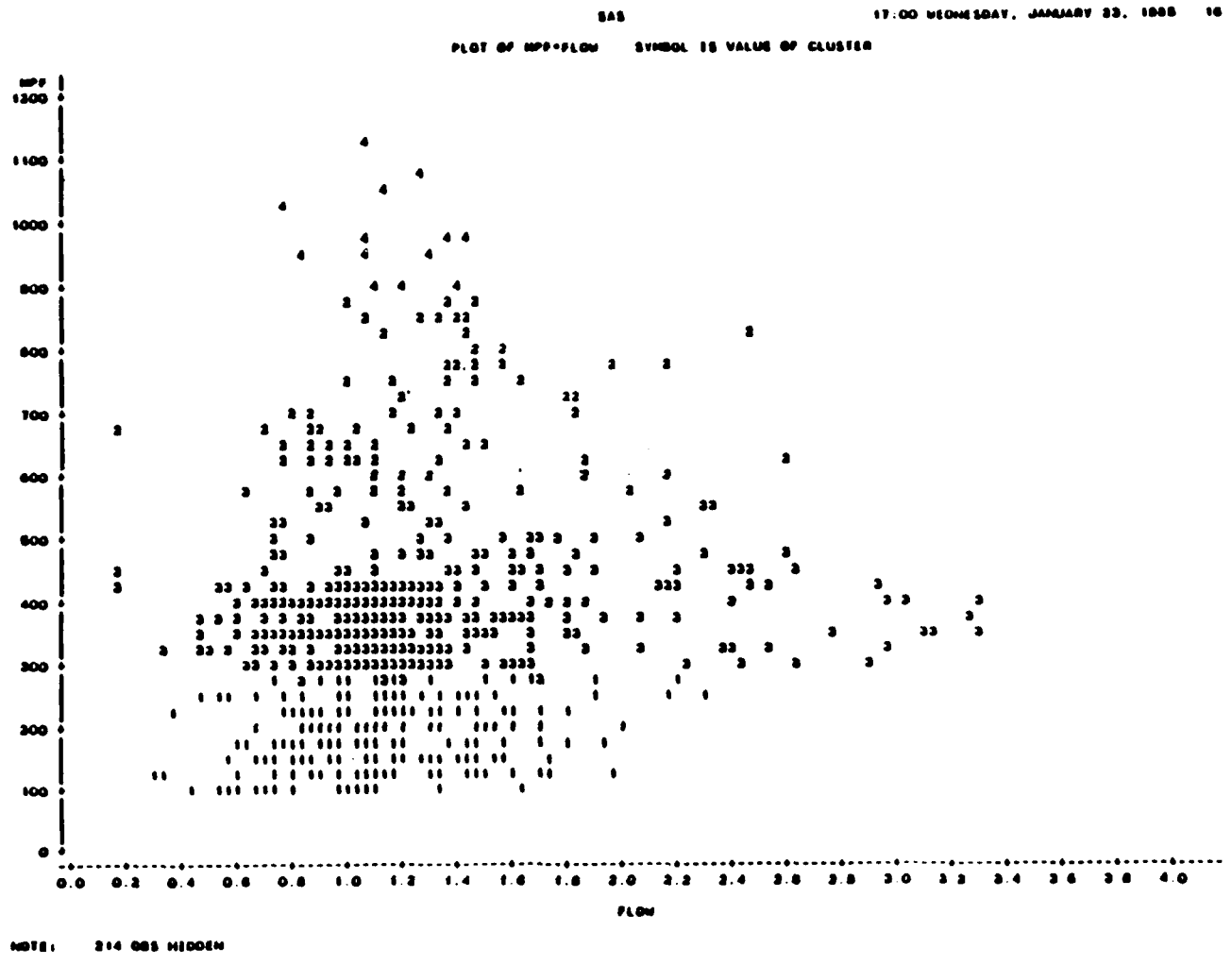

Figure 26. Cluster plot of Case 8, inspiration, with 4 cluster groups (Maxc=4).

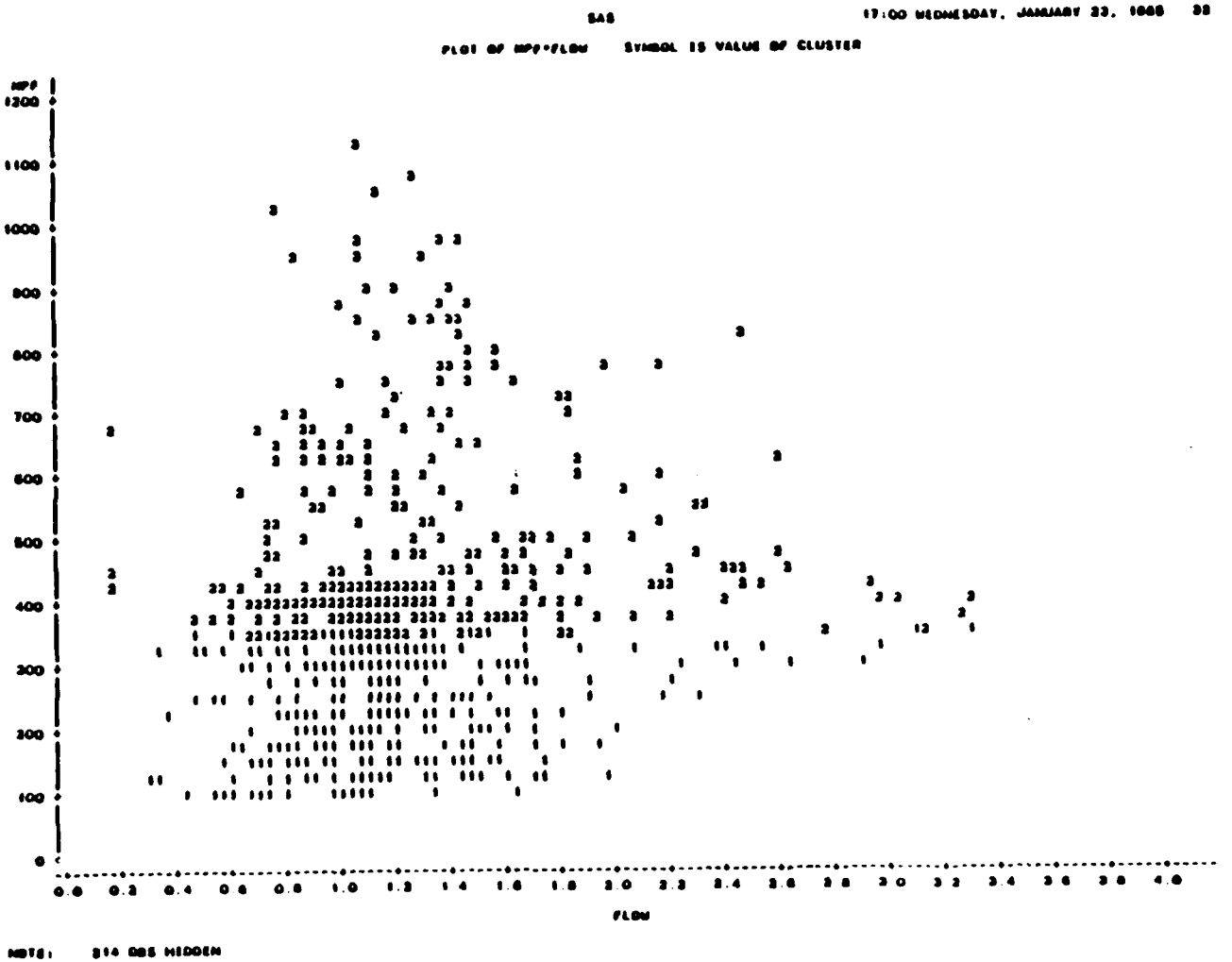

Figure 27. Cluster plot of Case 8, inspiration, with 3 cluster groups (Maxc=3).

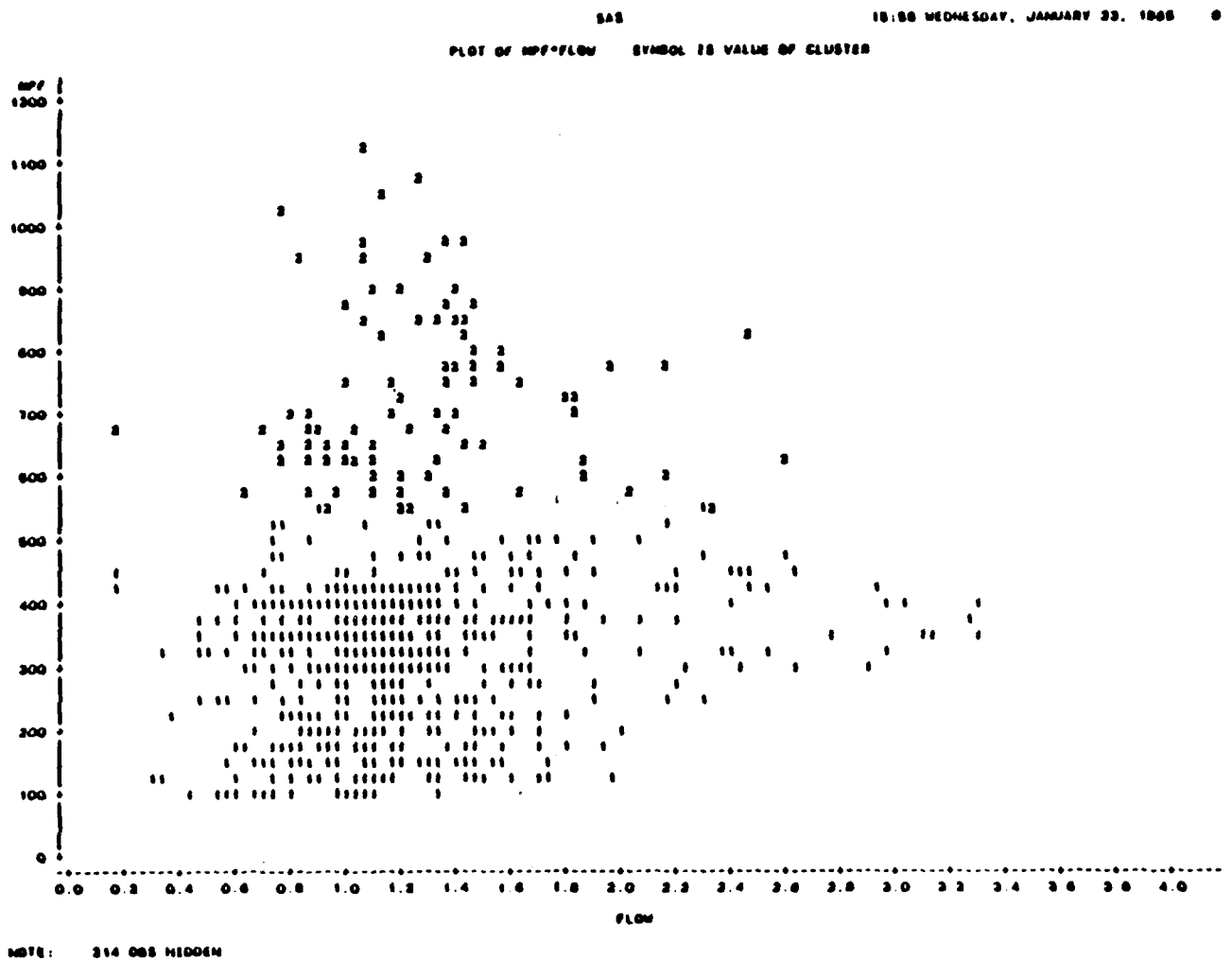

Figure 28. Cluster plot of Case 8, inspiration, with 2 cluster groups (Maxc=2).

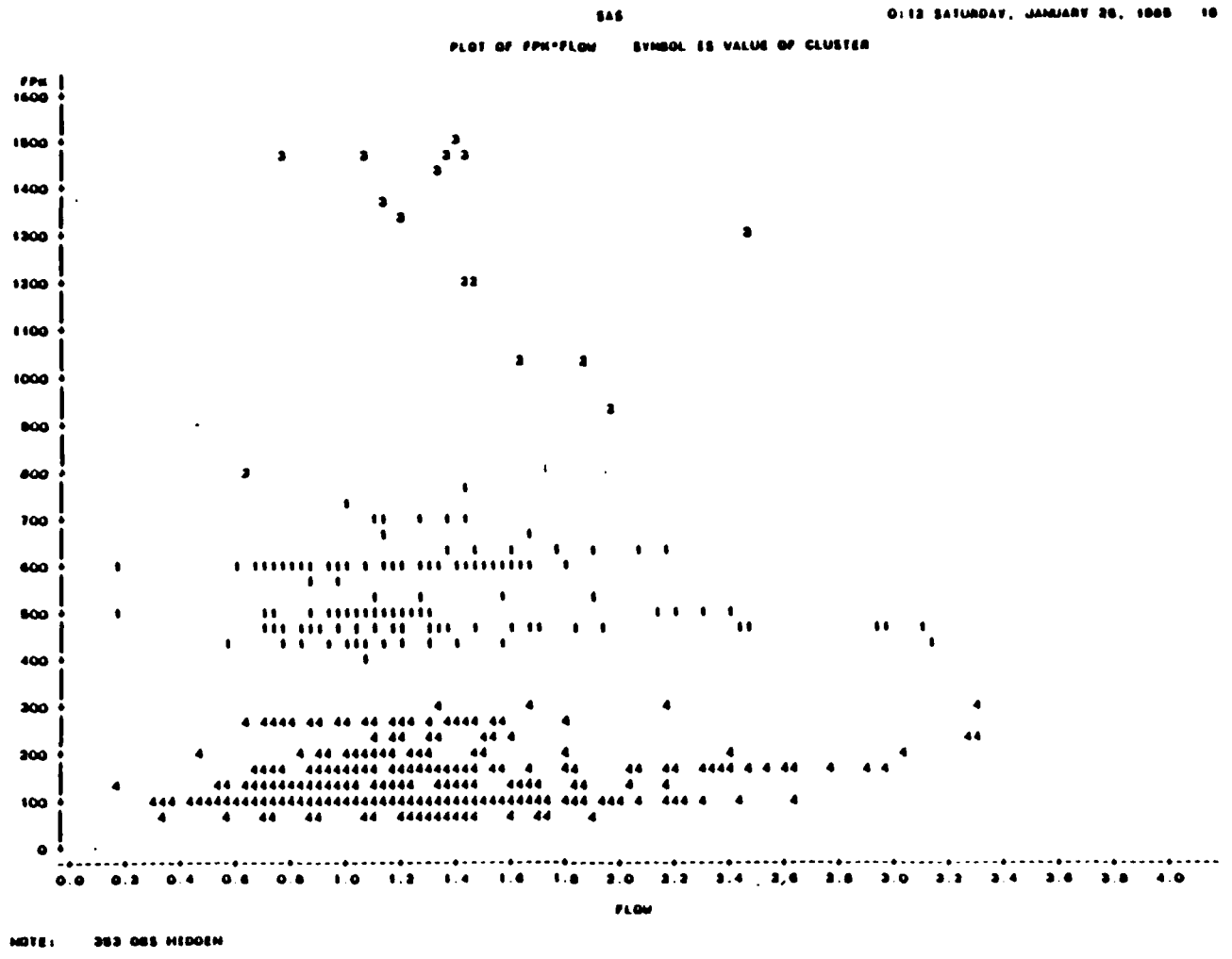

Figure 29. Cluster plot of Case 9, inspiration, with 4 cluster groups (Maxc=4).

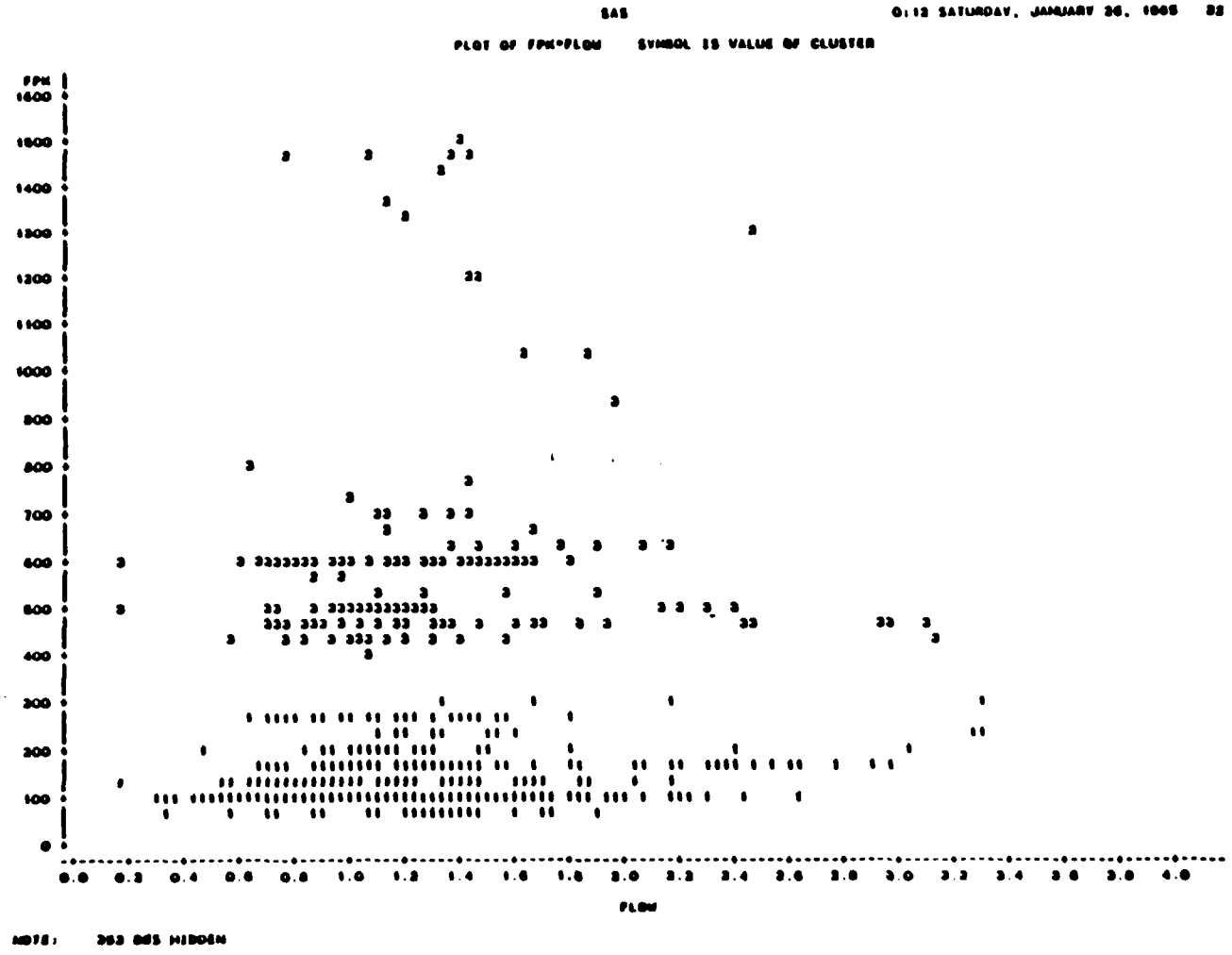

Figure 30. Cluster plot of Case 9, inspiration, with 3 cluster groups (Maxc=3).

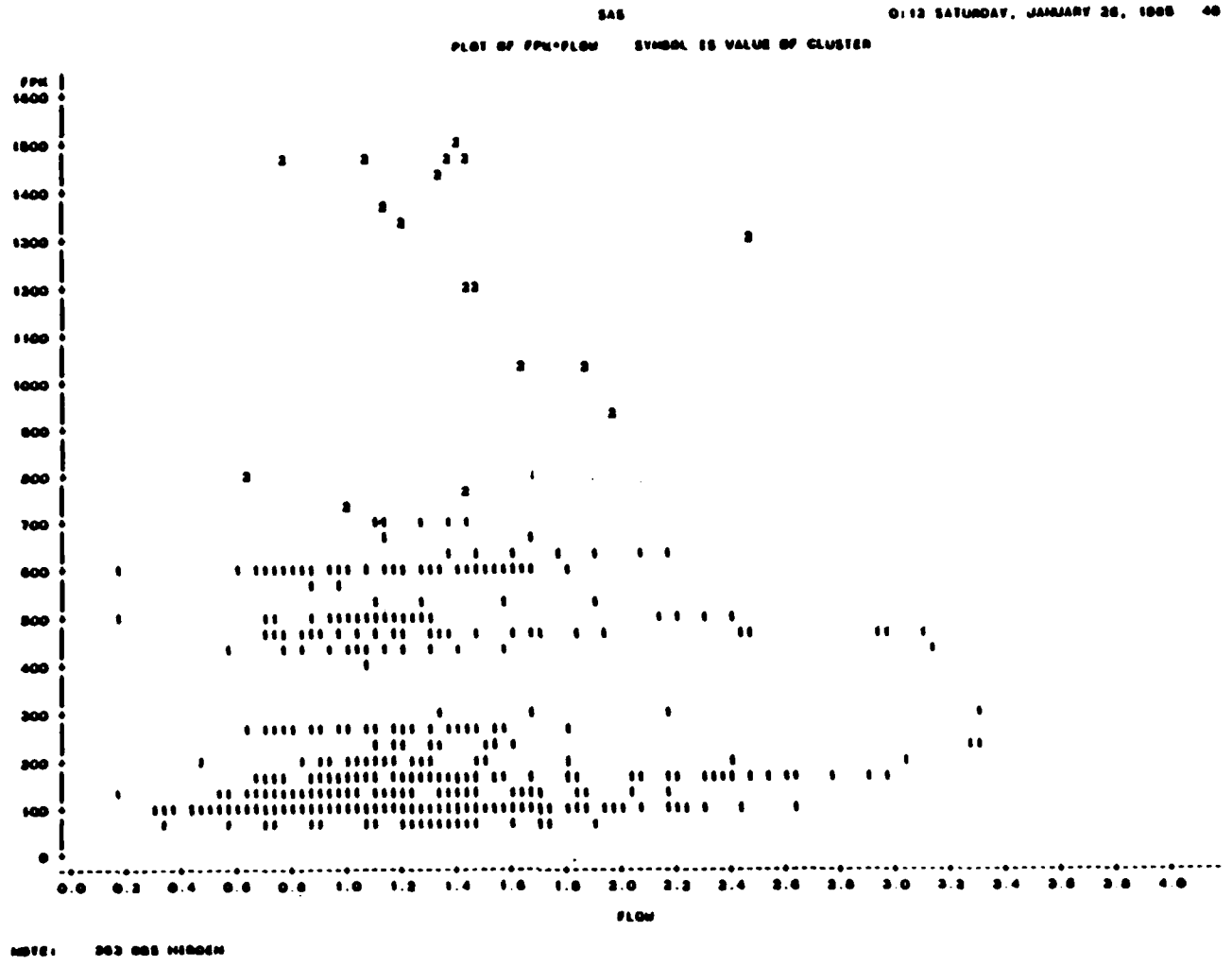

Figure 31. Cluster plot of Case 9, inspiration, with 2 cluster groups (Maxc=2).

Case 10 clusters the data by the variables FMAX and FLOW. Figure 32 shows a plot of FMAX vs. FLOW for a maximum of 4 cluster groups. This plot appears to indicate 3 groups instead of 4. Cluster groups 3 and 4 do not appear to be distinctly separate groups. Figure 33 shows a plot of FMAX vs. FLOW for a maximum of 3 clusters. The plot appears to have 3 separate groups. The boundaries drawn appear to be at FMAX values of 425 and 950. The groups appear to be separate from each other; however, cluster 2 is not a very dense group with some points scattered close to cluster 3. Figure 34 is a plot of 2 cluster groups and as in previous cases cluster group 1 appears to separate into 2 groups. In subsequent cases, results of clustering into 2 groups may be found in Appendix C. In summary, clustering the data by FMAX and FLOW appears to cluster the data into 3 groups. This result agrees with the expiratory data for the same case (FMAX,FLOW) which appear to cluster the data into 3 groups.

The next case discussions are results from clustering the data according to the various combinations of the indices obtained from the power spectra. Cases 11 through 13 correspond to the combinations of 2 indices, and case 14 corresponds to the combination of all 3 indices. Case 11 clusters the data by the indices MPF and FPK. Figure 35 is a cluster plot of the data into 4 cluster groups. The data appear to be grouped into 4 clusters with boundaries between the clusters as follows:

Cluster 1	100	MPF	425	20	FPK	310
Cluster 2	625	MPF	1200	920	FPK	1500
Cluster 3	275	MPF	830	430	FPK	810
Cluster 4	475	MPF	1200	80	FPK	420

Figure 36 is the plot resulting from trying cluster into 3 groups. This plot agrees with Figure 35 in that the data appear to be grouped into 4 cluster groups as opposed to 3 cluster groups. Cluster 2 appears to be 2 separate groups instead of 1 cluster group. Clustering the data according to MPF and FPK, therefore, appears to cluster the data into 4 groups. Cluster 1 (Fig. 35) or cluster 3 (Fig. 36) appear to be the denser cluster groups. In Case 12 the data is clustered by the indices MPF and FMAX. Figure 37 is a plot of MPF and FMAX for 4 cluster groups. Cluster 1 is not a dense cluster group. There appears to be a zone between cluster groups 1 and 3 in which there are data points assigned to either cluster group, signifying that there is not a distinct boundary between these groups. Also, clusters 2 and 4 are not well defined or distinguished from each other. Figure 38 is clustering by the variables MPF vs. FMAX into 3 groups. Cluster group 2 appears to be a separate group from cluster groups 1 and 3. Cluster group 1 is not as dense a group as cluster group 2. The boundaries between the cluster group appear to be as follows:

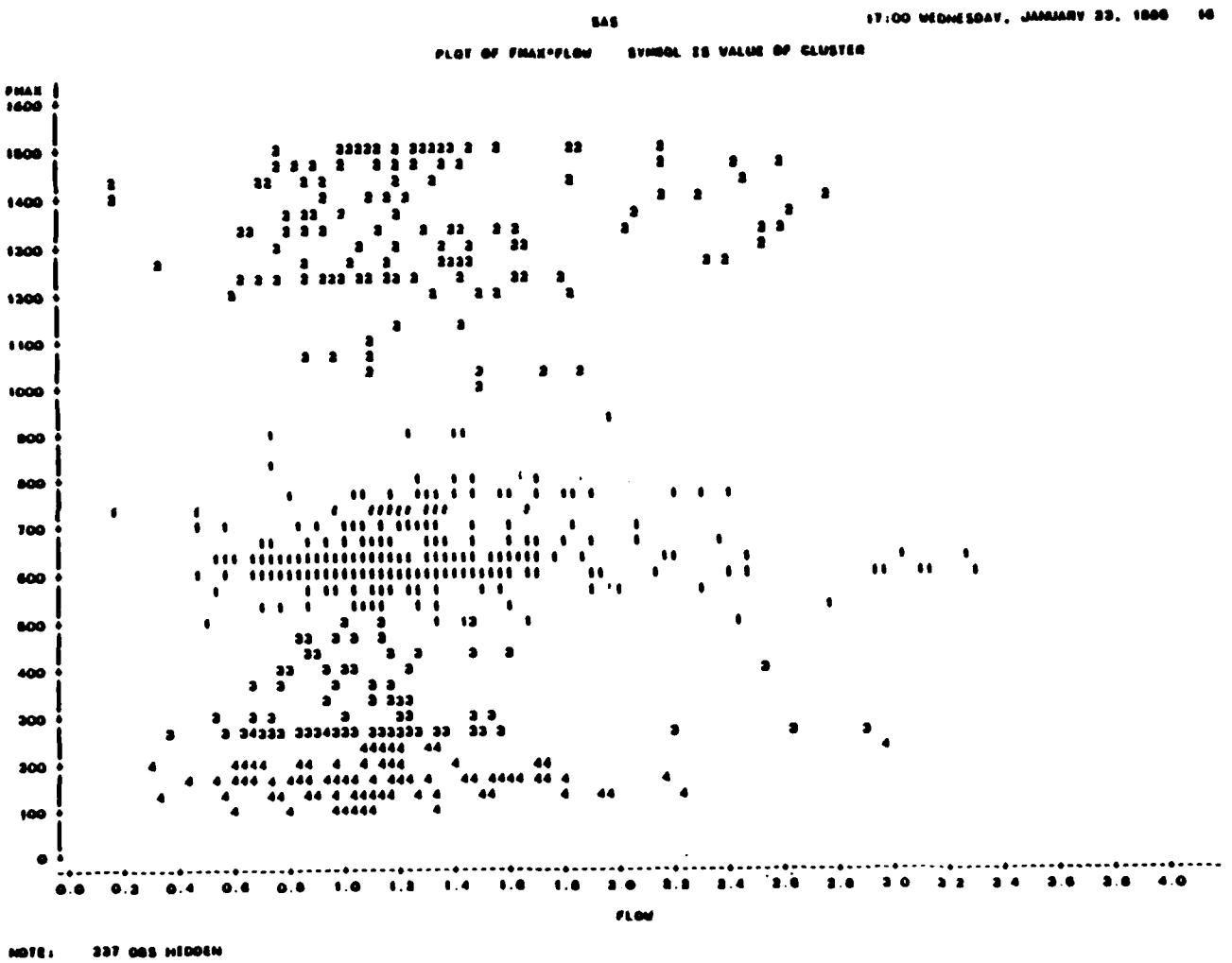

Figure 32. Cluster plot of Case 10, inspiration, with 4 cluster groups (Maxc=4).

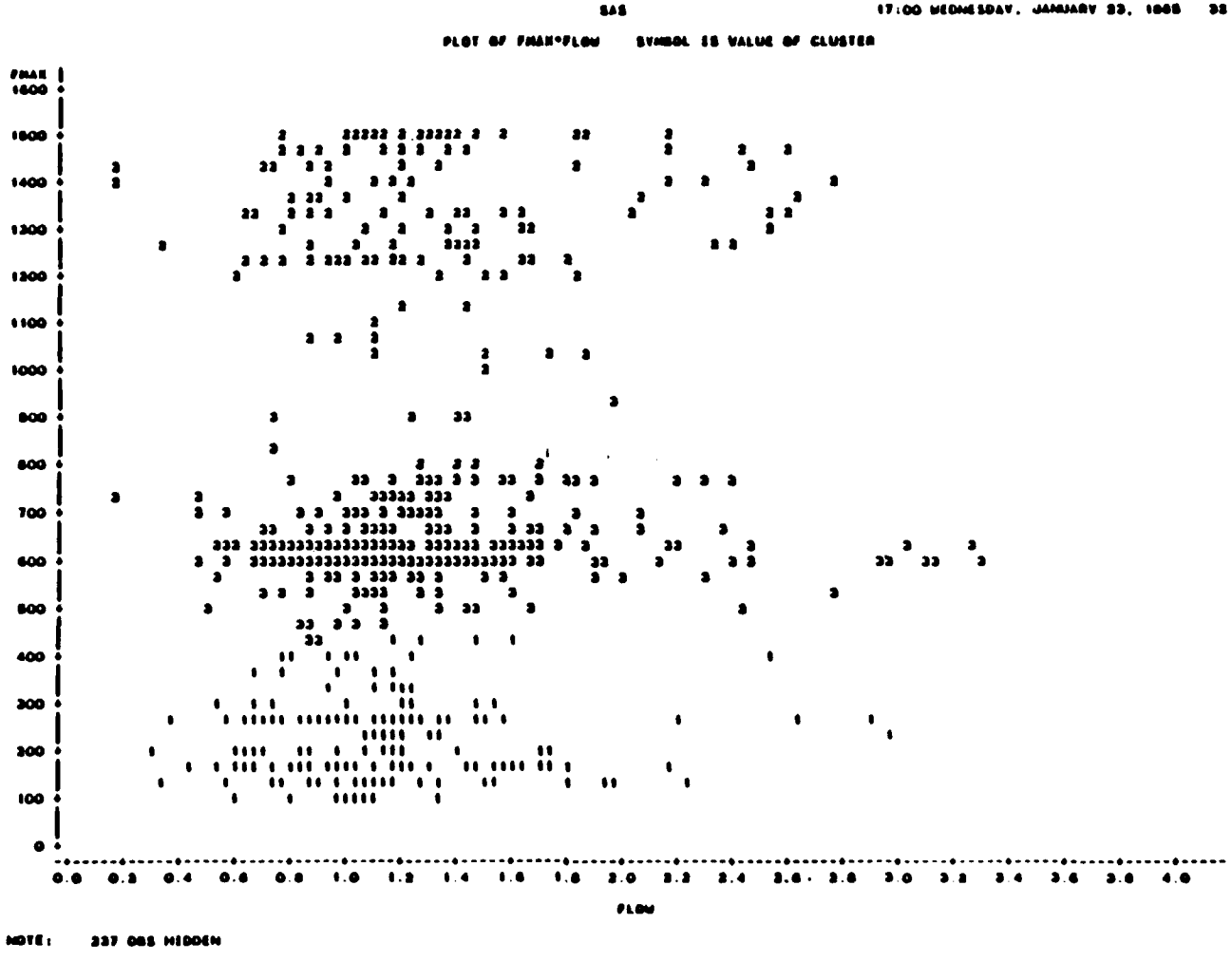

Figure 33. Cluster plot of Case 10, inspiration, with 3 cluster groups (Maxc=3).

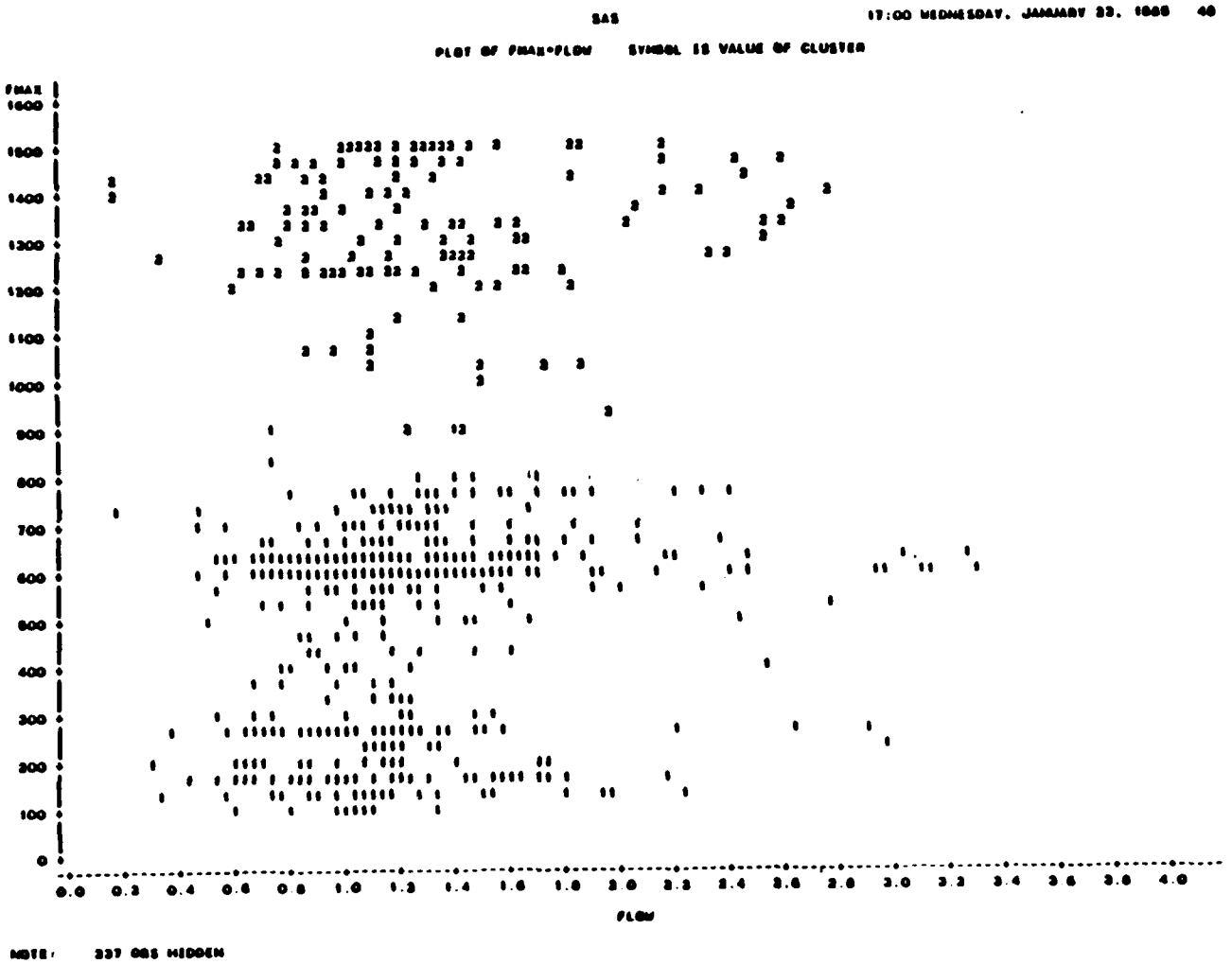

Figure 34. Cluster plot of Case 10, inspiration, with 2 cluster groups (Maxc=2).

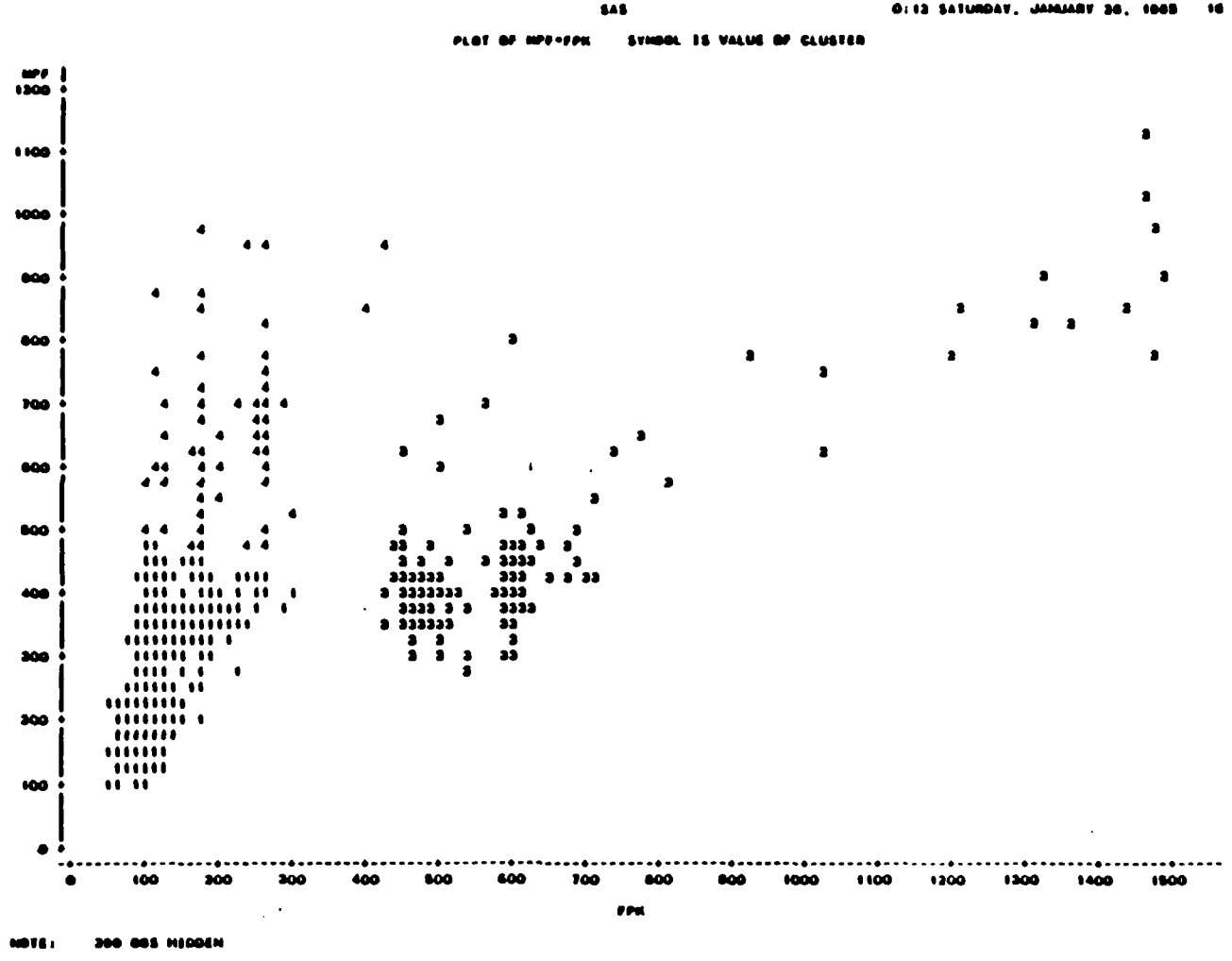

Figure 35. Cluster plot of Case 11, inspiration, with 4 cluster groups (Maxc=4).

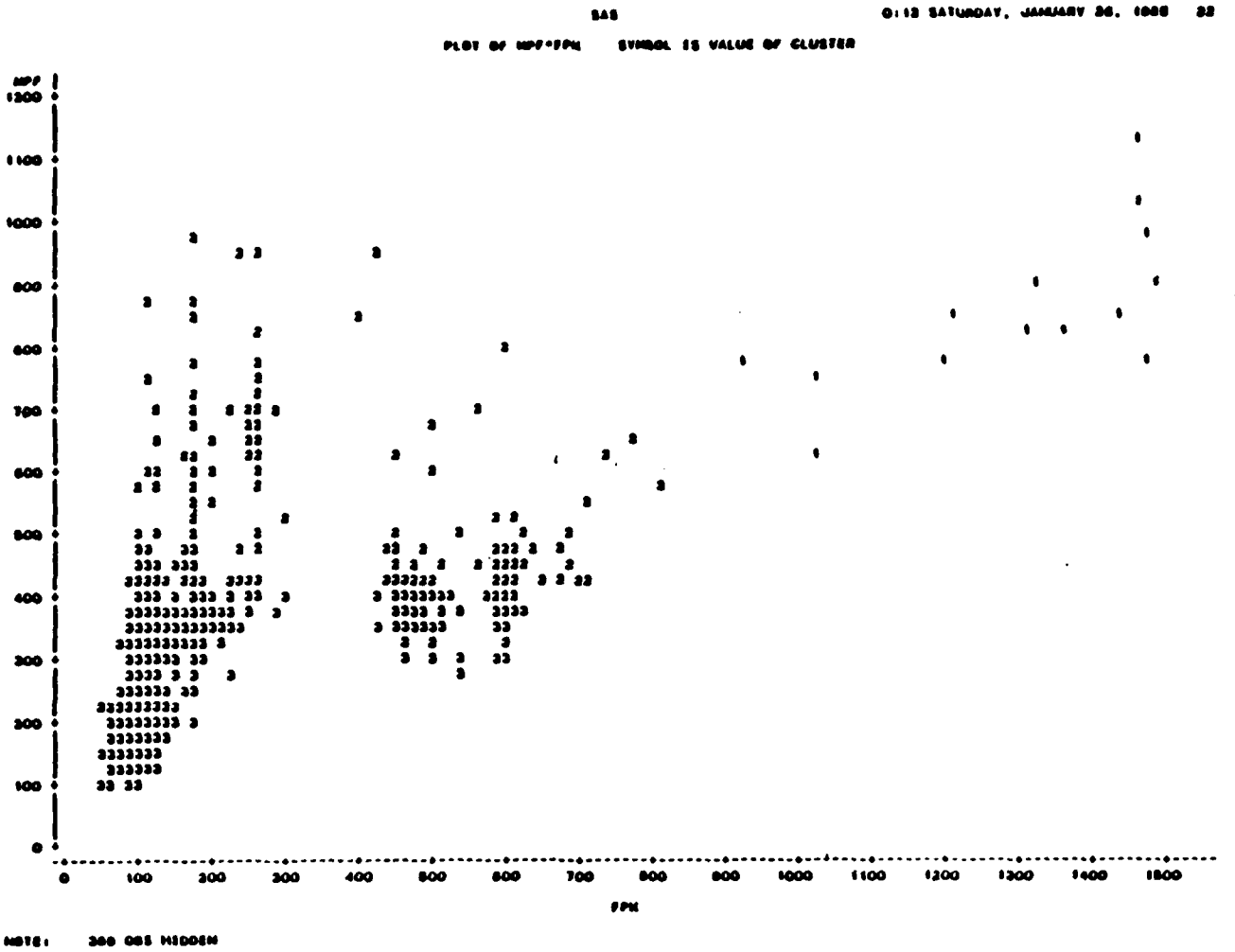

Figure 36. Cluster plot of Case 11, inspiration, with 3 cluster groups (Maxc=3).

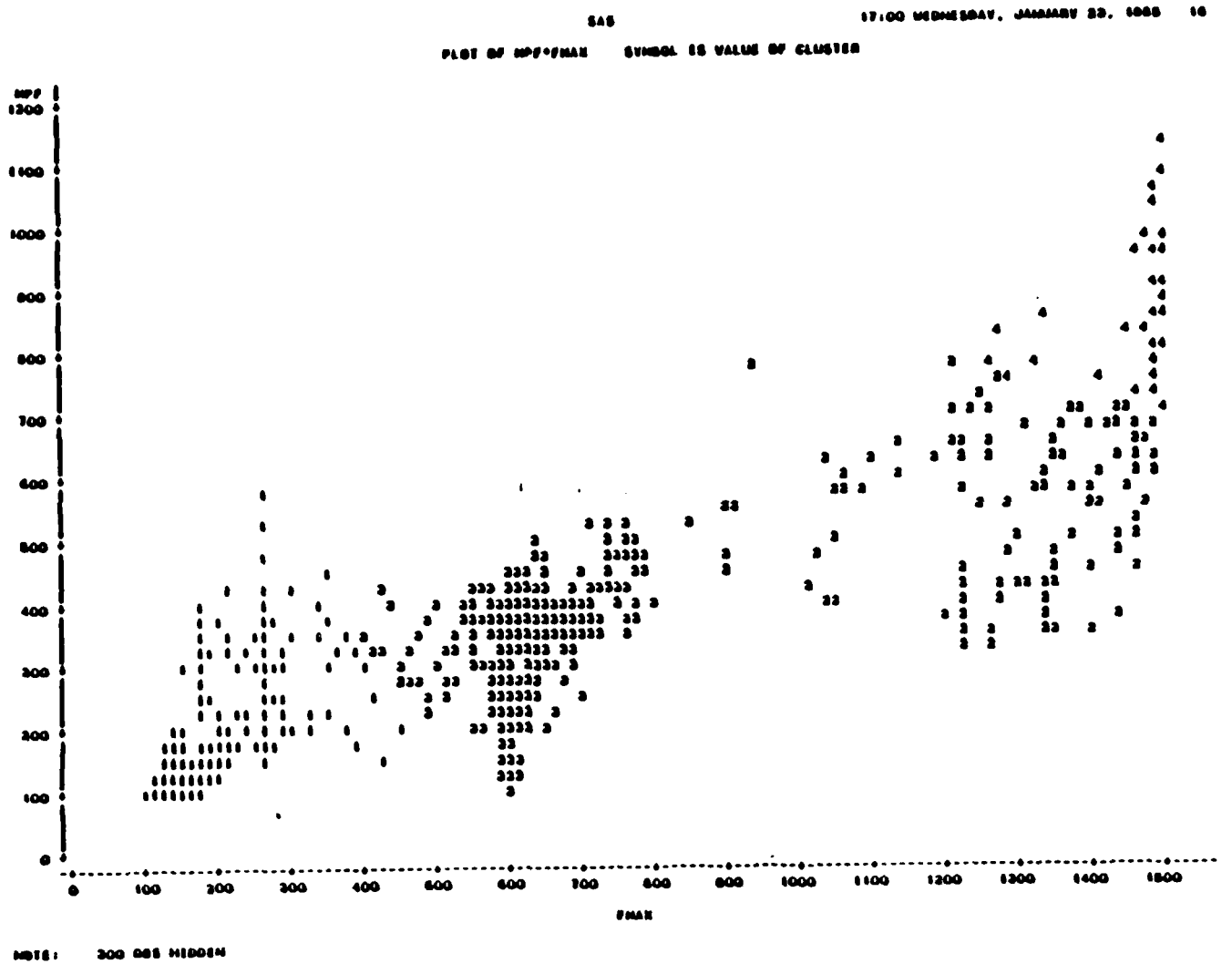

Figure 37. Cluster plot of Case 12, inspiration, with 4 cluster groups (Maxc=4).

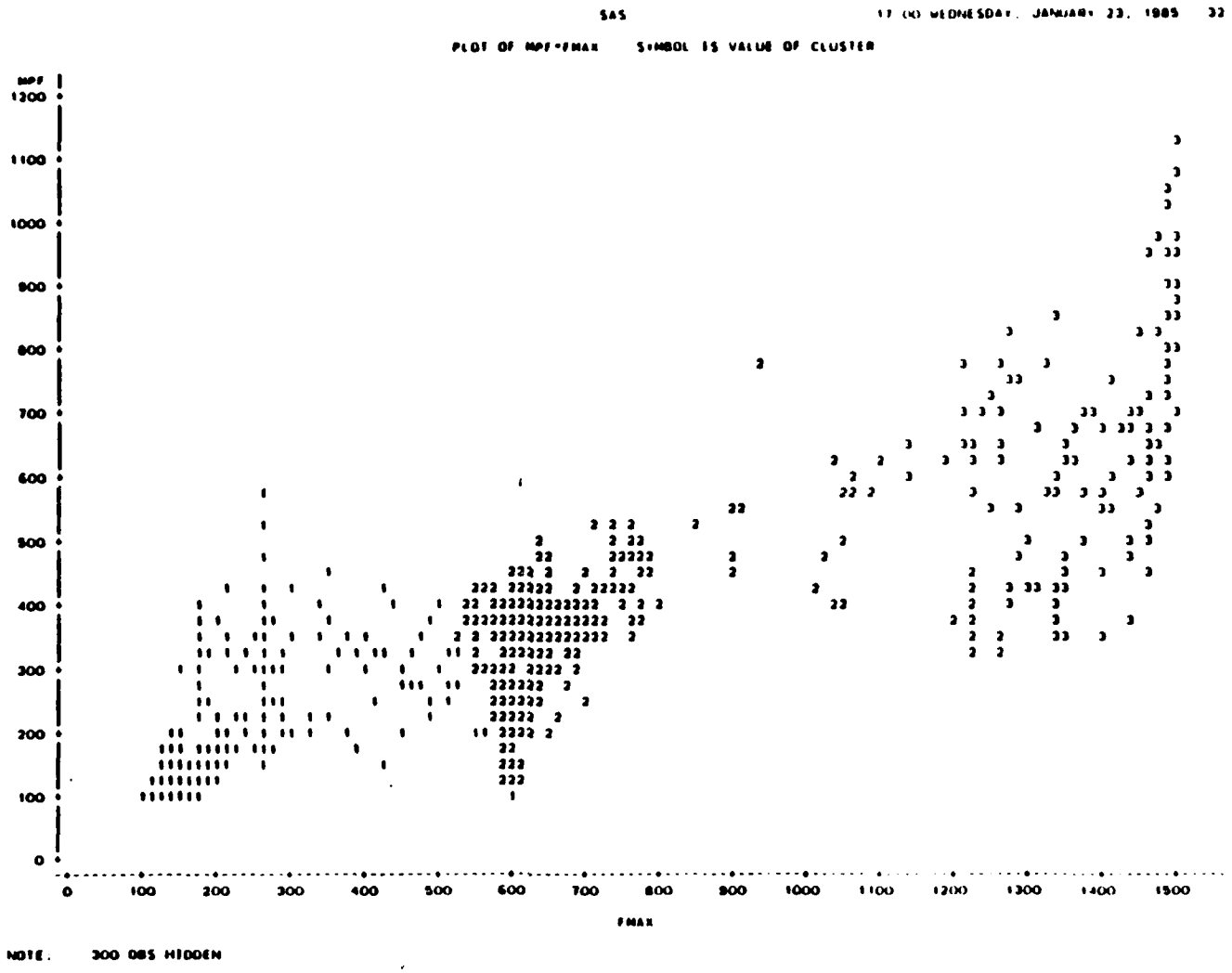

Figure 38. Cluster plot of Case 12, inspiration, with 3 cluster groups (Maxc=3).

Cluster 1	100	MPF	575	100	FMAX	600
Cluster 2	125	MPF	775	625	FMAX	1263
Cluster 3	350	MPF	1125	1138	FMAX	1500

In summary, clustering the data according to the indices MPF and FMAX appears to cluster the data into 3 groups.

Case 13 clusters the data by the indices FPK and FMAX. Figure 39 is a plot of FPK vs. FMAX into 4 groups. This plot does not appear to show 4 distinguishable clusters. Cluster groups 1 and 4 appear to be separate groups; however, cluster group 1 has a dispersion of points in cluster groups 4 and 2. Cluster group 2 appears to be a separate group, but Cluster group 3 does not show a distinct grouping. Figure 40 is a plot of FPK vs. FMAX into 3 cluster groups. This plot does not clear up the picture in any way. The previous cluster groups 1 and 4 are now grouped into cluster group 3. This grouping does not appear to give an accurate representation of the clustering of the data.

In summary, clustering the data by the indices FPK and FMAX does not give a clear distinction of cluster groups in any of the plots. This grouping does not agree with the expiratory data for the same case, which tended to cluster the data into 4 groups.

The previous cases studied are not consistent. Some combinations appear to show 3 clusters; others appear to show 4 clusters, and some do not reveal any distinct clusters at all. The next case, Case 14, is an attempt to give a clearer indication of the relationship between the three indices of the power spectra (MPF vs. FPK vs. FMAX) by a three-dimensional cluster plot.

The inspiratory three-dimensional plots of Case 14 are analyzed in the same fashion as the expiratory plots of Case 7. The same angles are used for the plots and a boundary is drawn around the normal subjects of Wong's study. The individual plots of normal subjects and USAF data are found in Appendix D.

In Figure 41, we noted a similar pattern to the expiratory plot. The normal subjects appear to veer out at an angle and the other data points follow a more vertical line. There is some overlapping of points as in Figure 24.

Figure 42 does not appear to show any distinct groups. This pattern is similar to the pattern in Figure 25. Observing the data from the viewing angle of 5° in Figure 43 appears to give the same conclusion as Figure 26. The normal data is clustered centrally and there appears to be 2 groups of data outside the normal boundary. The viewing angles of 85° and 5° appear to be better angles than 45°. From these 2 angles, the appearance of clusters seems to be forming. The viewing angle of 5° in both Case 7 and Case 14 shows a distinct group at a higher maximum frequency than the normal subjects.

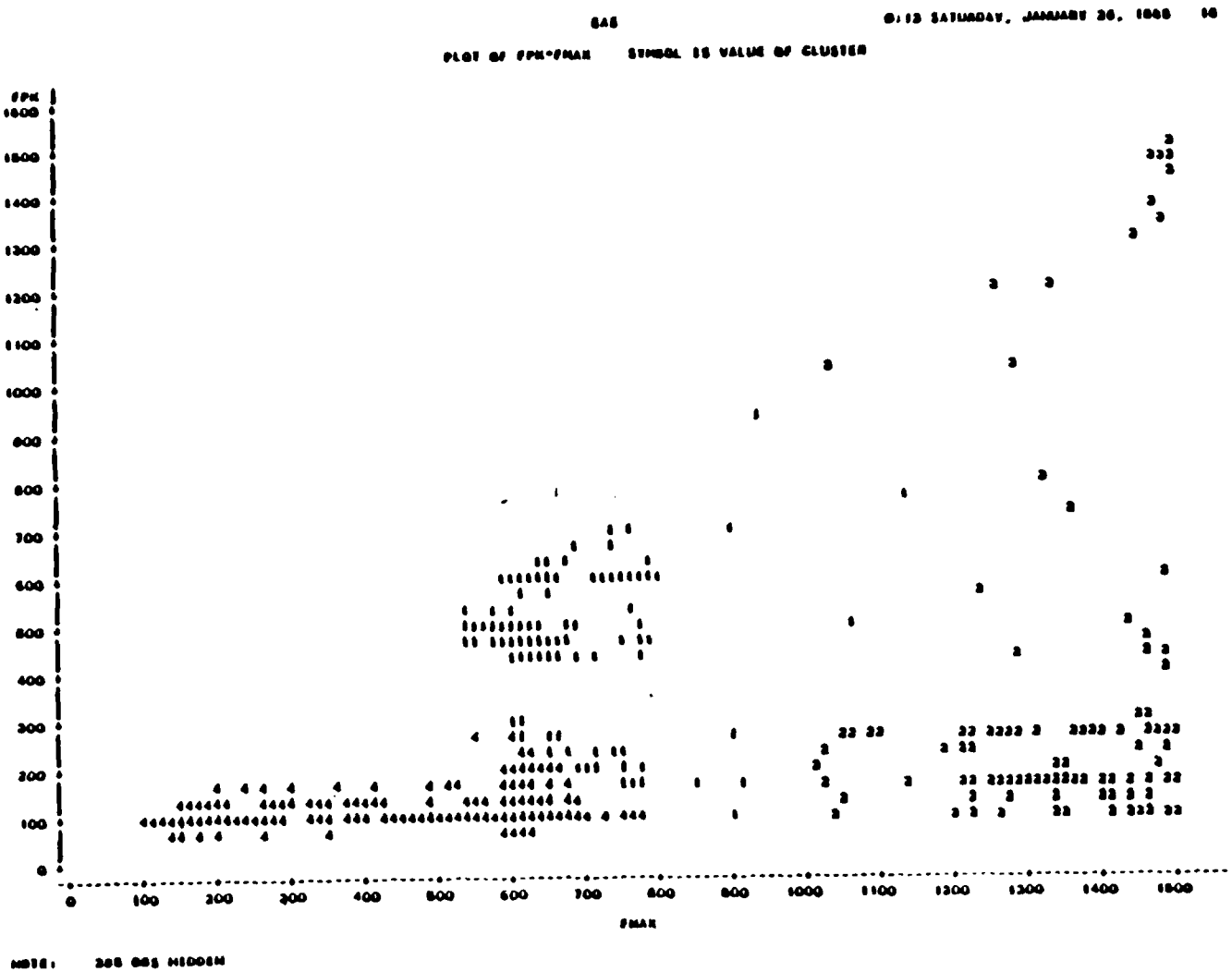

Figure 39. Cluster plot of Case 13, inspiration, with 4 cluster groups (Maxc=4).

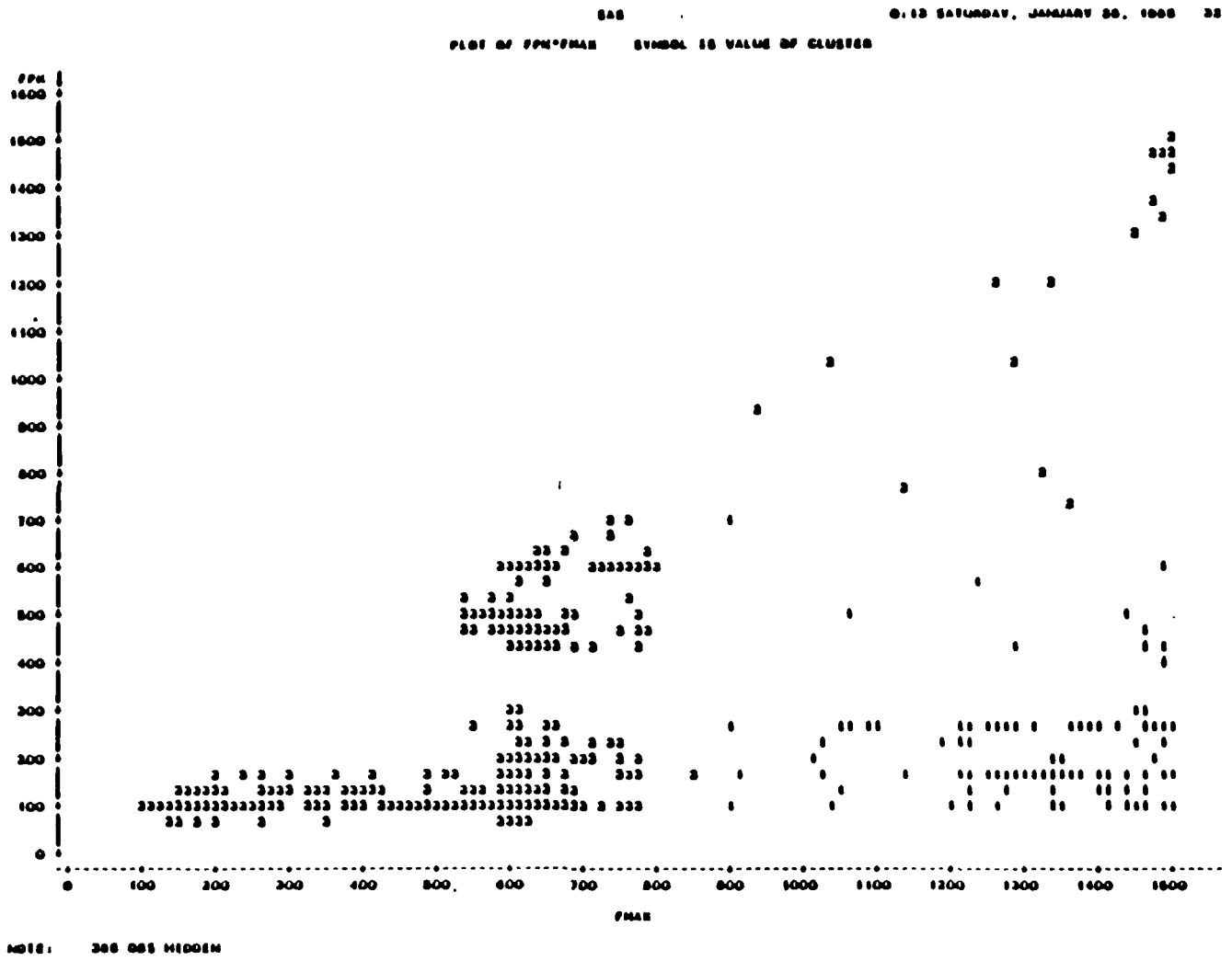

Figure 40. Cluster plot of Case 13, inspiration, with 3 cluster groups (Maxc=3).

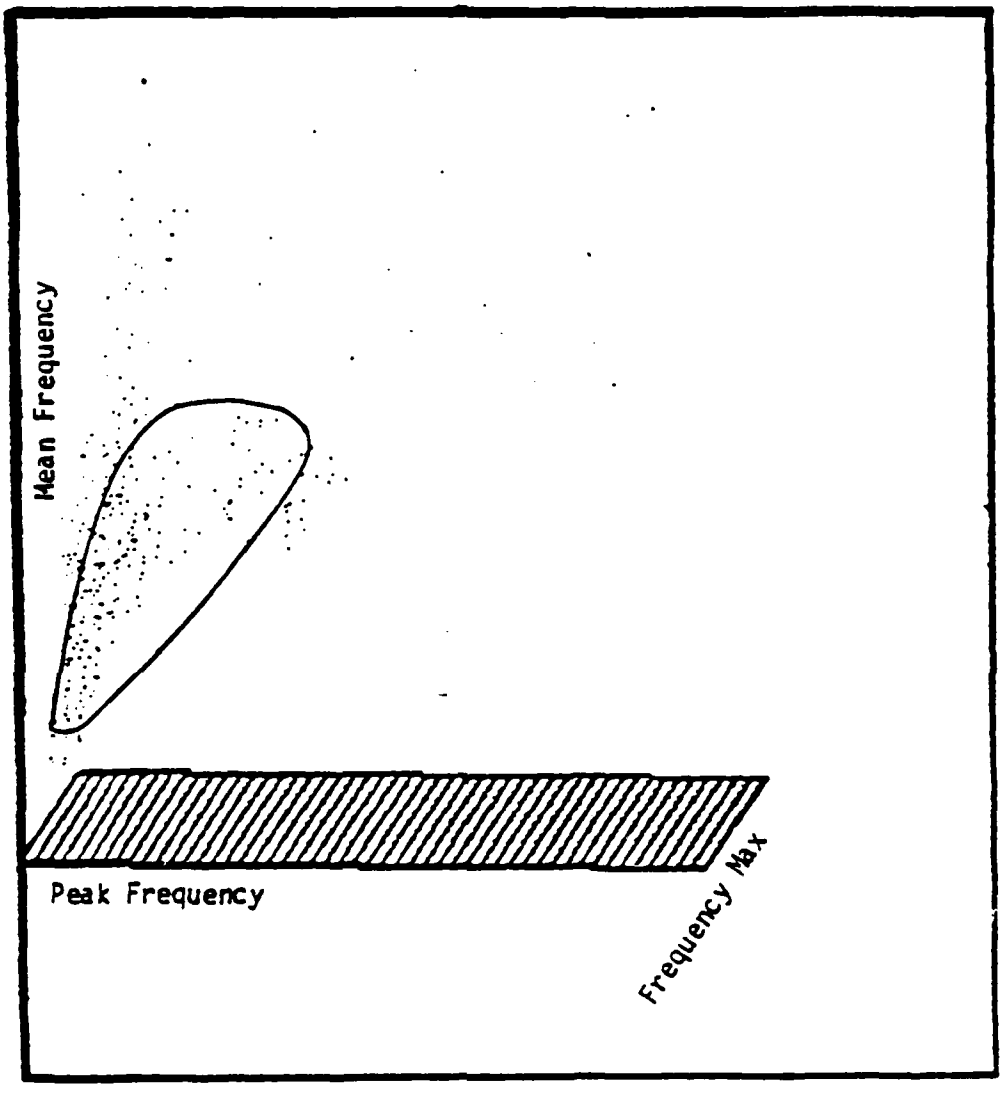

Figure 41. 3-D plot of Case 14, inspiration, rotation = 85° and tilt = 5°.

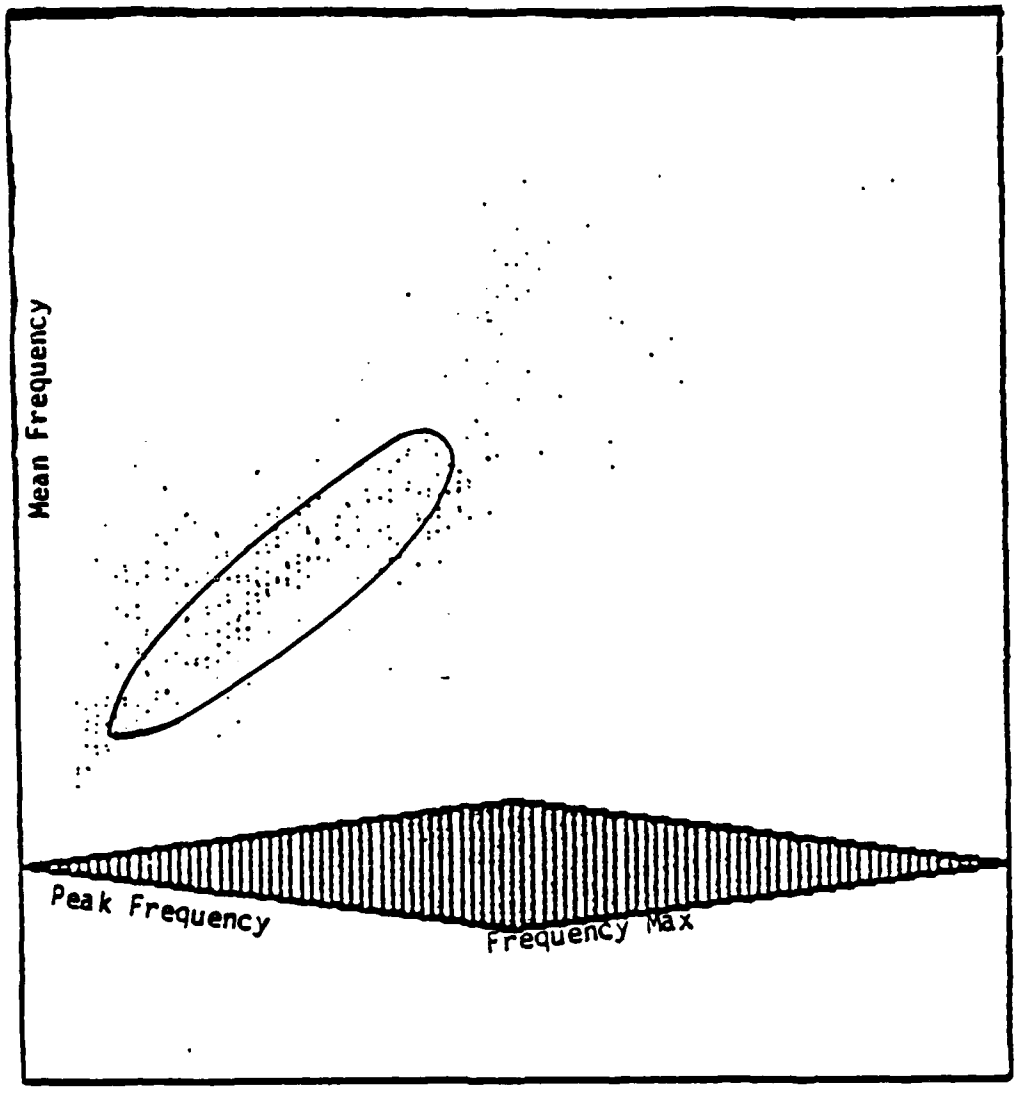

Figure 42. 3-D plot of Case 14, inspiration, rotation = 45° and tilt = 5°.

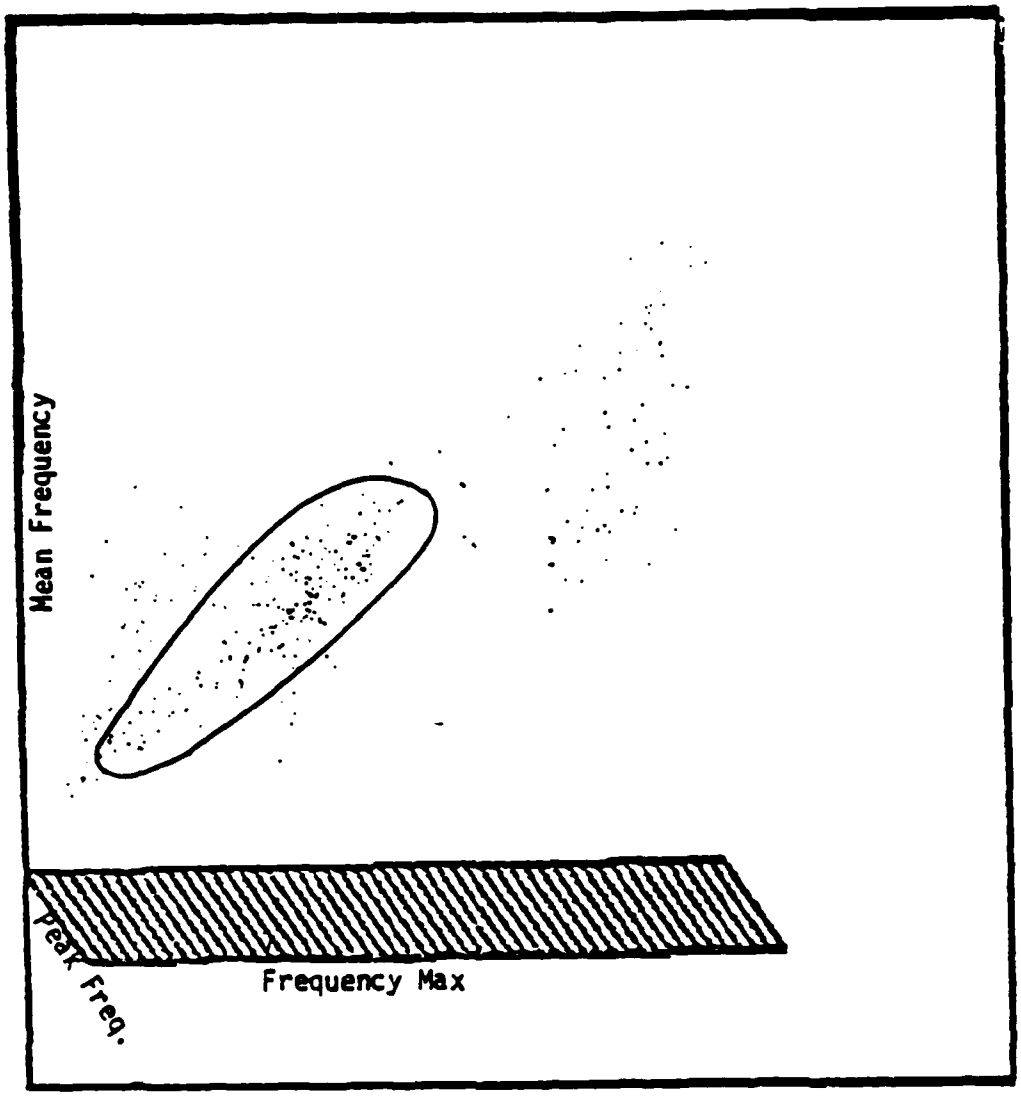

Figure 43. 3-D plot of Case 14, inspiration, rotation = 5° and tilt = 5°.

CONCLUSIONS

The objective of this study was to determine whether respiratory sound data of normal volunteers and pulmonary insufficiency subjects reveals groupings or clusters of the data. Cases 1 through 6 of the expiratory data, and Cases 8 through 13 of the inspiratory data, dealt with 1 or 2 parameters of the power spectra. The plots appear to indicate that the data may be clustered into 3 or 4 groups but not necessarily agreeing in the number of cluster groups for the same variables during expiration and inspiration.

The three-dimensional plots appeared to give a clearer picture of the situation. The viewing angles of 85° and 5° with a 5° table angle appeared to show 3 possible cluster groups from the data.

RECOMMENDATIONS

A recommendation is made to perform a discriminant analysis of the data to establish whether the clustering that appears in the three-dimensional plots actually represents distinct populations.

The power spectra plots revealed the appearance of a bimodal distribution that was not evident from the normal subjects of Wong's study. This may be a very important finding that should be taken into account in the future studies. A recommendation is made to study a better method of calculating the power spectra of such a distribution, and to repeat the study in the three-dimensional realm and compare the results.

According to the paper by Grassi et al. [19], the ratio of the inspiratory and expiratory sound intensity was used as an index. A recommendation is made to repeat the study and collect sequential samples of expiratory and inspiratory respiratory sounds, calculate the ratio of the power spectra parameters, and compare the ratio and the combination of the 3 parameters of the power spectra as estimators for discrimination between normal and pulmonary insufficiency patients.

REFERENCES

1. Bates, B. *A Guide to Physical Examination*. J. B. Lippincott Co. Philadelphia, 128,1979.

2. Bullar, J. P. Experiments to determine the origin of respiratory sound. *Proc. Roy. Soc. London* 37:411-426(1884).

3. Bunin, N. and R. Loudon. Lung sound terminology in case reports. *Chest* 76:690-692(1979).

4. Bushnell, G. E. The mode of production of the so-called vesicular murmur of respiration. *JAMA* 77:2104-2106(1921).

5. Cabot, R. C. and H. F. Dodge. Frequency characteristics of heart and lung sounds. *JAMA* 84:1793-1795(1925).

6. Charbonneau, G., J. L. Racineux, M. Sudraud,and E. Tukchais. An accurate recording system and its use in breath sounds spectral analysis. *J. Appl. Physiol.* 55:1120-1127(1983).

7. Chowdhury, S. K. and A. K. Majumder. Digital spectrum analysis of respiratory sound. *IEEE Trans. Biomed. Eng.* 28:784-788(1981).

8. Dekker, E. The transition between laminar and turbulent flow in the trachea. *J. Appl. Physiol.* 16:1060(1961).

9. Dosani, R. and S. S. Kraman. Lung sound intensity variability in normal man. *Chest* 84:628-631(1983).

10. Druzgalski, C. Breath sounds in pulmonary diagnosis. *IEEE Frontiers of Eng. in Health Care* 383-385(1981).

11. Ertel, P. Y., M. Lawrence, R. K. Brown, and A. M. Stern. Stethoscope acoustics. *Circulation* 33:889(1966).

12. Fahr, G. The acoustics of the bronchial breath sounds. *Arch. Int. Med.* 39:286-302(1927).

13. Fletcher, H. and W. Munson. Loudness, its definition, measurement and calculation. *J. Acoust. Soc. Amer.* 5:82-108(1933).

14. Forgacs, P., A. R. Nathoo, and H. D. Richardson. Breath sounds. *Thorax* 26:288-295(1971).

15. Forgacs, Paul. The functional significance of clinical signs in diffuse airway obstruction. *Brit. J. Dis. Chest* 65:170(1971).

16. Forgacs, Paul. *Lung Sounds*. p.56, Balliere Tindall, London, 1978.

17. Grassi, C., G. Marinone, G. C. Morandini, A. Pernice, and M. Puglis. Normal and pathological respiratory sounds analyzed by means of a new phonopneumographic apparatus. *Respiration* 33:315-324(1976).

18. Gavriely, N., Y. Palti, and G. Alroy. Spectral characteristics of normal breath sounds. *J. Appl. Physiol.* 50:307-314(1981).

19. Guyton, A. C. *Textbook of Medical Physiology*. Sixth Edition, W.B. Saunders Co., Philadelphia, 1981.

20. Hardin, J. C. and J. L. Patterson. Monitoring the state of the human airways by analysis of respiratory sound. *Acta Astronautica* 6:1137-1151(1979).

21. Jaeger, M. J. and H. Matthys. *Airways Dynamics*. Thomas, Springfield, IL, 1970.

22. Laennec, R. T. H. *A Treatise On The Disease Of The Chest And Mediate Auscultation*. Translated from the French edition by John Forbes. Samuel Wood and Sons, New York, 1935.

23. Leblanc, P. Breath sounds and distribution of pulmonary ventilation. *Am. Rev. Resp. Dis.* 102:10-16(1970).

24. Martini, P. and H. Muller. Studies on bronchial breathing. *Deutsche. Arch. F. Klin. Med.* 143:159-173(1923).

25. McKusick, V., J. T. Jenkins, and G. N. Webb. The acoustic basis of the chest examination. *Am. Rev. Tuberc.* 72:12-34(1955).

26. Morris, S. The advent and development of the binaural stethoscope. *Practitioner* 199:674(1967).

27. Murphy, R. Human factors in chest ausculations. *Human Factors in Health Care*. D. C. Heath and Co., Lexington, MA., 1975.

28. Murphy, R. Ausculations of the lung: past lessons, future possibilities. *Thorax* 36:99-107(1981).

29. Nath, A. R. and L. H. Capel. Inspiratory crackles - early and late. *Thorax* 29:223(1974).

30. O'Donnell, D. M. and S. S. Kraman. Vesicular lung sound amplitude mapping by automated flow-gated phonopneumography. *J. Appl. Physiol.* 53:603-609(1982).

31. Ploysongsang, Y., R. R. Martin, and W. R. D. Ross. Breath sounds and regional ventilation. *Am. Rev. Resp. Dis.* 116:187-199(1978).

32. Ploysongsang, Y., P. T. Macklem, and W. R. D. Ross. Distribution of regional ventilation measured by breath sounds. *Am. Rev. Resp. Dis.* 117:657-664(1978).

33. Schroter, R. C. and M. F. Sudlow. Flow patterns in models of the human bronchial airways. *Resp. Physiol.* 7:341(1969).

34. Stanley, W. D. *Digital Signal Processing*. pp. 279-280, Reston Publishing Co., Reston, VA,1975.

35. West, J .B. and P. Hugh-Jones. Patterns of gas flow in the upper bronchial tree. *J. Appl. Physiol.* 14:753-759(1959).

36. Wong, W. C. A Thesis. Correlation of Respiration Flow Rate with Frequency Spectrum of Respiratory Sound at Trachea of Normal Young Adults. Texas A & M University, College Station; 1984.

APPENDIX A

PLOTS OF TEN CLUSTER GROUPS

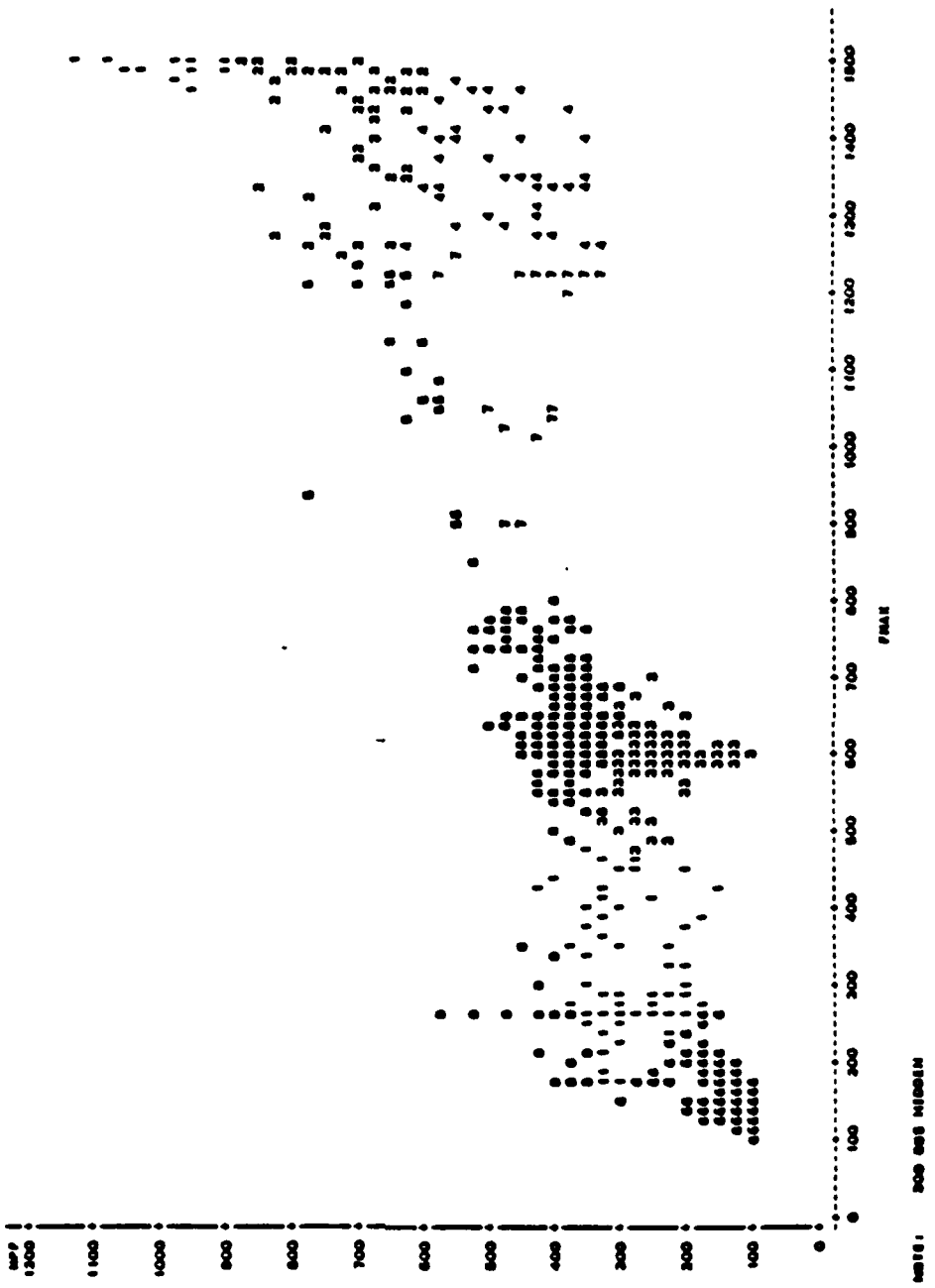
SAS
PLOT OF DEP*FRAN SYMBOL IS VALUE OF CLUSTER
DEP
FRAN

PLOT OF FPK*FMAX SYMBOL IS VALUE OF CLUSTER

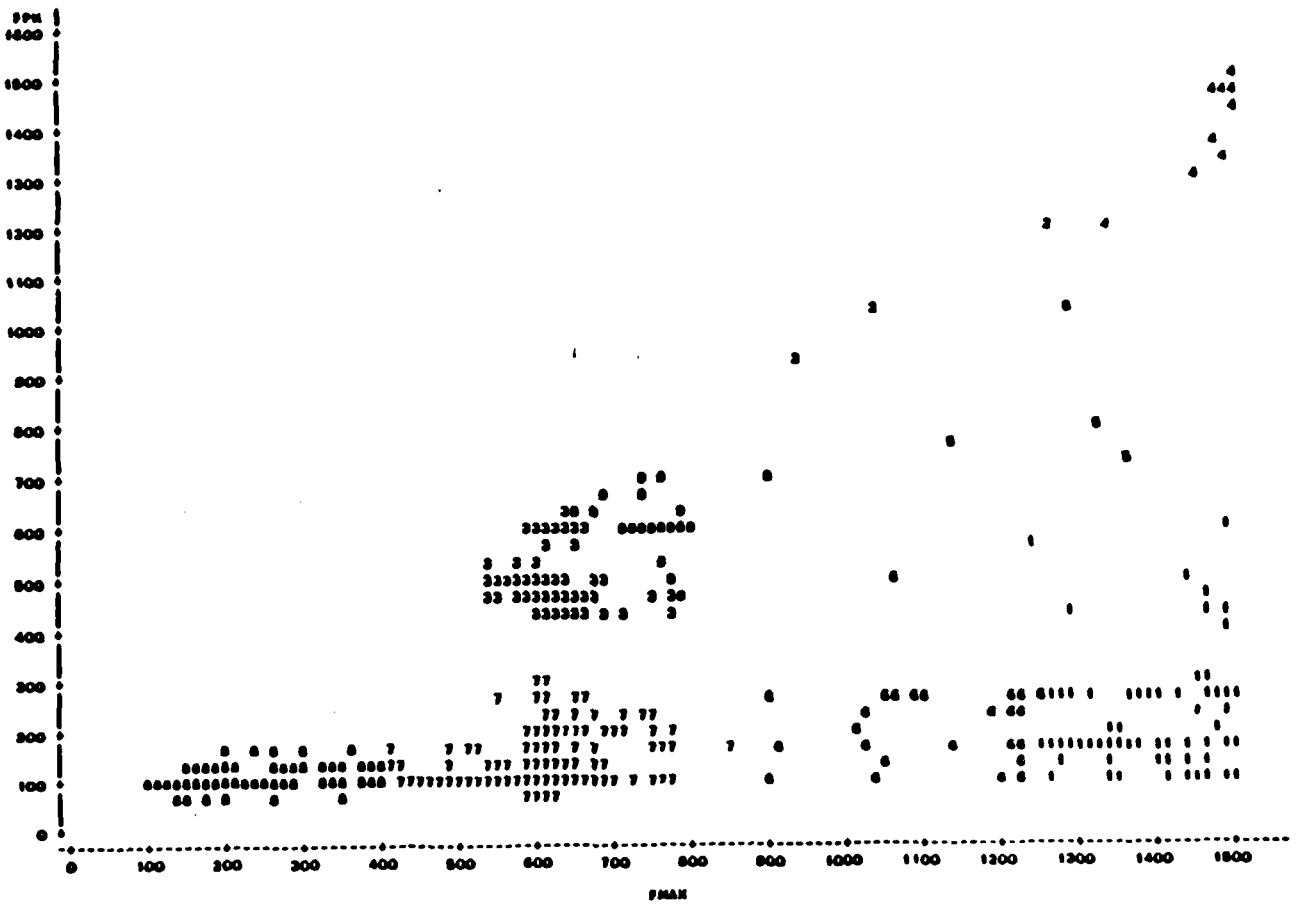

NOTE: 368 OBS HIDDEN

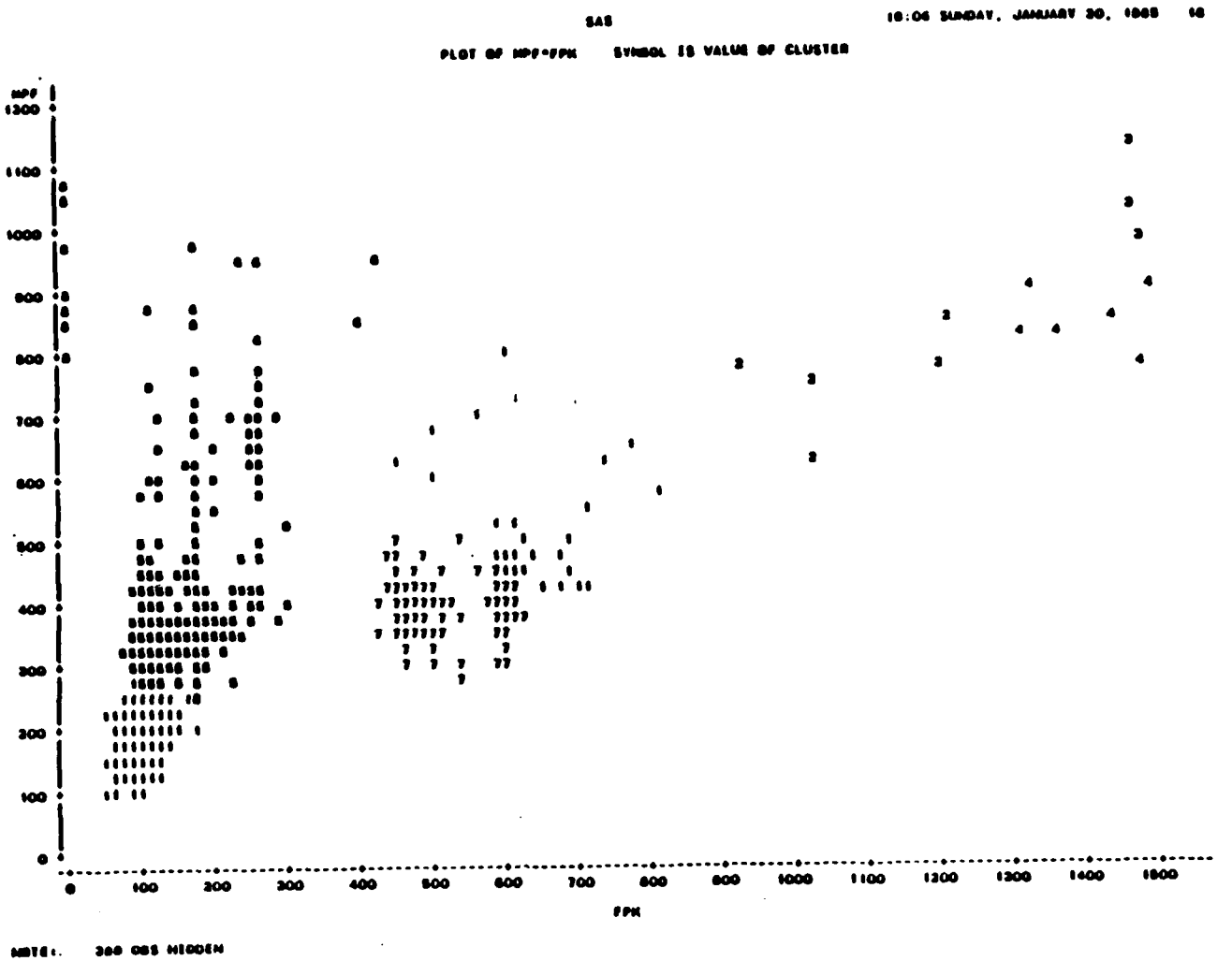
SAS
16:06 SUNDAY, JANUARY 30, 1983 16
PLOT OF MPG*FPK SYMBOL IS VALUE OF CLUSTER
MPG
1200
1100
1000
900
800
700
600
500
400
300
200
100
0
0 100 200 300 400 500 600 700 800 900 1000 1100 1200 1300 1400 1500
FPK
NOTE: 388 OBS HIDDEN

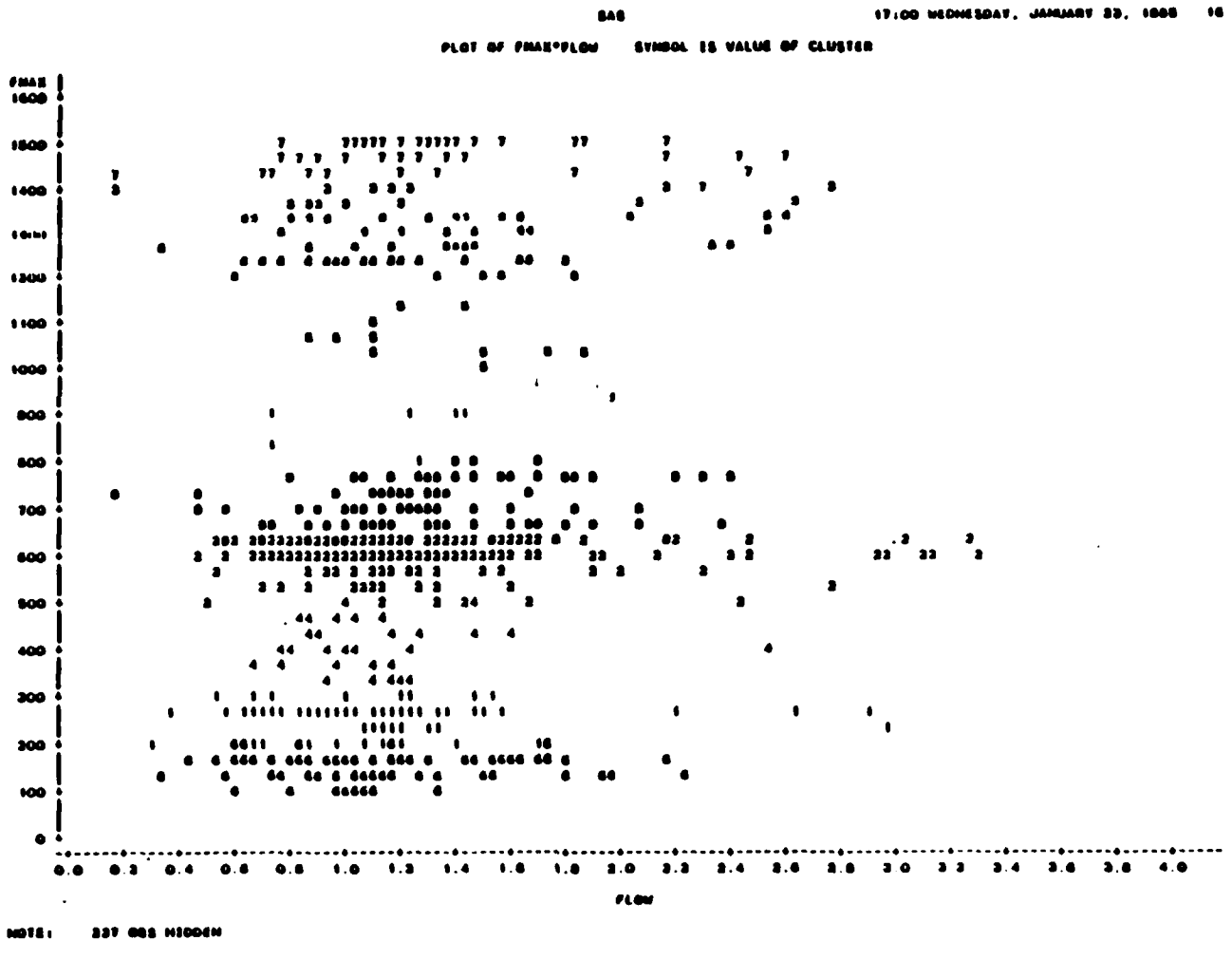
SAS 17:00 WEDNESDAY, JANUARY 23, 1985 16
PLOT OF PMAX*FLOW SYMBOL IS VALUE OF CLUSTER
PMAX
1600
1500
1400
1300
1200
1100
1000
900
800
700
600
500
400
300
200
100
0
0.0 0.2 0.4 0.6 0.8 1.0 1.2 1.4 1.6 1.8 2.0 2.2 2.4 2.6 2.8 3.0 3.2 3.4 3.6 3.8 4.0
FLOW
NOTE: 337 OBS HIDDEN

SAS 0:12 SATURDAY, JANUARY 28, 1989 16

PLOT OF FPM*FLOW SYMBOL IS VALUE OF CLUSTER

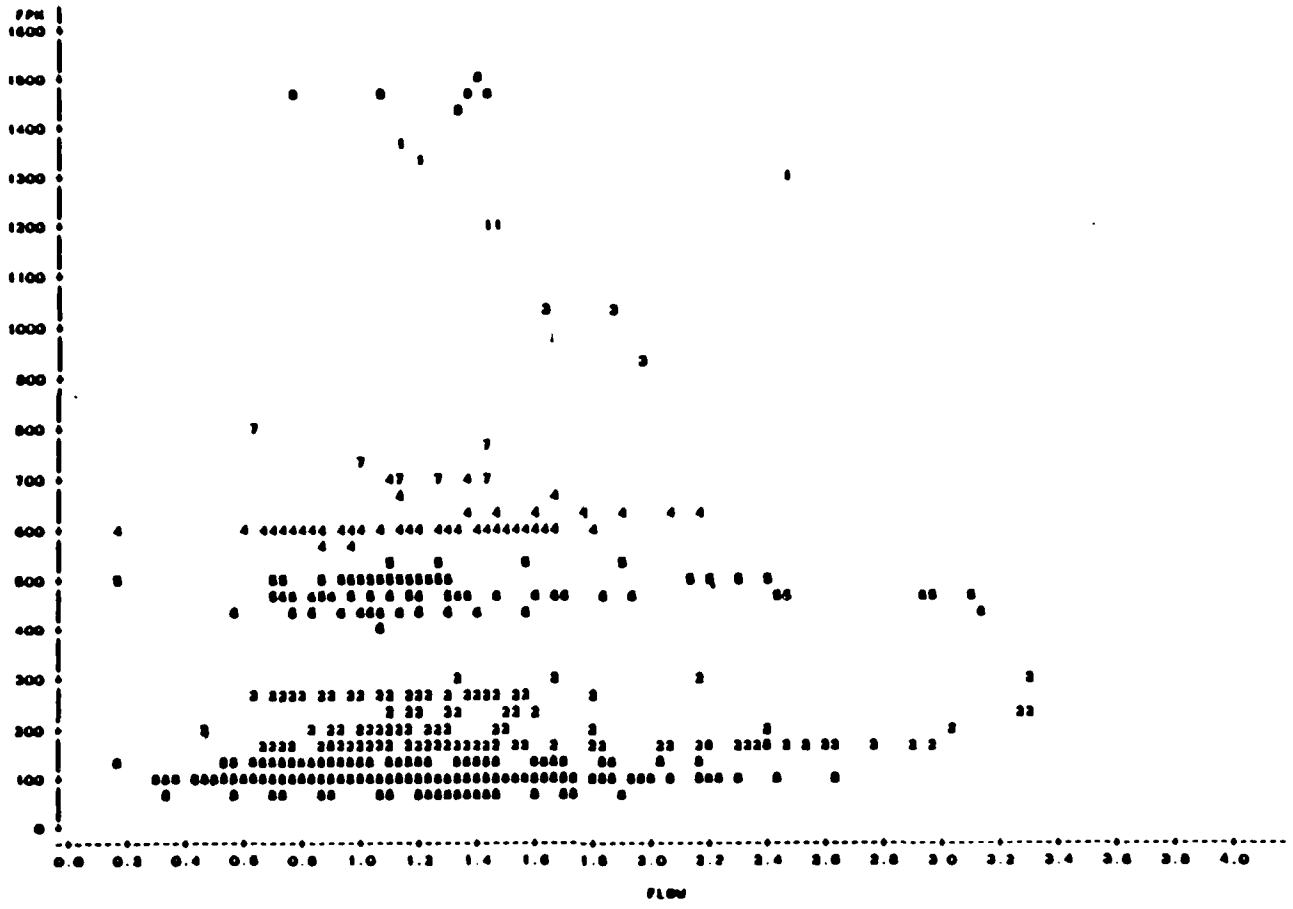

NOTE: 263 OBS HIDDEN

PLOT OF MPP*FLOW SYMBOL IS VALUE OF CLUSTER

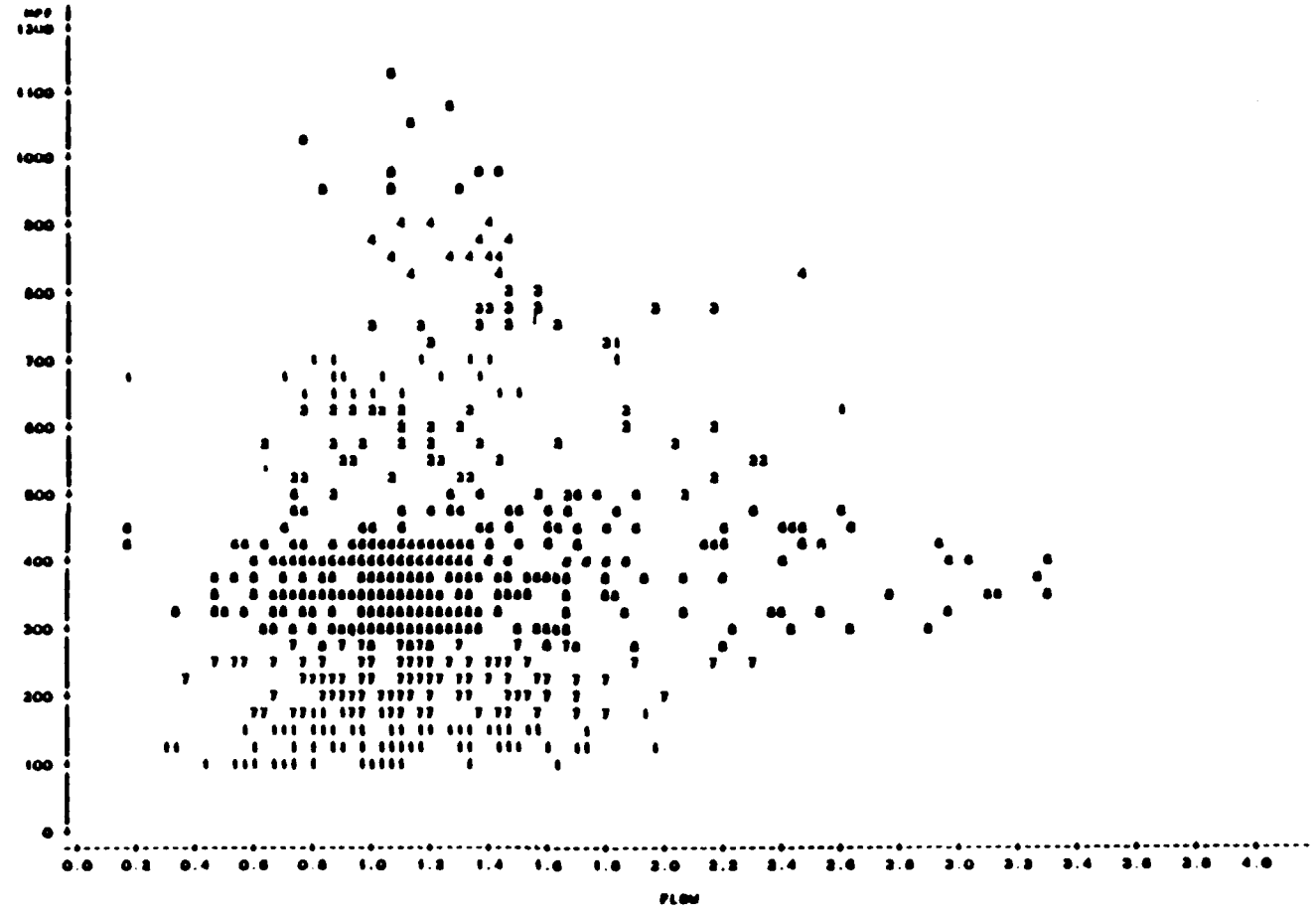

NOTE: 314 OBS HIDDEN

APPENDIX B

PLOTS OF FIVE CLUSTER GROUPS

SAS 10:07 SUNDAY, JANUARY 20, 1985 32

PLOT OF MPF*FMAX SYMBOL IS VALUE OF CLUSTER

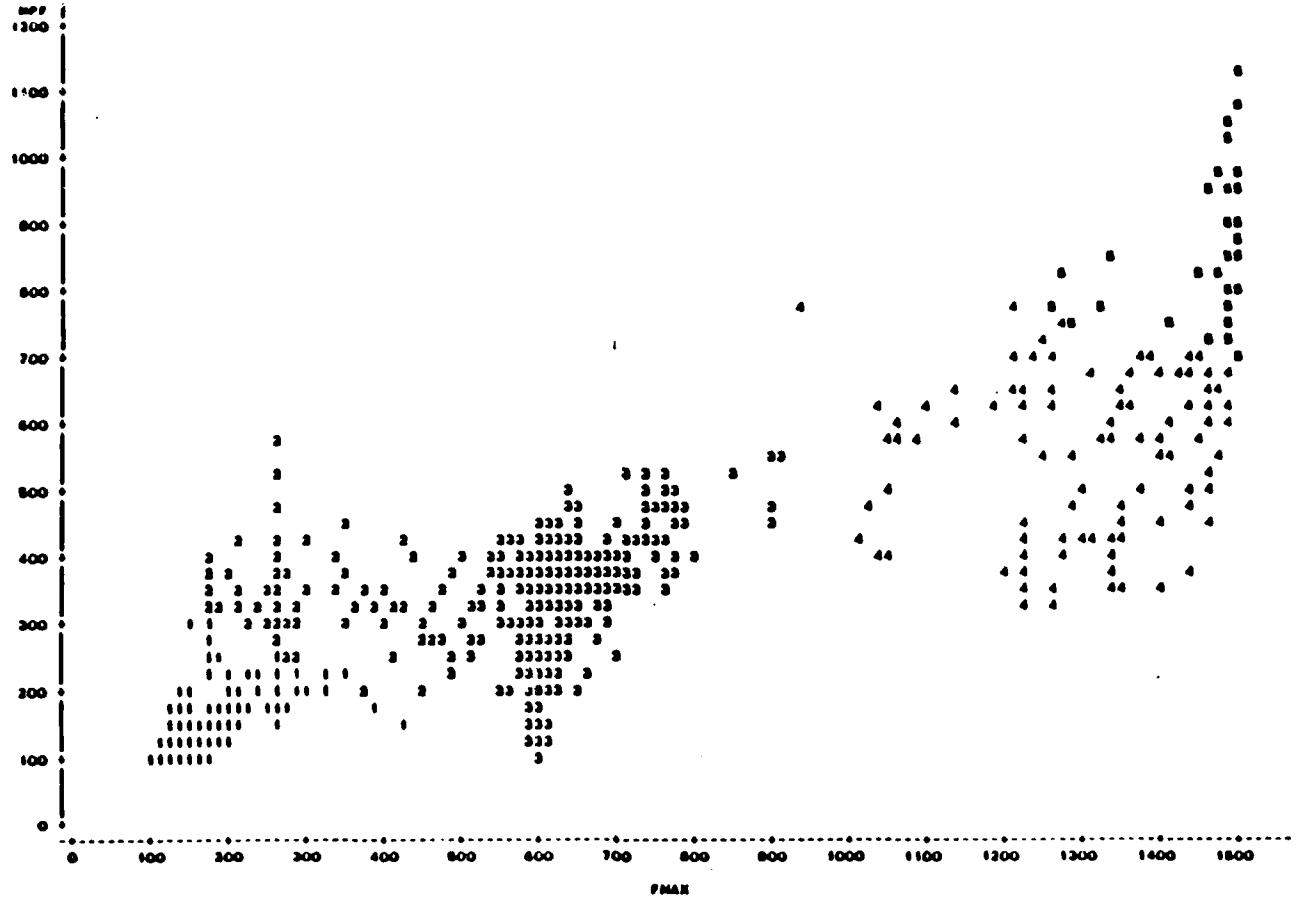

NOTE: 300 OBS HIDDEN

SAS 0:12 SATURDAY, JANUARY 26, 1985 33

PLOT OF FPK*FMAX SYMBOL IS VALUE OF CLUSTER

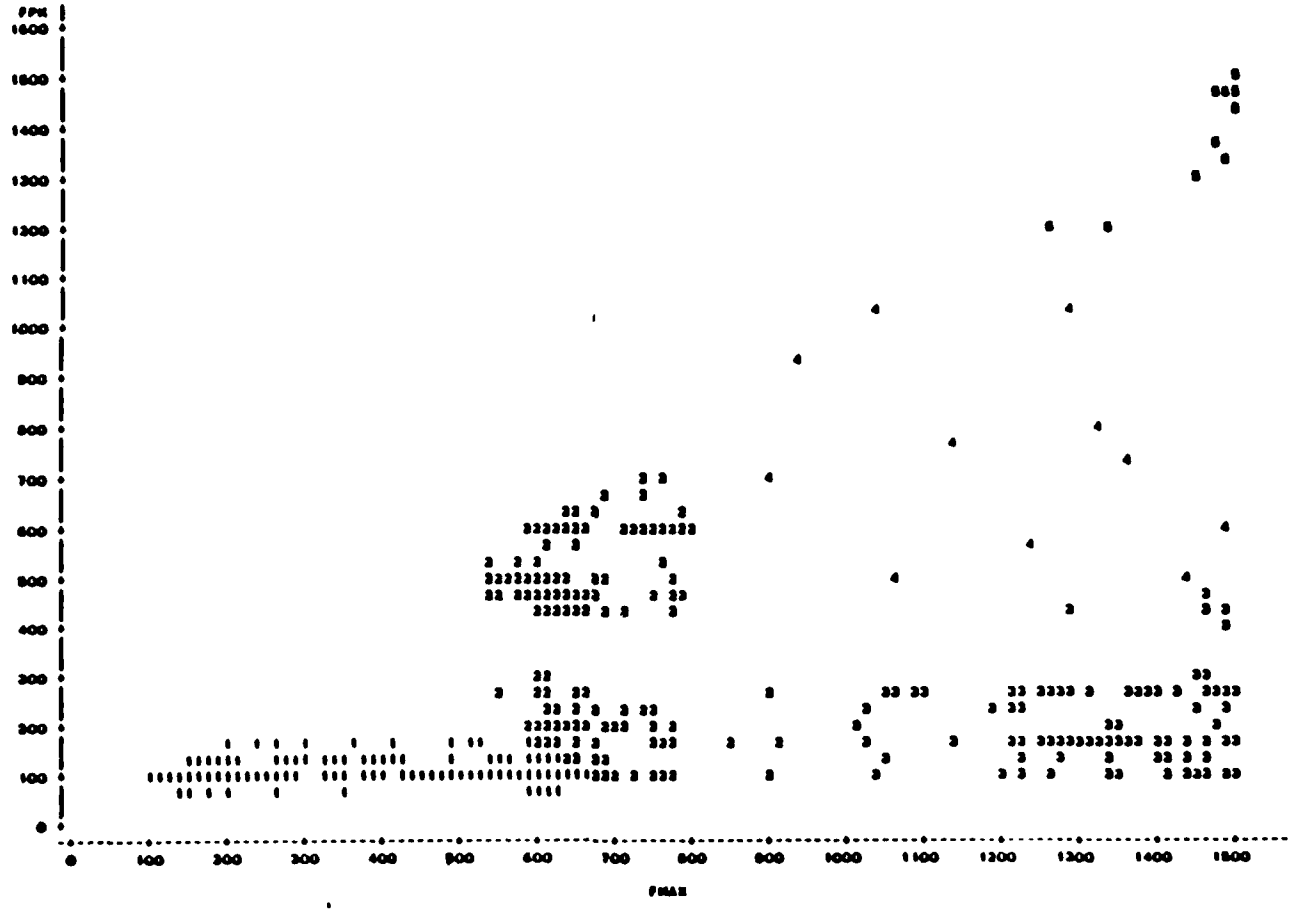

NOTE: 306 OBS HIDDEN

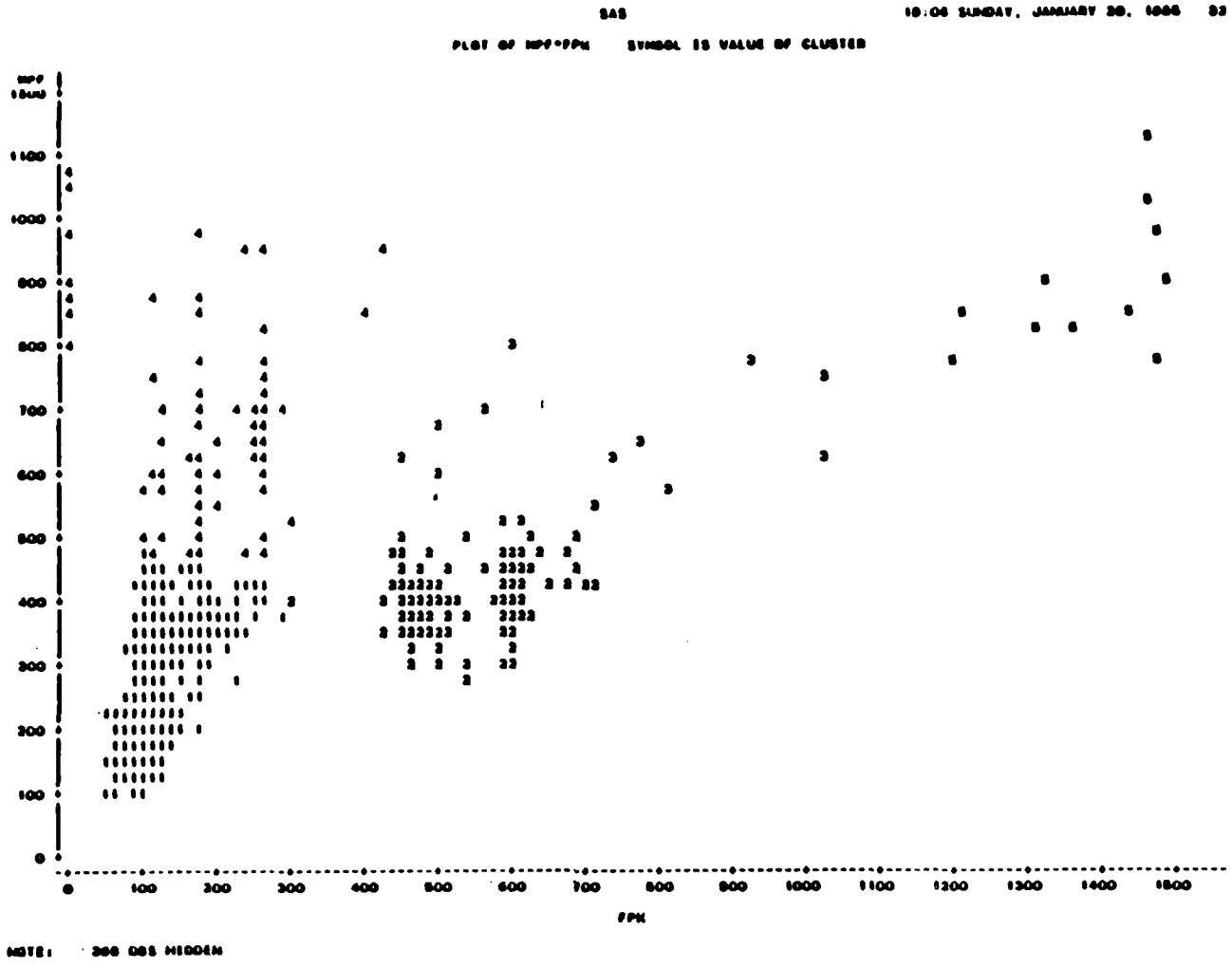
SAS
10:06 SUNDAY, JANUARY 20, 1985 53
PLOT OF MPG*FPK SYMBOL IS VALUE OF CLUSTER
MPG
1100
1000
900
800
700
600
500
400
300
200
100
0
0 100 200 300 400 500 600 700 800 900 1000 1100 1200 1300 1400 1500
FPK
NOTE: 300 OBS HIDDEN

PLOT OF FMAX*FLOW SYMBOL IS VALUE OF CLUSTER

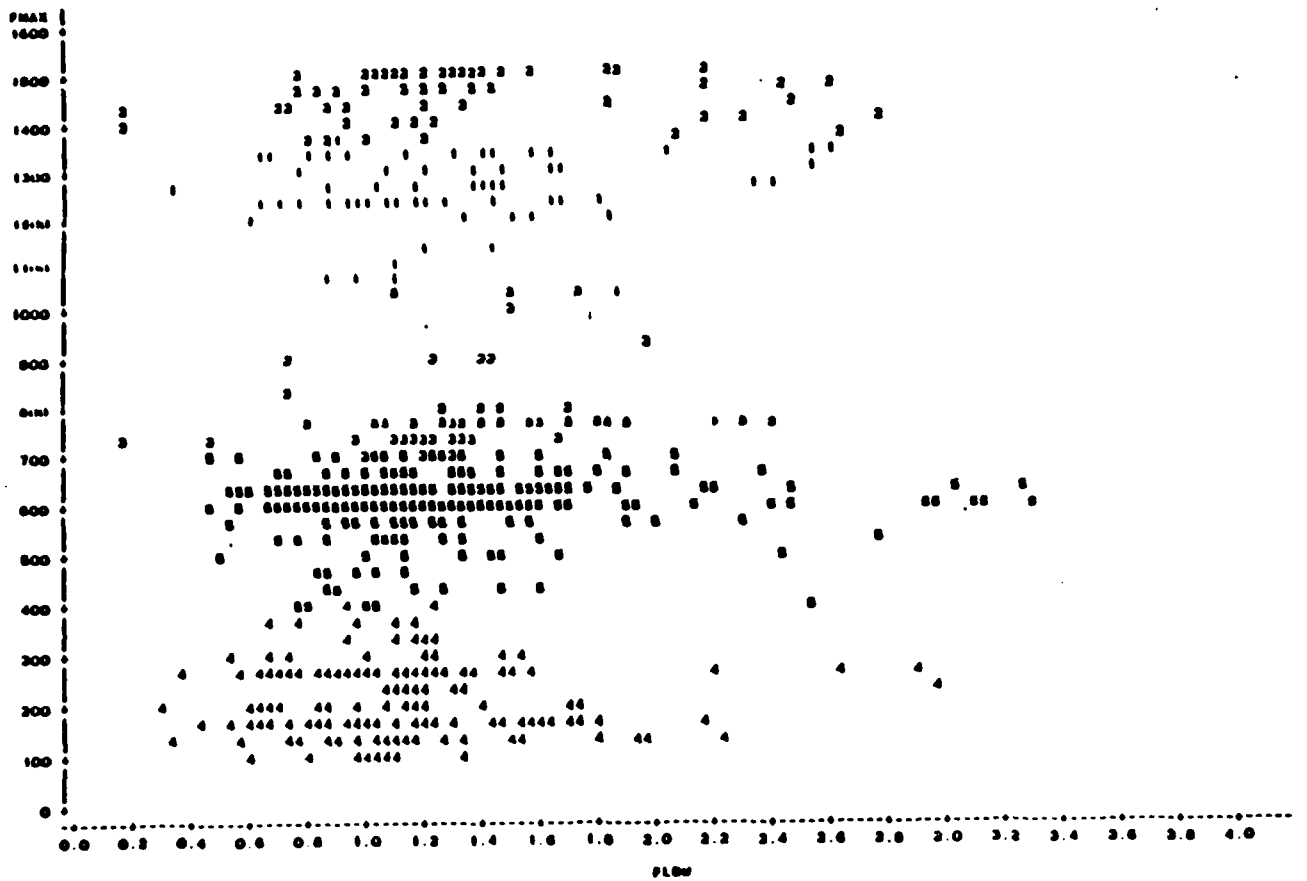

NOTE: 897 OBS MISSING

PLOT OF FPK*FLOW SYMBOL IS VALUE OF CLUSTER

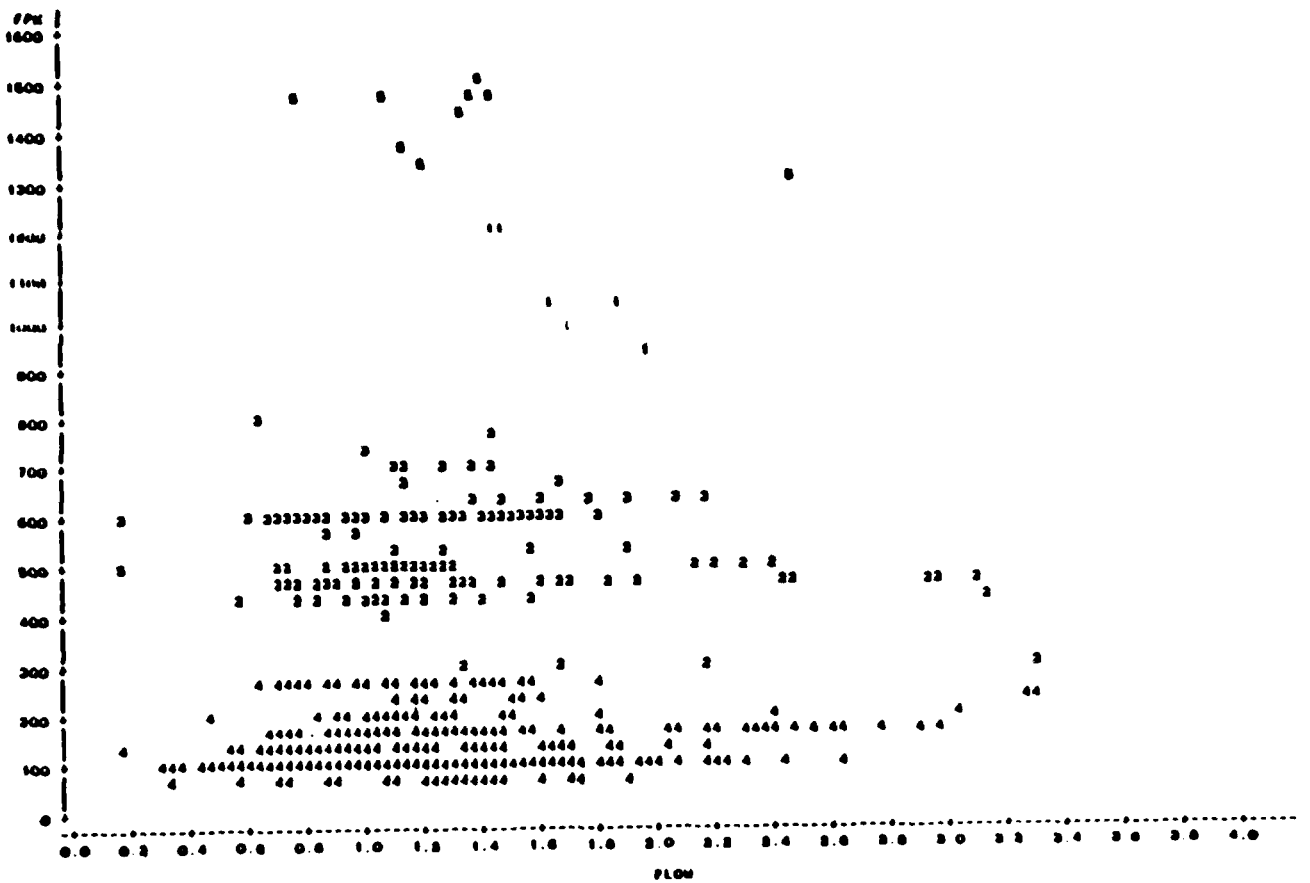

NOTE: 383 OBS HIDDEN

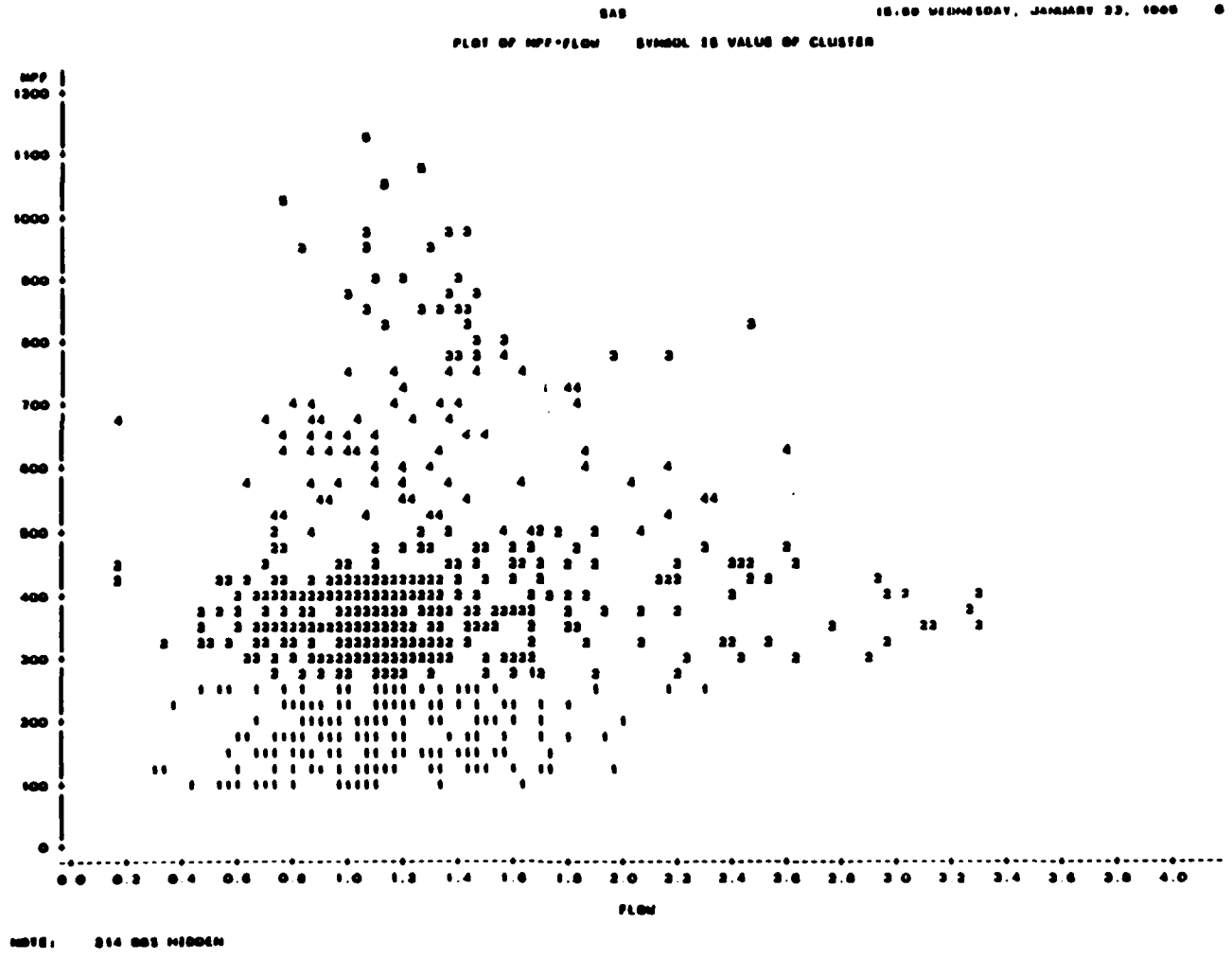
SAS
PLOT OF MPF*FLOW SYMBOL IS VALUE OF CLUSTER
MPF
FLOW
NOTE: 814 OBS HIDDEN

APPENDIX C

PLOTS OF TWO CLUSTER GROUPS

PLOT OF FPH*FLOW SYMBOL IS VALUE OF CLUSTER

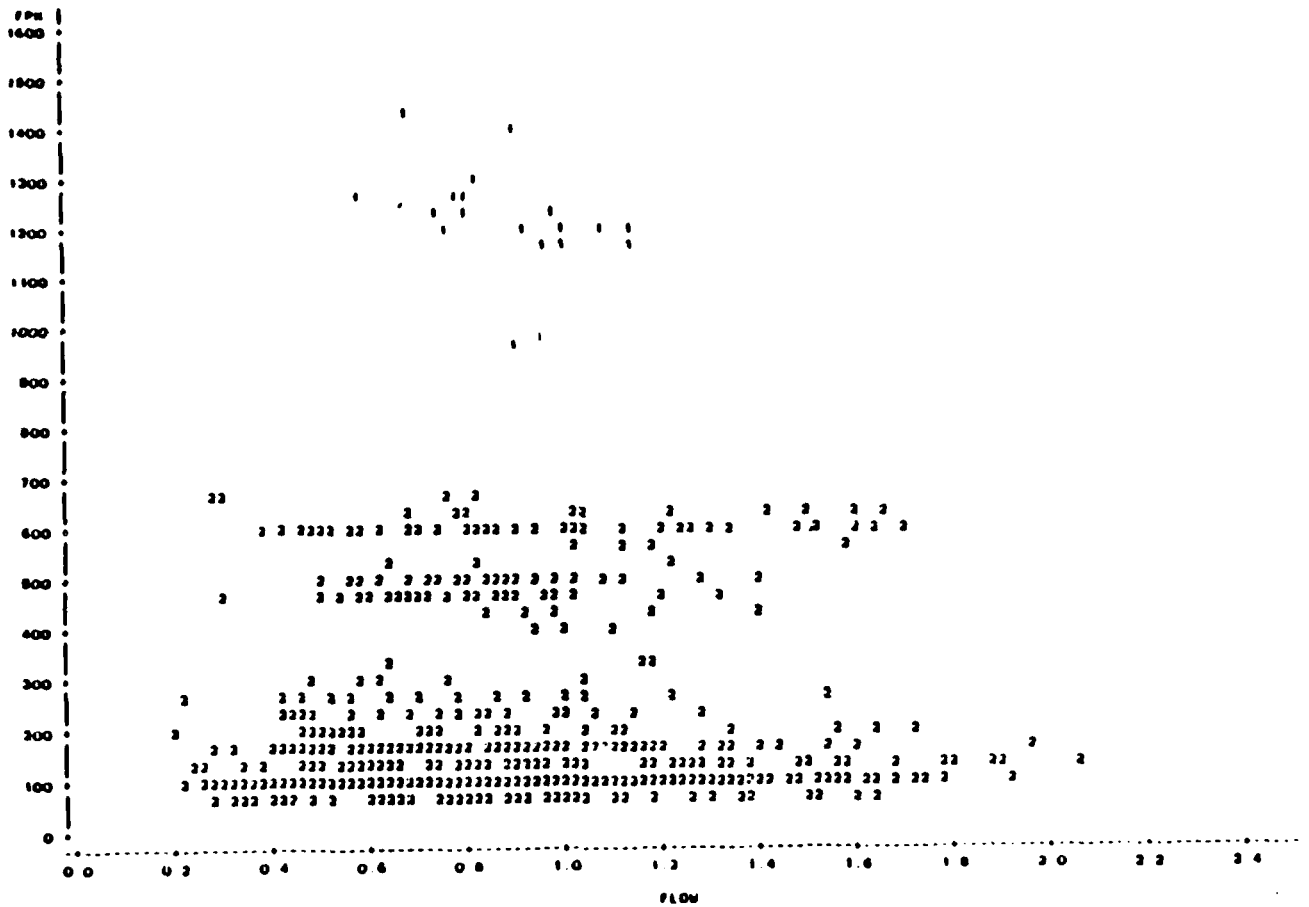

NOTE: 300 OBS HIDDEN

SAS 0:33 WEDNESDAY, JANUARY 23, 1985 9

PLOT OF FMAX*FLOW SYMBOL IS VALUE OF CLUSTER

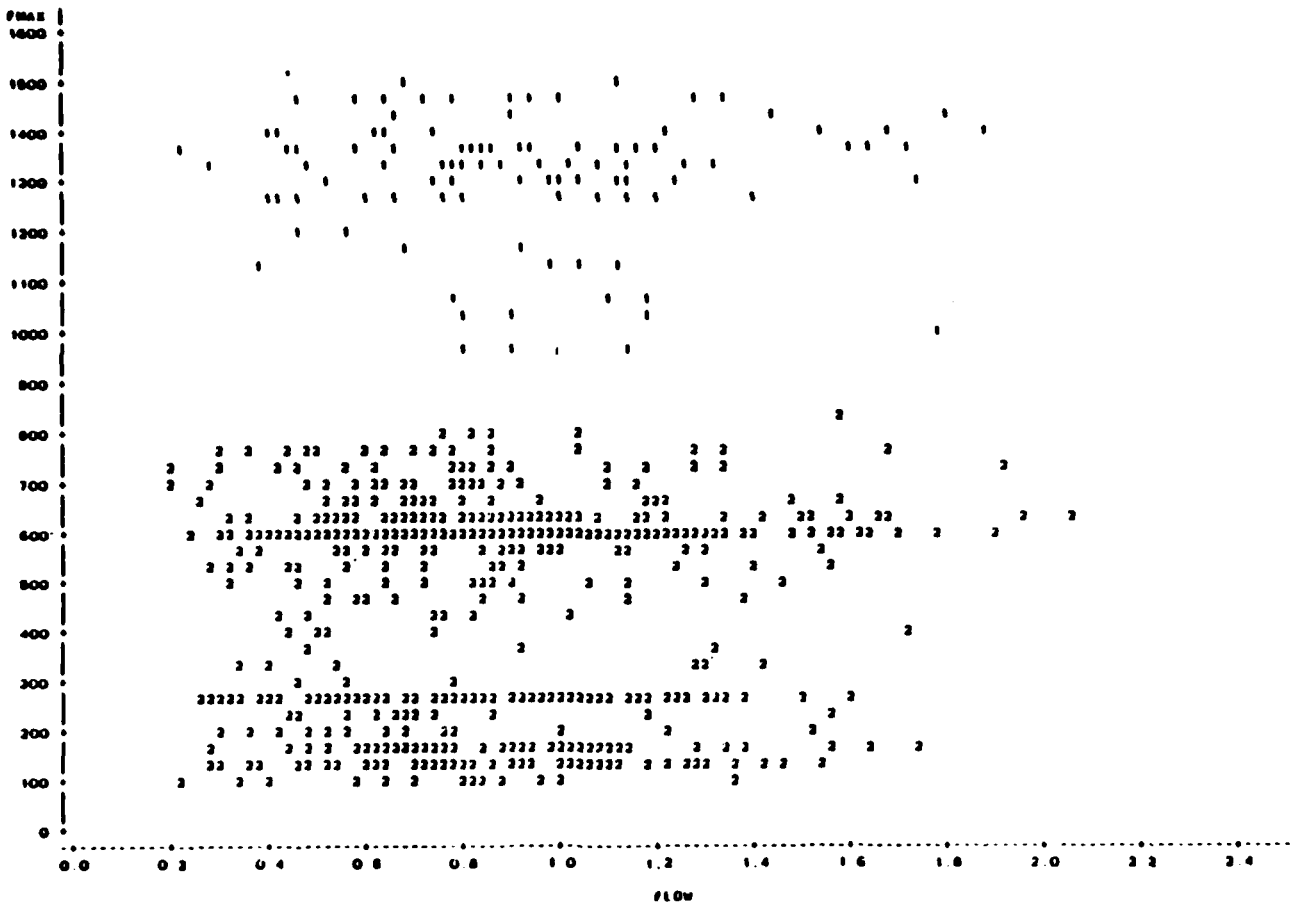

NOTE: 376 OBS HIDDEN

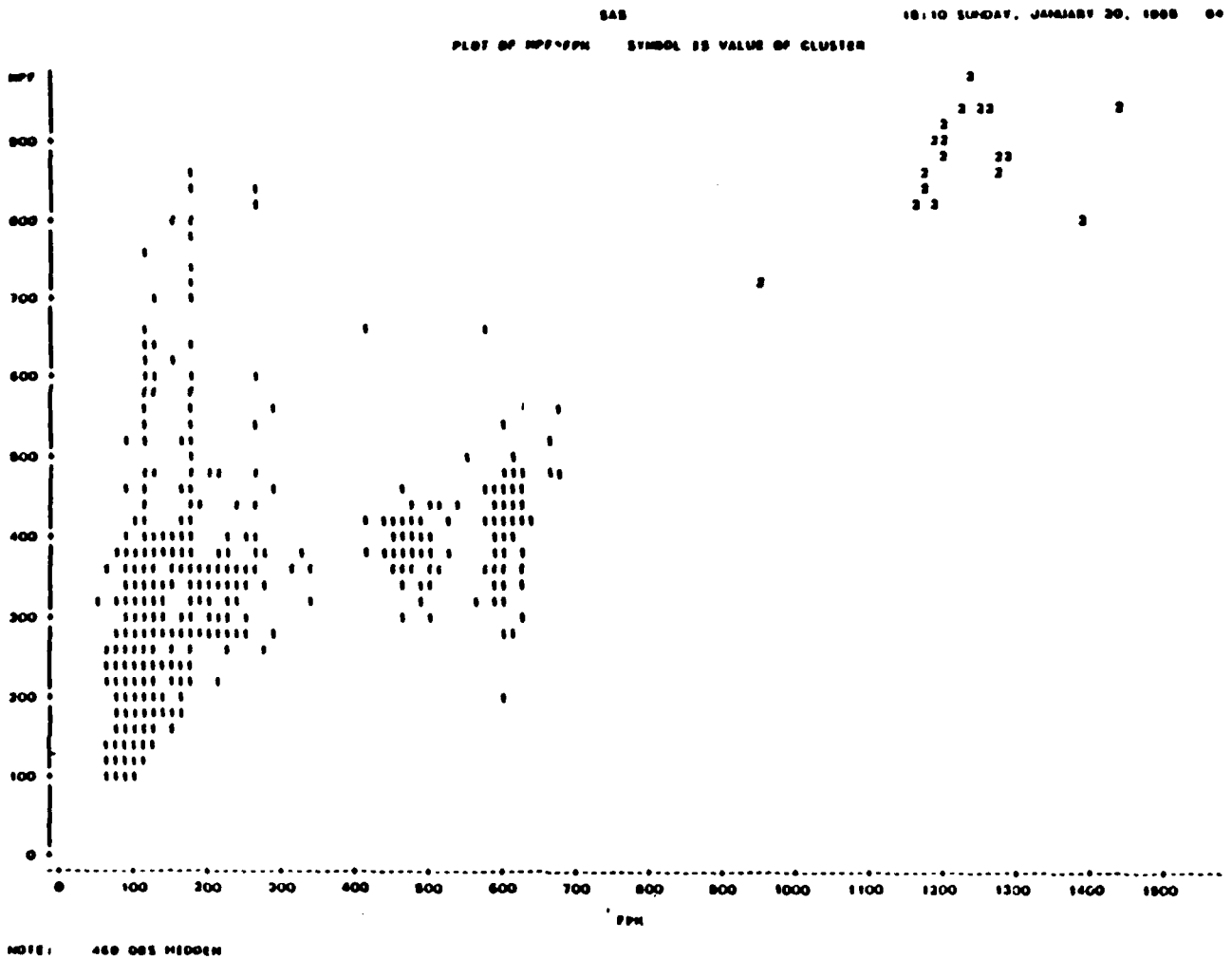
SAS
18:10 SUNDAY, JANUARY 20, 1985
PLOT OF MPF*PPH SYMBOL IS VALUE OF CLUSTER
MPF
PPH
NOTE: 460 OBS HIDDEN

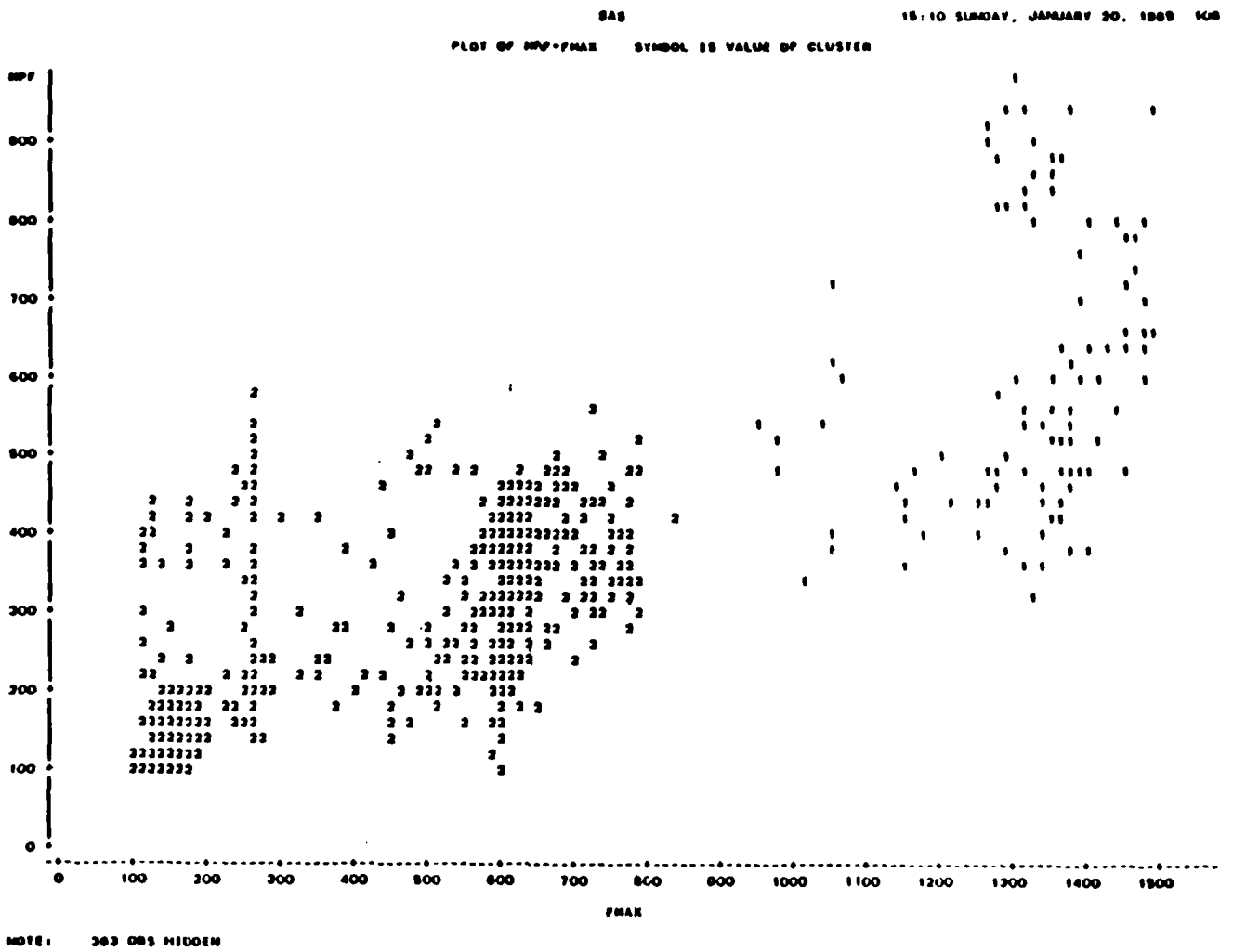

NOTE: 303 OBS HIDDEN

PLOT OF FPH*FMAX SYMBOL IS VALUE OF CLUSTER

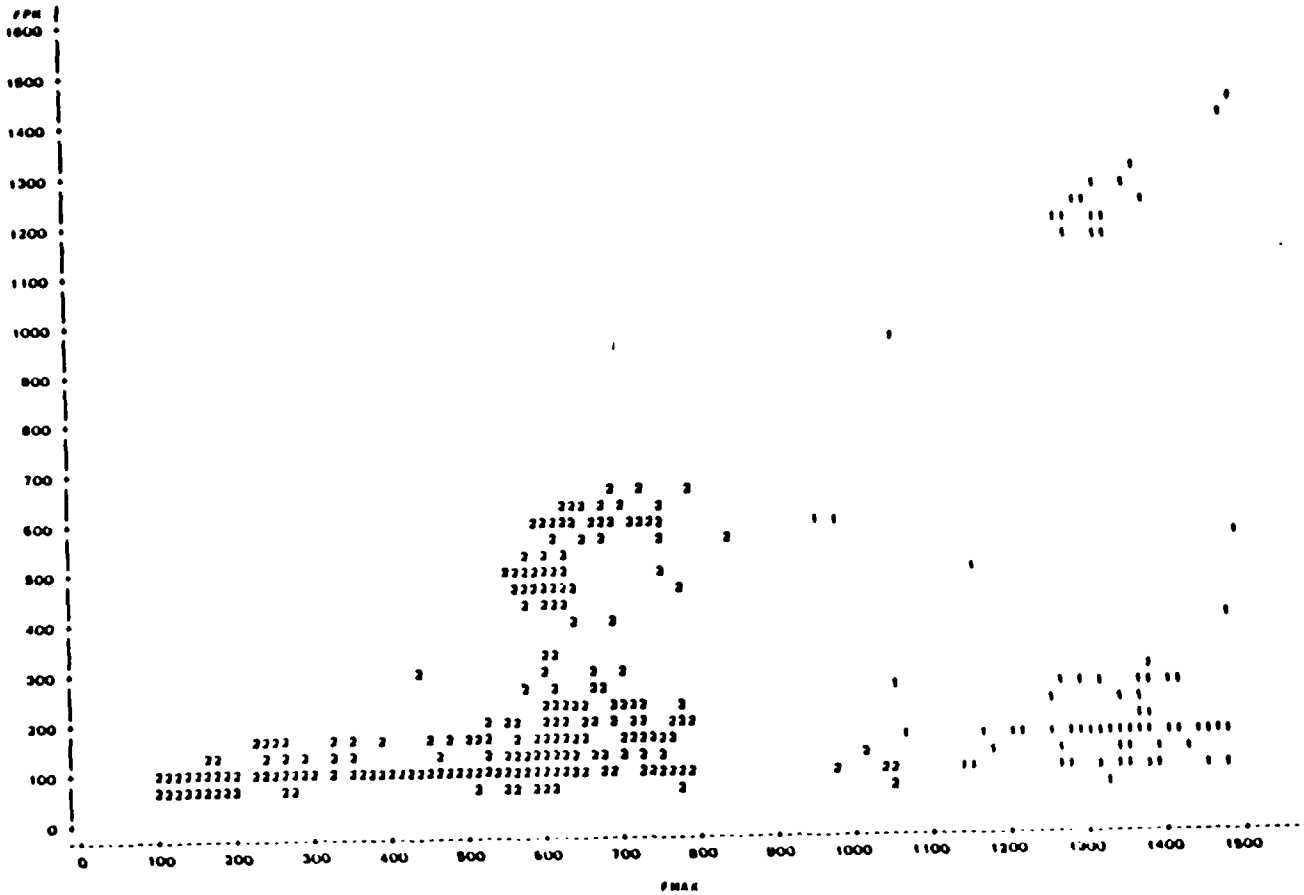

NOTE: 509 OBS HIDDEN

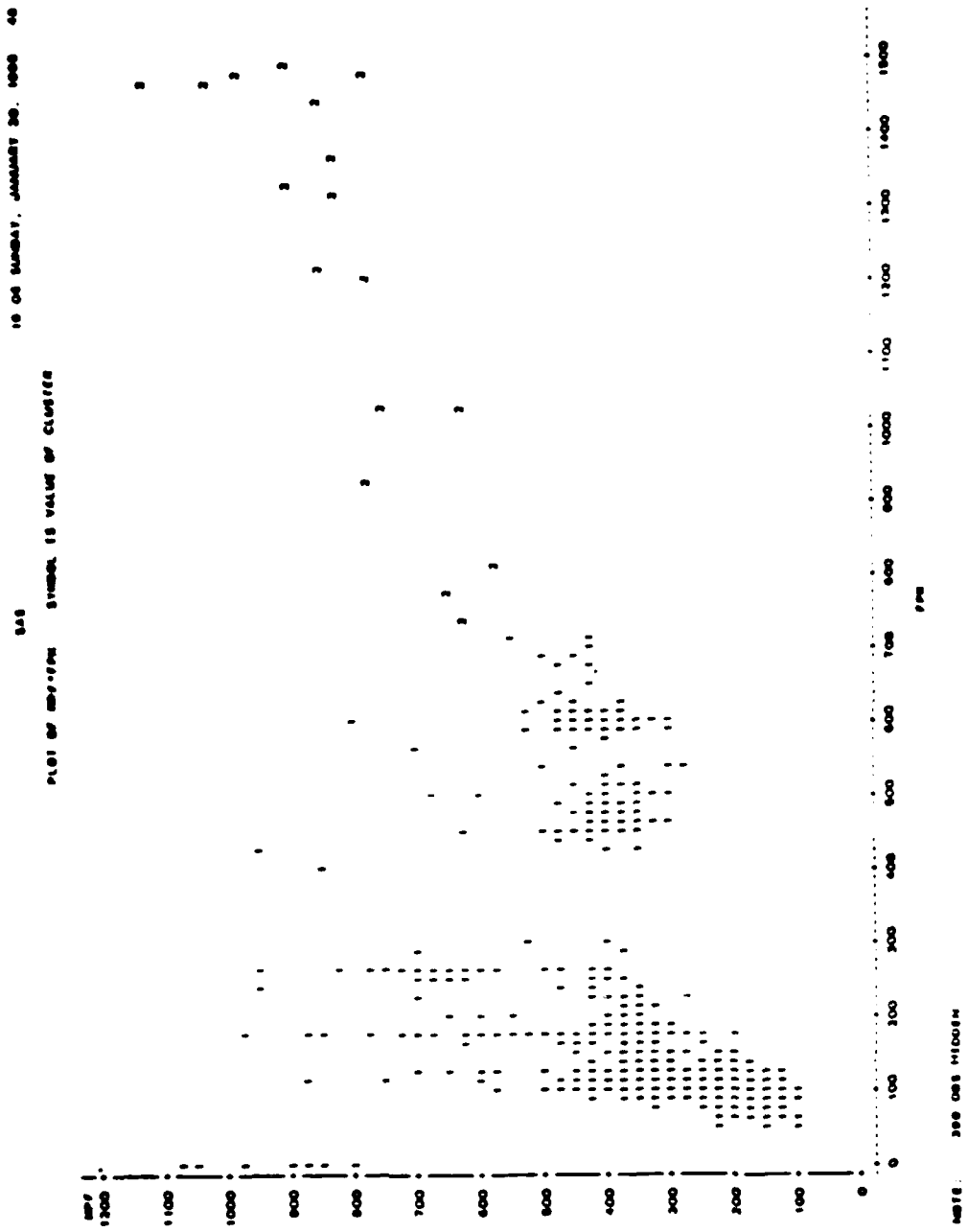

PLOT OF MPF*FMAX SYMBOL IS VALUE OF CLUSTER

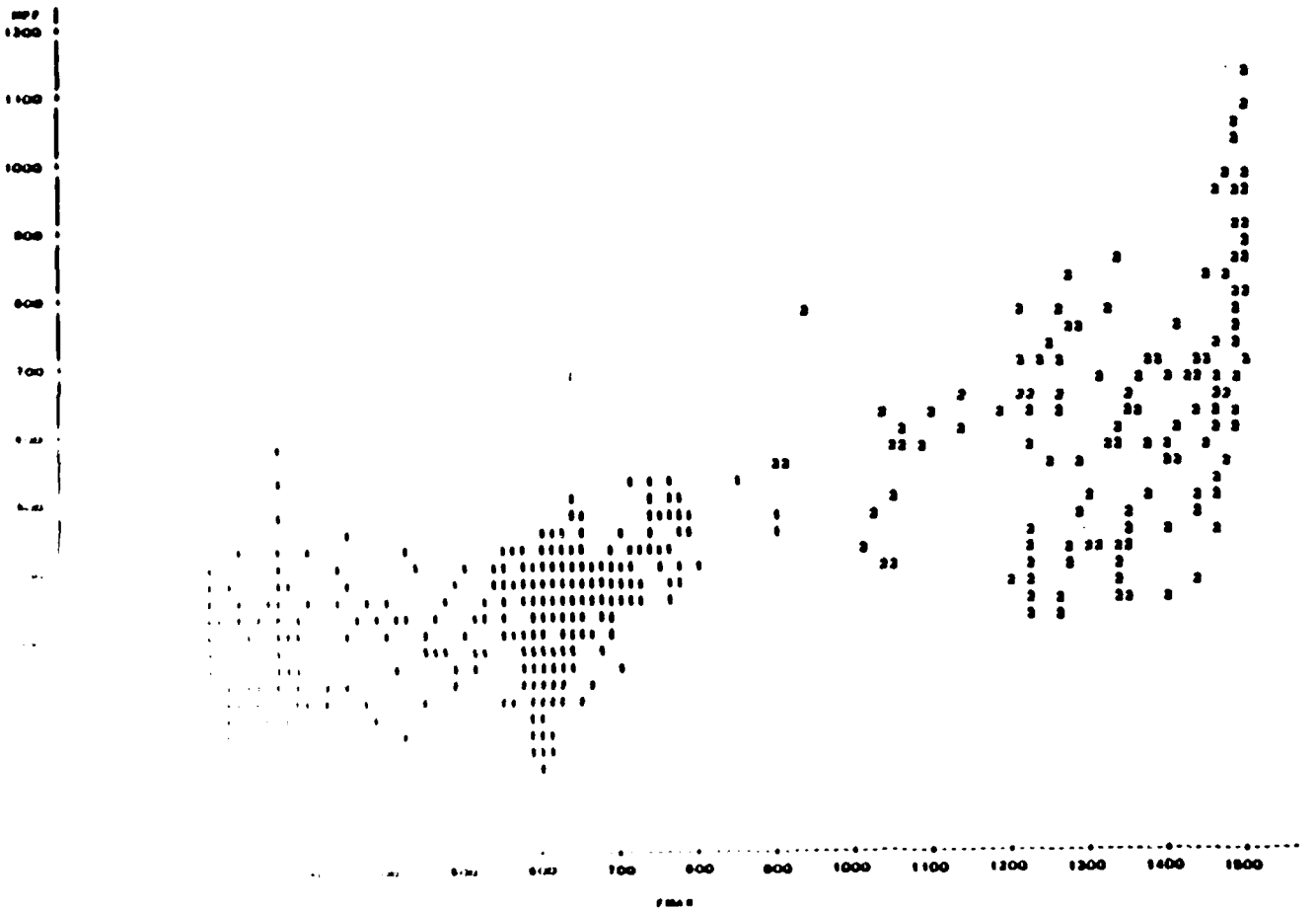

AD-A175 926 CLUSTER ANALYSIS OF RESPIRATORY SOUNDS OF PULMONARY INSUFFICIENT PATIENTS (U) TEXAS A AND M UNIV COLLEGE STATION DEPT OF INDUSTRIAL ENGINEE 2/2

UNCLASSIFIED C S LESSARD ET AL OCT 86 USAFSAM-TR-86-13 F/G 6/5 NL

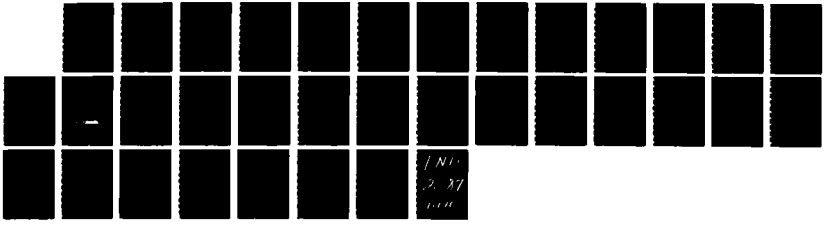

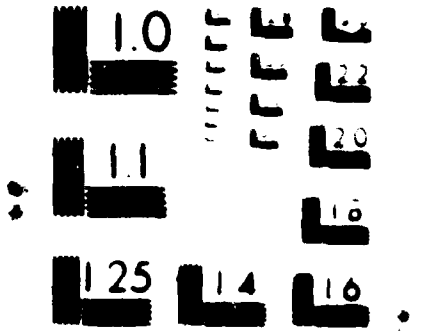
1.0
1.1
1.25
1.4
1.6
2.2
2.0
1.8

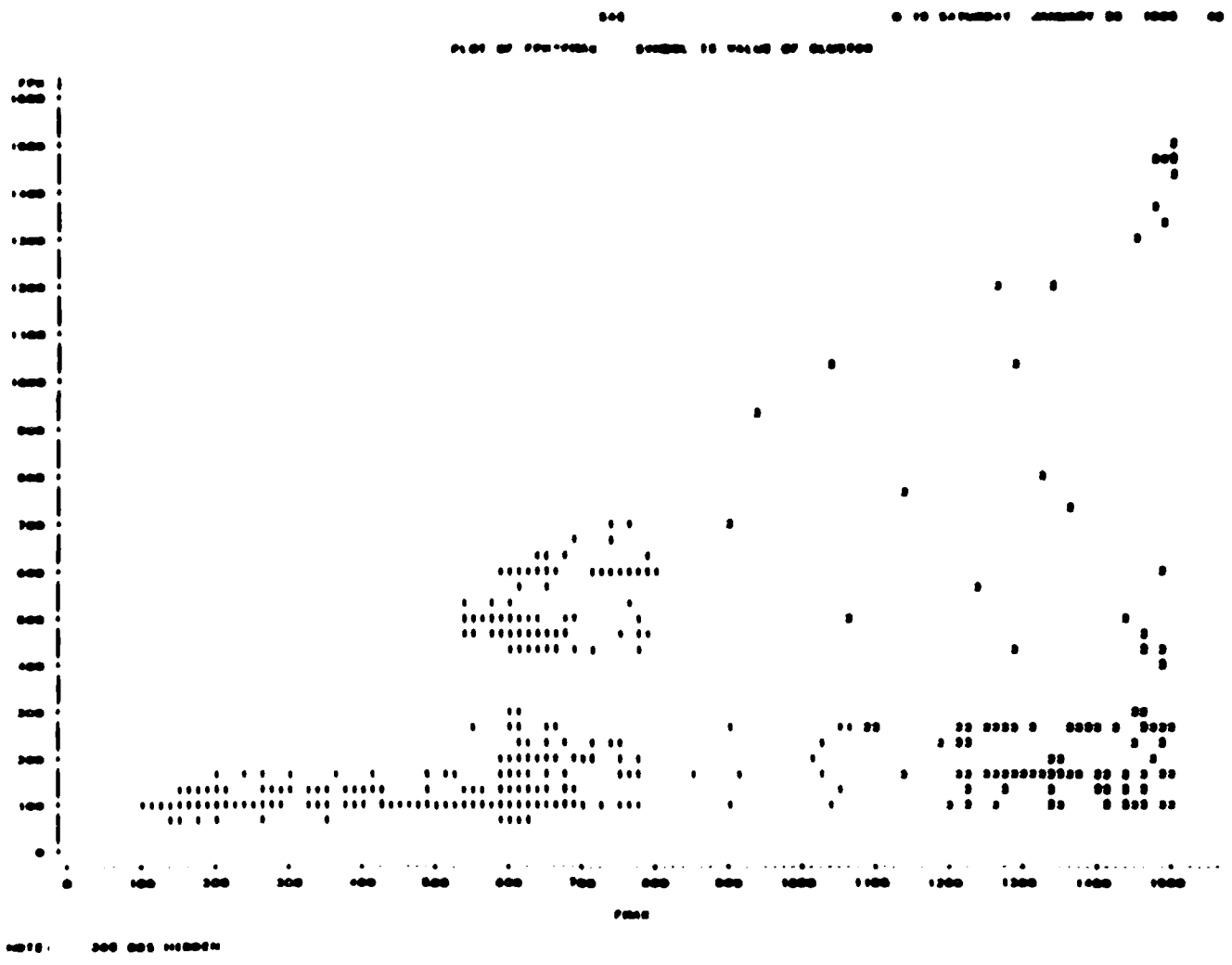

APPENDIX D

THREE-DIMENSIONAL CLUSTER PLOTS

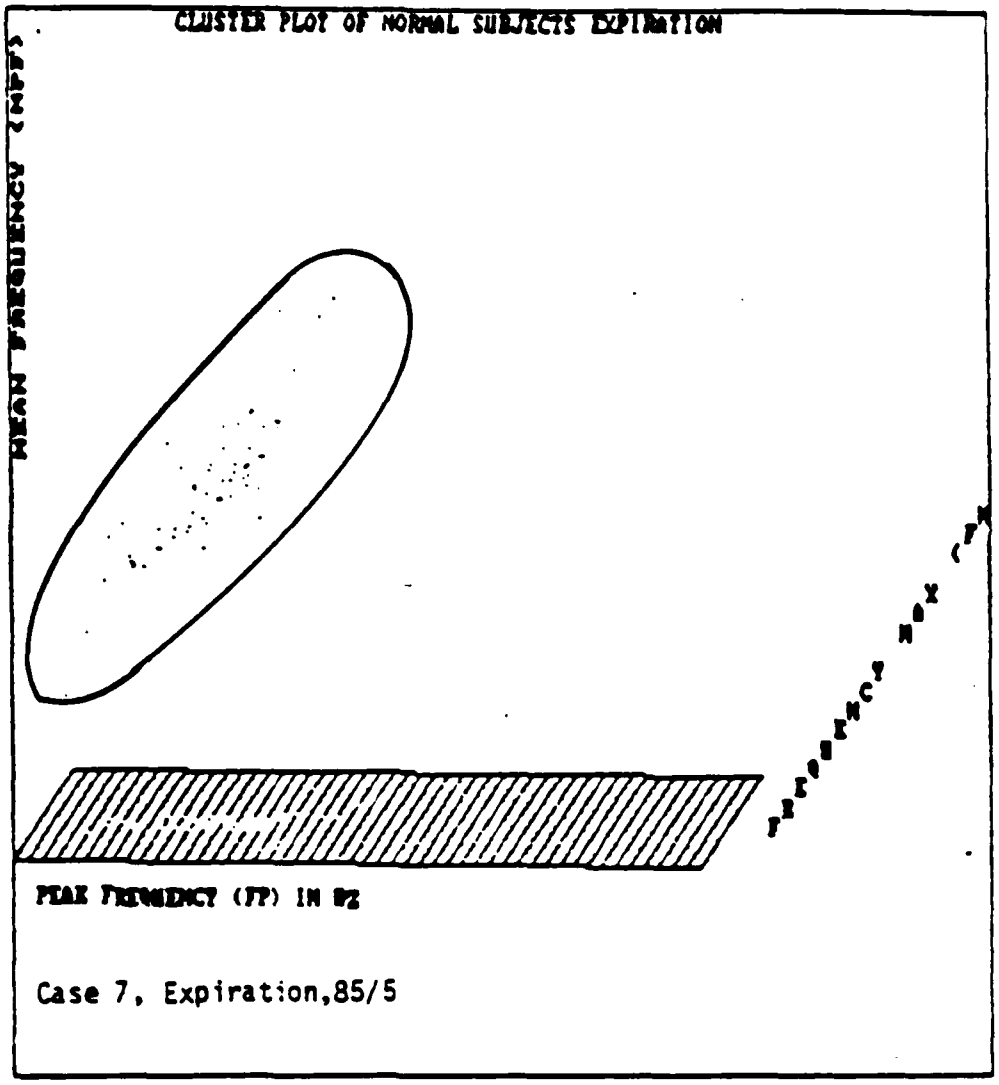

Case 7, Expiration,85/5

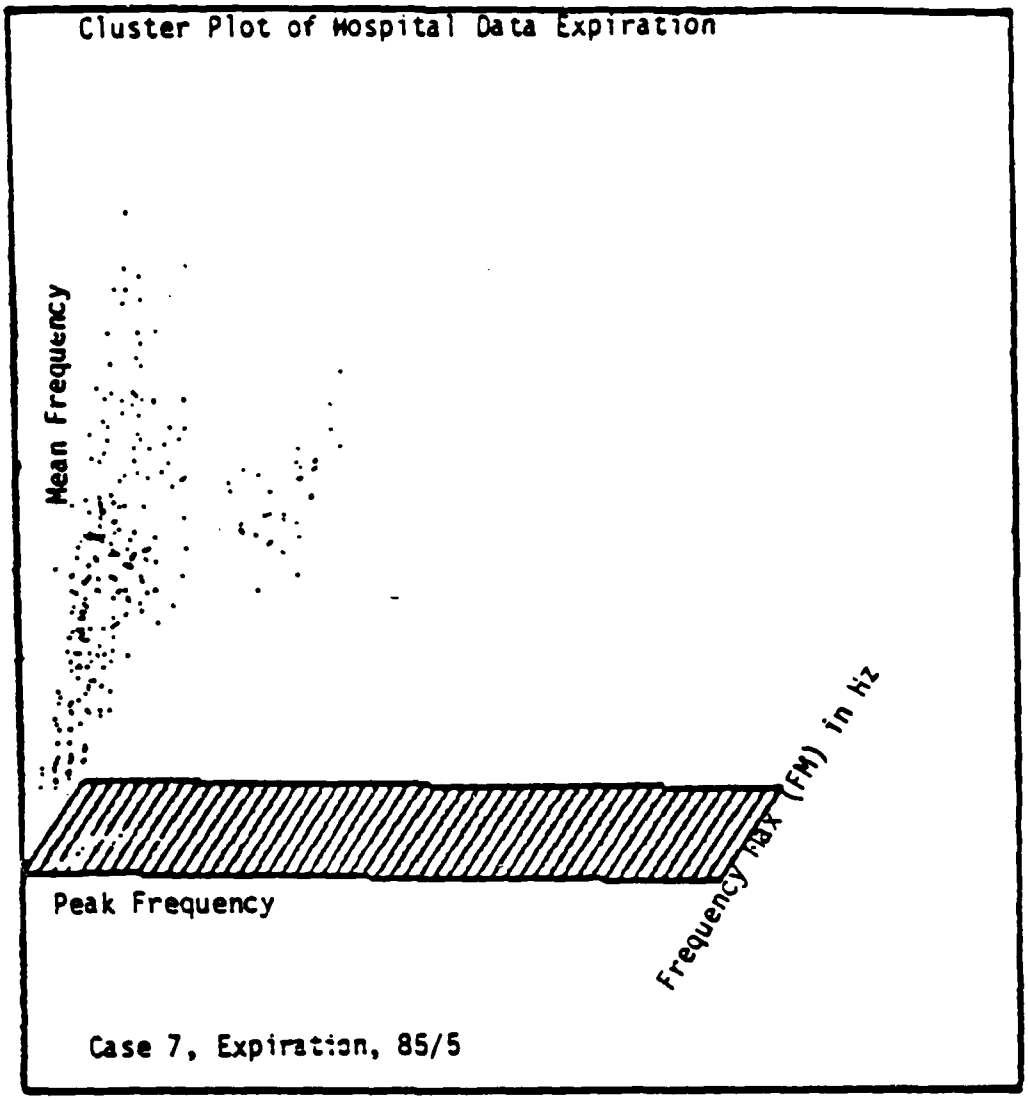
Cluster Plot of Hospital Data Expiration
Mean Frequency
Peak Frequency
Frequency Max (FM) in Hz
Case 7, Expiration, 85/5

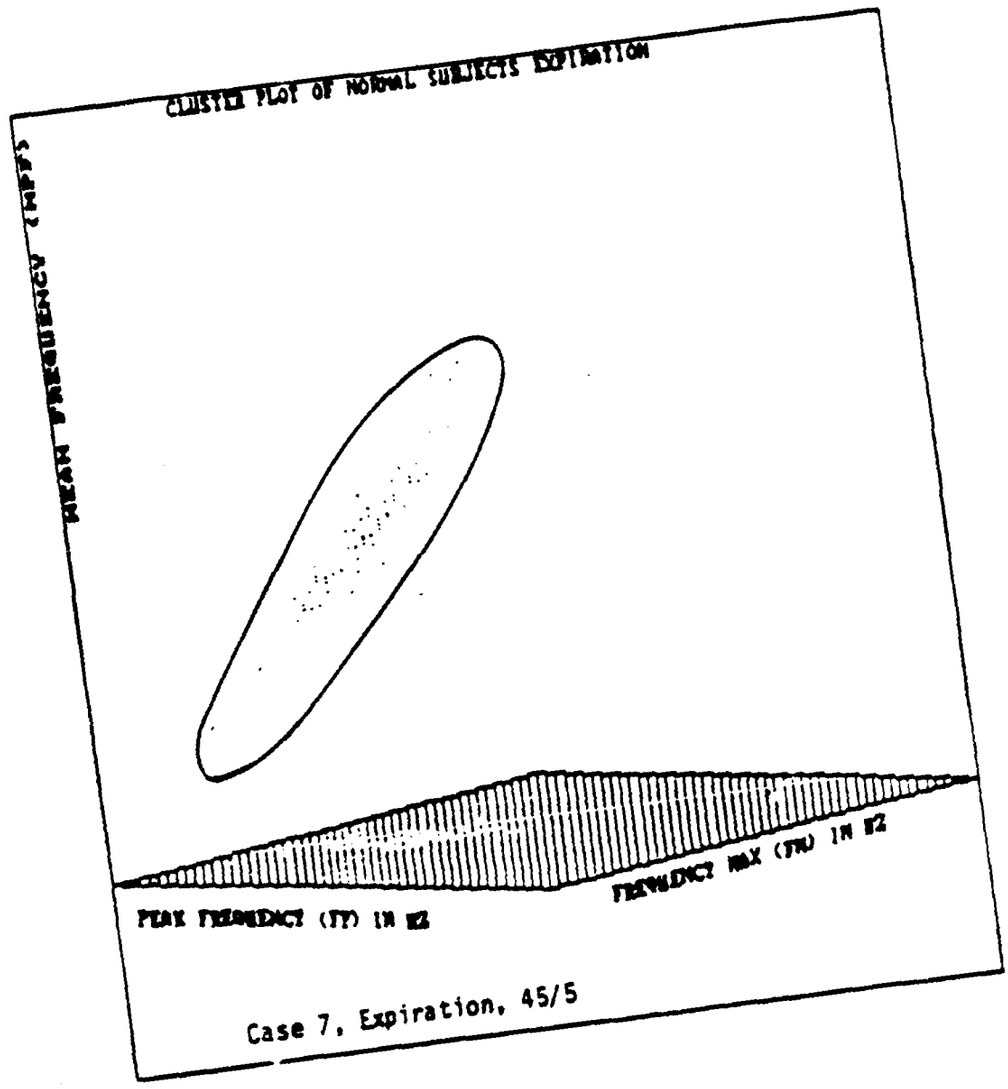

Case 7, Expiration, 45/5

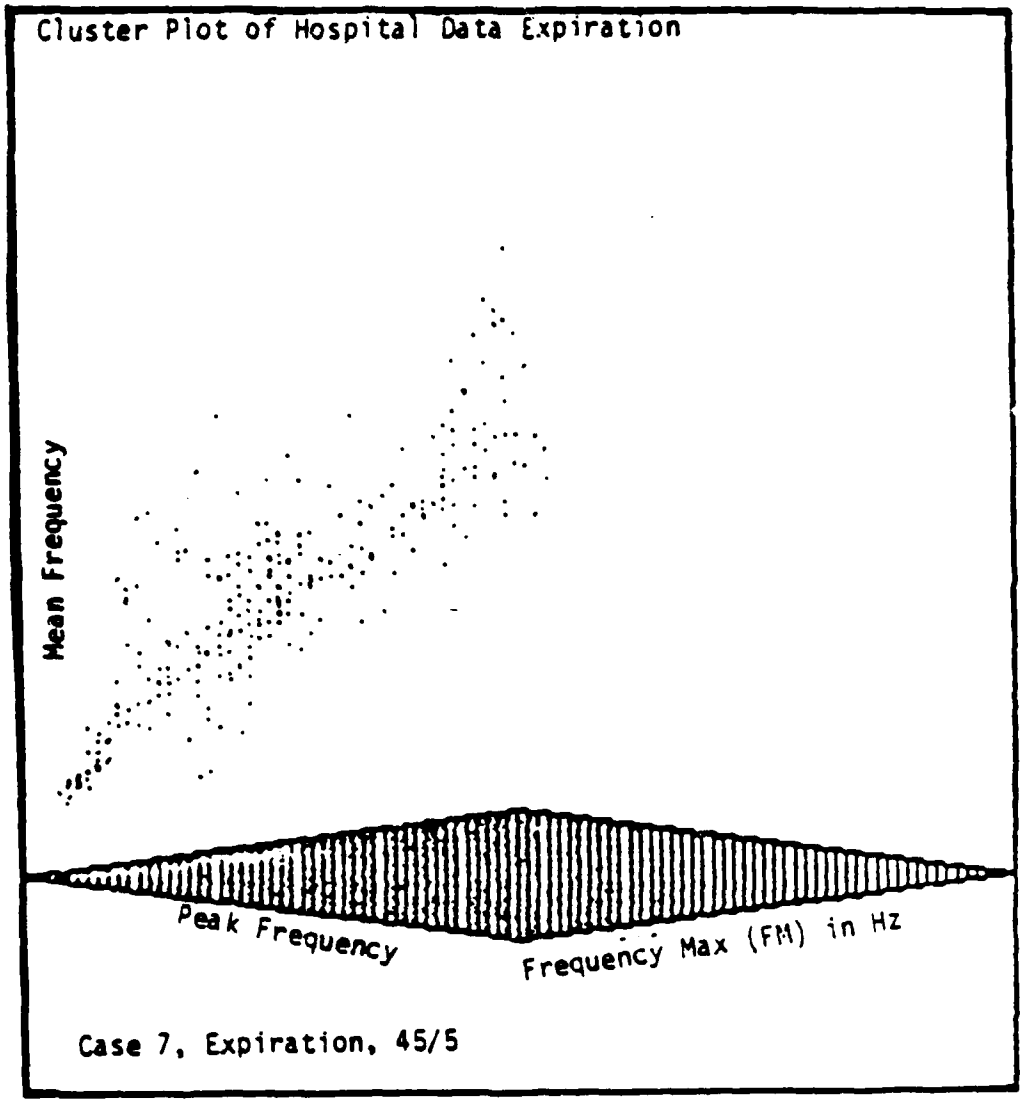
Cluster Plot of Hospital Data Expiration
Mean Frequency
Peak Frequency
Frequency Max (FM) in Hz
Case 7, Expiration, 45/5

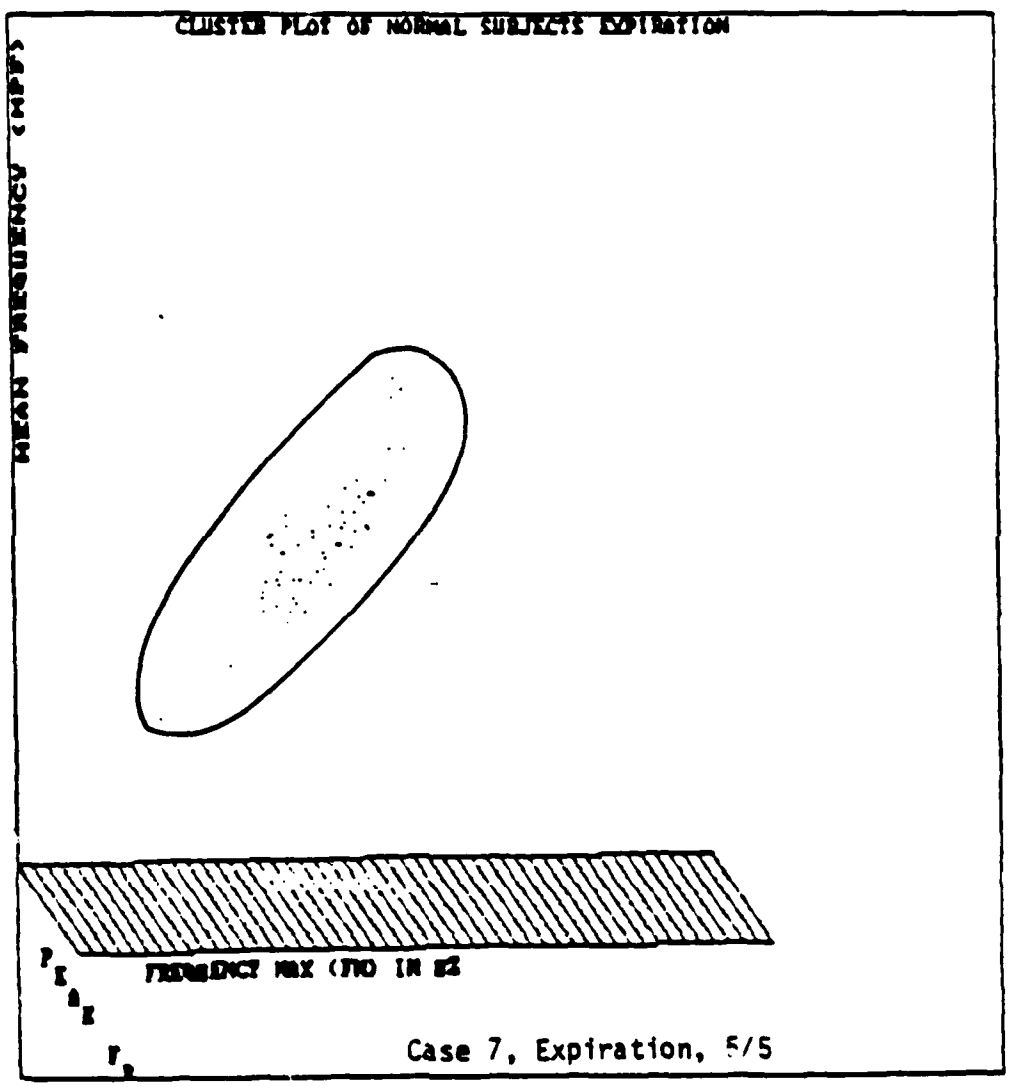
CLUSTER PLOT OF NORMAL SUBJECTS EXPIRATION
MEAN FREQUENCY (HPS)
FREQUENCY MAX (TWO IN 82
Case 7, Expiration, 5/5

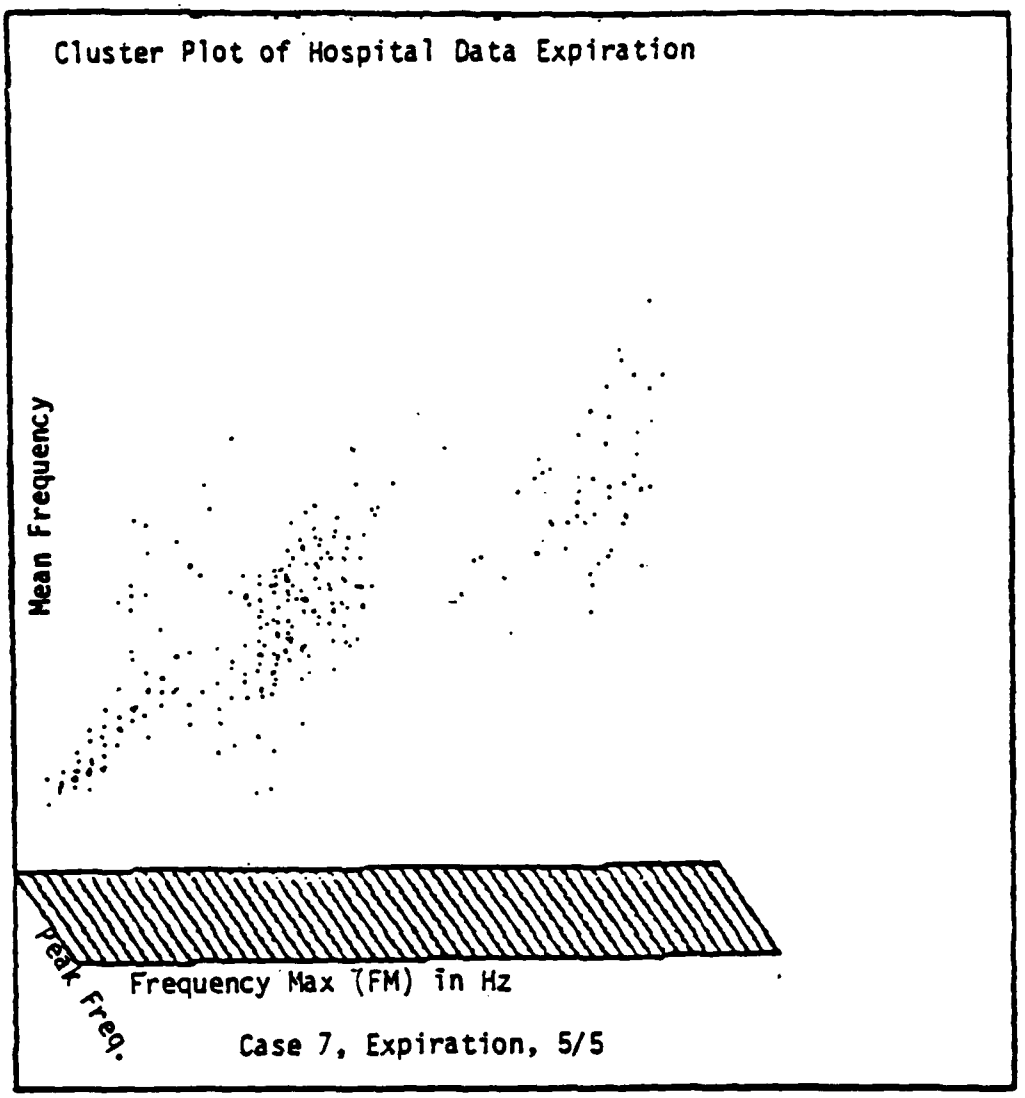
Cluster Plot of Hospital Data Expiration
Mean Frequency
Peak Freq.
Frequency Max (FM) in Hz
Case 7, Expiration, 5/5

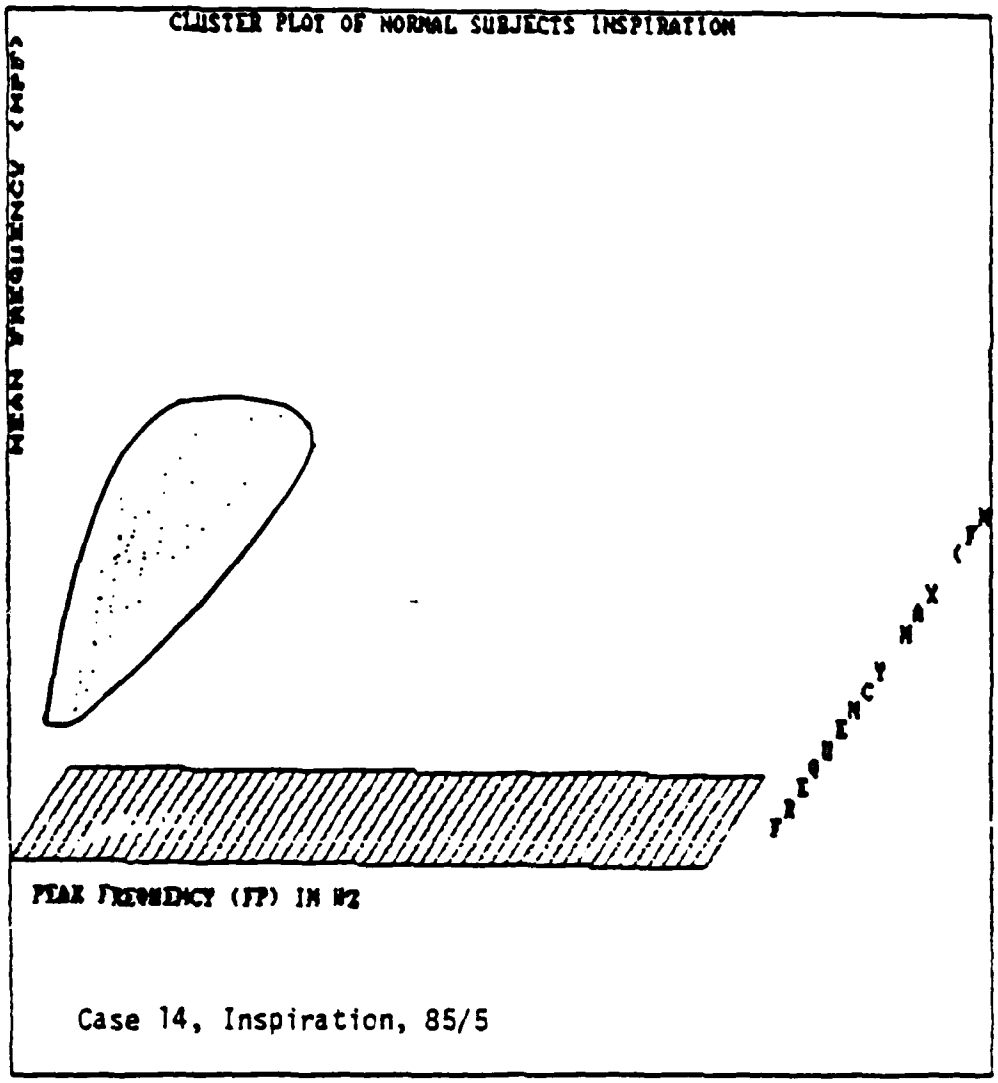

Case 14, Inspiration, 85/5

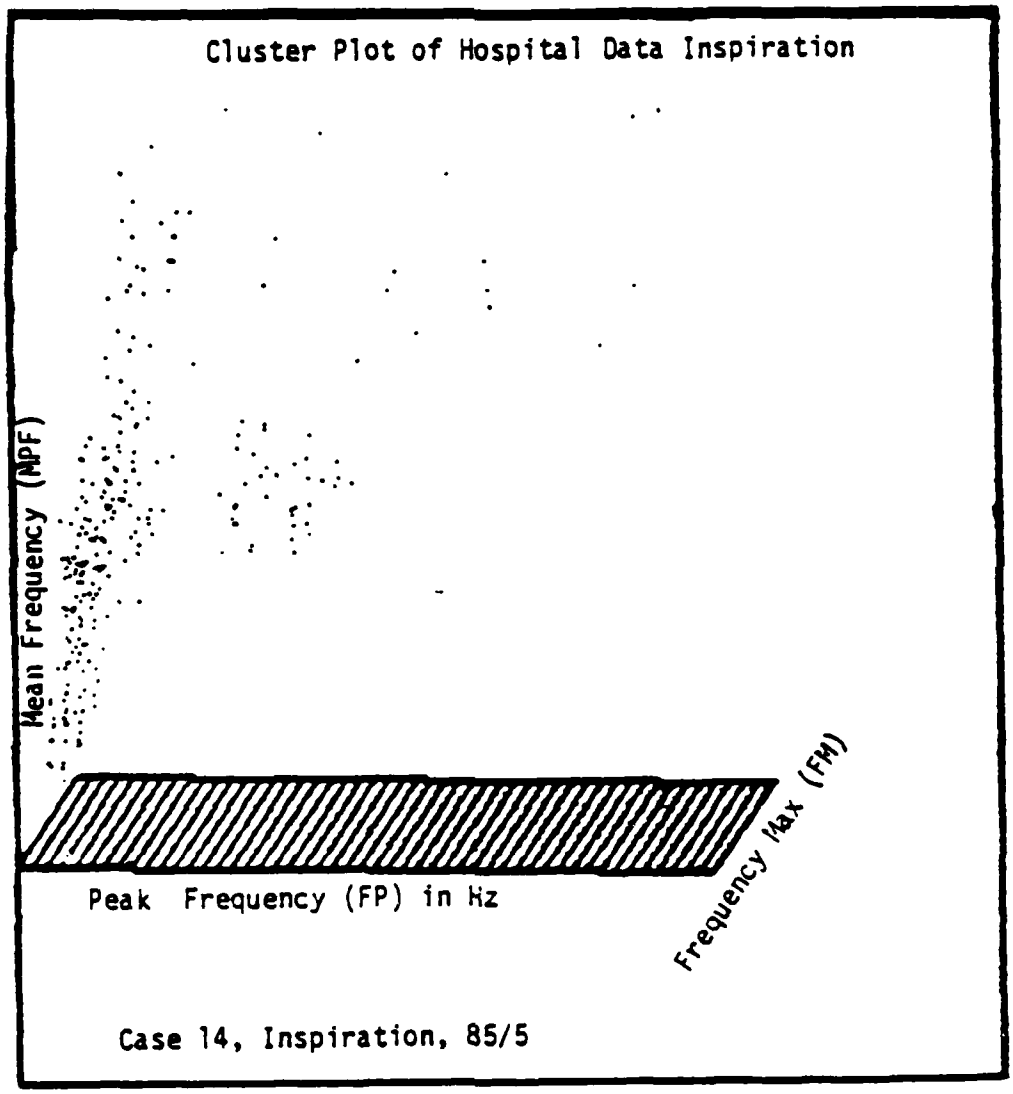
Cluster Plot of Hospital Data Inspiration
Mean Frequency (MPF)
Peak Frequency (FP) in Hz
Frequency Max (FM)
Case 14, Inspiration, 85/5

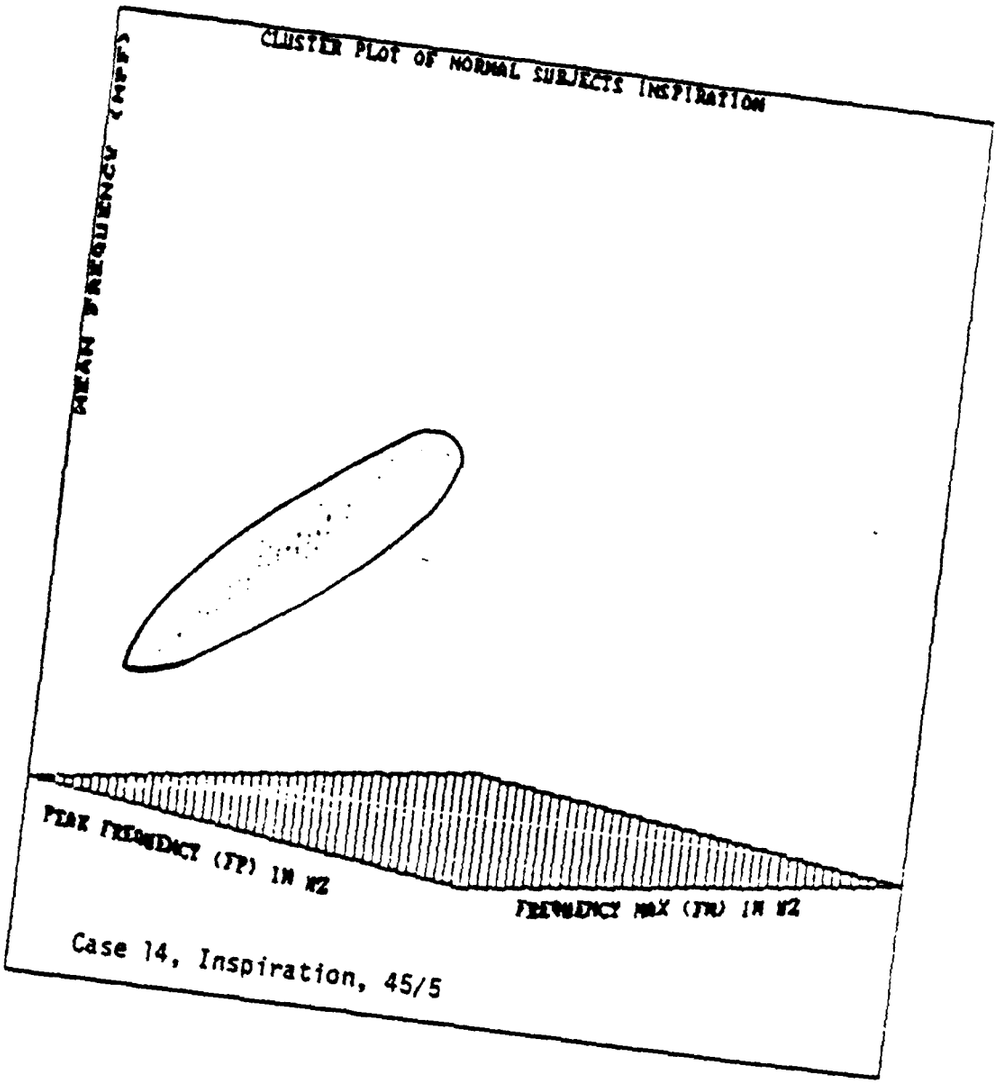

Case 14, Inspiration, 45/5

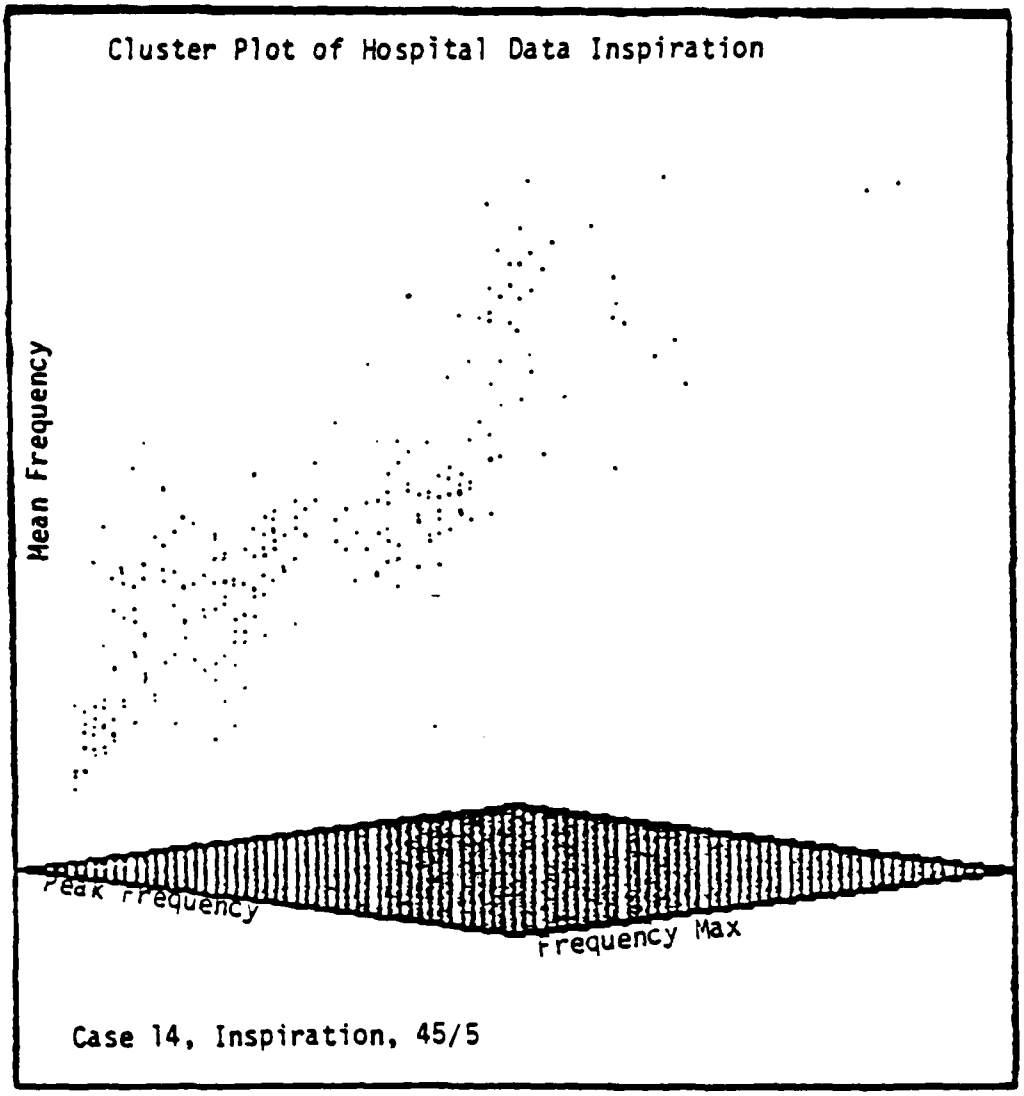
Cluster Plot of Hospital Data Inspiration
Mean Frequency
Peak Frequency
Frequency Max
Case 14, Inspiration, 45/5

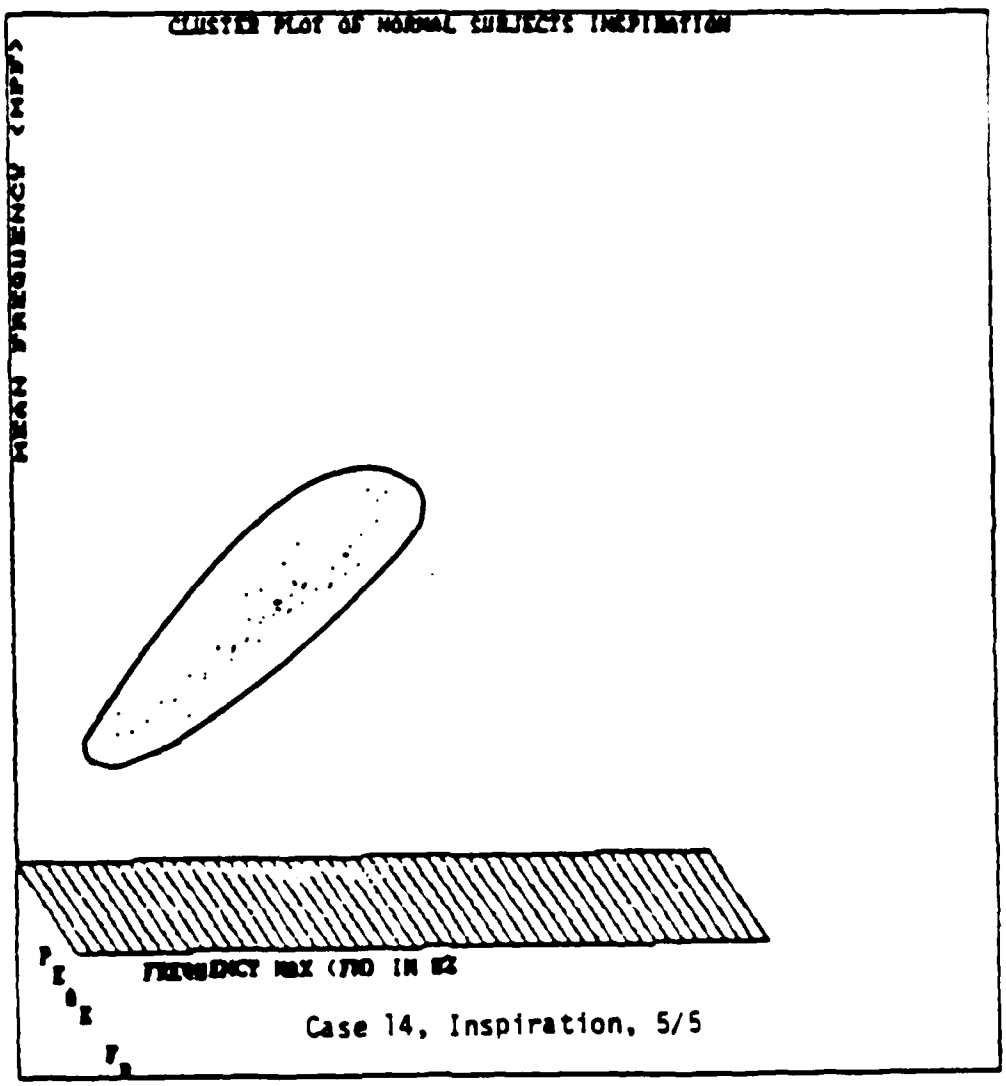
CLUSTER PLOT OF NORMAL SUBJECTS INSPIRATION
MEAN FREQUENCY (MPS)
FREQUENCY MAX (FFD IN HZ
Case 14, Inspiration, 5/5

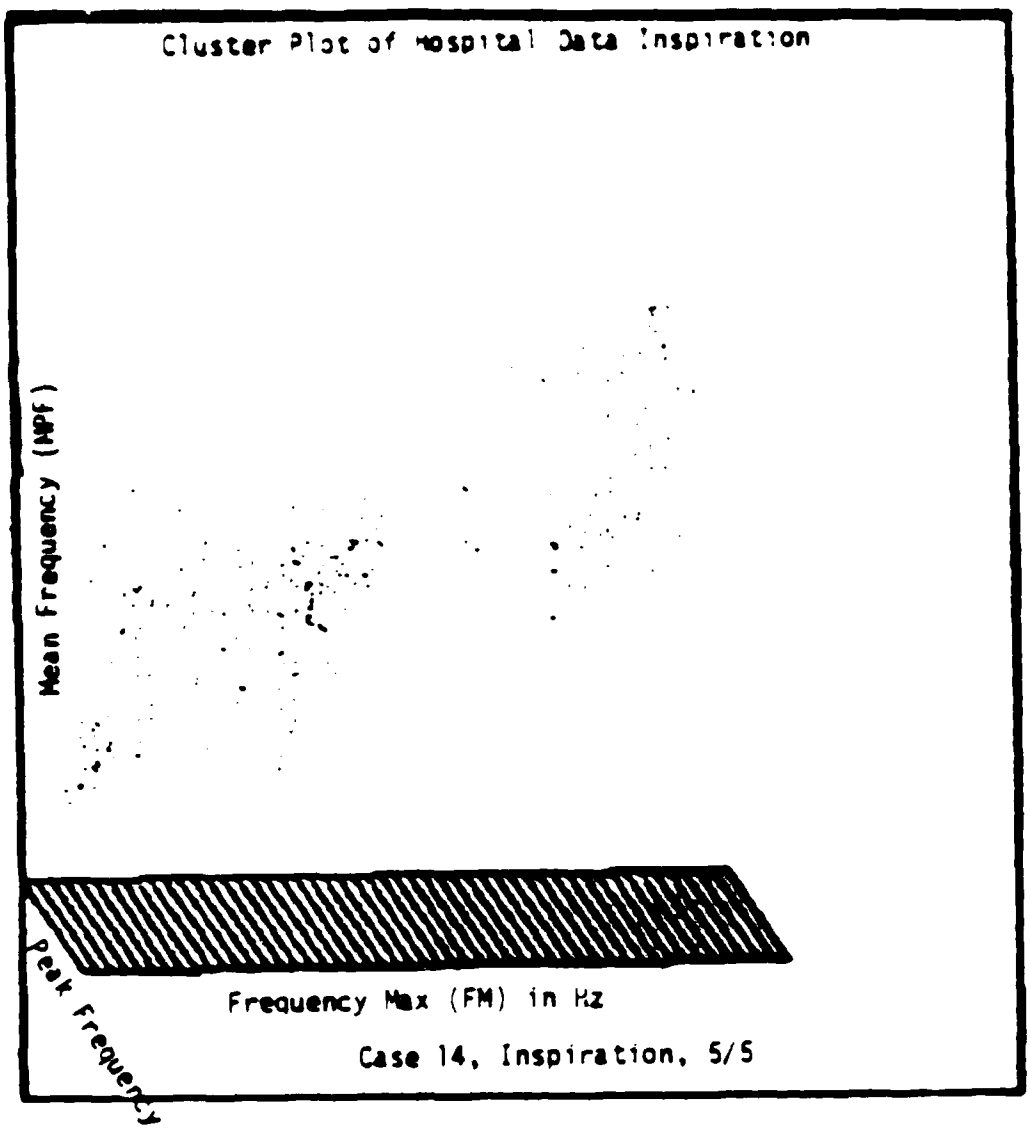
Cluster Plot of Hospital Data Inspiration
Mean Frequency (MPf)
Peak Frequency
Frequency Max (FM) in Hz
Case 14, Inspiration, 5/5

APPENDIX E

EXPIRATORY AND INSPIRATORY DATA

Expiration

```
COMMENT STATE  NORMAL= 1  ABNORMAL= 0:
INPUT ID $ FVC FEV1 FEV1P STATE FLOW MPF FPK FMAX;
CARDS;
 B   82  70  85  0    99      707.3  172.0 1480.0
 B   82  70  85  0   1.0      651.7  412.0  1476.0
 B   82  70  85  0    90      799.8  152.0  1440.0
 B   82  70  85  0    77      777.6  172.0  1468.0
 B   82  70  85  0    65      723.7  172.0  1448.0
 B   82  70  85  0  1.12      665.0  572.0  1488.0
 B   82  70  85  0  1.18      603.4  172.0  1068.0
 B   82  70  85  0  1.12      636.0  172.0  1364.0
 B   82  70  85  0  0.93      634.7  116.0  1472.0
 B   82  70  85  0    74      797.8  172.0  1404.0
 B   82  70  85  0    62      756.8  108.0  1388.0
 B   82  70  85  0    58      782.1  172.0  1456.0
 B   82  70  85  0    71      730.7  172.0  1464.0
 B   82  70  85  0    90      720.2  956.0  1048.0
 B   82  70  85  0  0.80      614.1  112.0  1044.0
 B   82  70  85  0    63      648.7  112.0  1456.0
 B   82  70  85  0    52      606.3  172.0  1300.0
 B   82  70  85  0    46      661.4  108.0  1456.0
 B   82  70  85  0    40      646.2  172.0  1404.0
 B   82  70  85  0    90      489.3  596.0   980.0
 B   82  70  85  0    80      479.1  620.0   680.0
 B   82  70  85  0    74      443.5  584.0   636.0
 B   82  70  85  0    62      454.6  288.0   700.0
 B   82  70  85  0    52      427.1  592.0   688.0
 B   82  70  85  0    44      278.9  112.0   604.0
 C   77  78  99  0    64      323.9  332.0   604.0
 C   77  78  99  0   1.1      414.1  412.0   684.0
 C   77  78  99  0  1.03      396.0  452.0   616.0
 C   77  78  99  0    83      429.5  436.0   624.0
 C   77  78  99  0    63      311.4  124.0   620.0
 C   77  78  99  0    65      354.5  468.0   612.0
 C   77  78  99  0    83      440.0  592.0   620.0
 C   77  78  99  0    97      441.5  472.0   632.0
 C   77  78  99  0    86      464.2  464.0   632.0
 C   77  78  99  0    70      384.8  480.0   620.0
 C   77  78  99  0    68      328.6  592.0   616.0
 C   77  78  99  0  1.00      475.5  600.0   620.0
 C   77  78  99  0  1.00      476.9  600.0   624.0
 C   77  78  99  0  1.00      447.8  604.0   604.0
 C   77  78  99  0    89      464.8  592.0   628.0
 C   77  78  99  0    73      414.3  608.0   632.0
 C   77  78  99  0    39      217.6   76.0   584.0
 C   77  78  99  0    99      475.8  600.0   620.0
 C   77  78  99  0    99      473.3  600.0   624.0
 C   77  78  99  0    99      459.9  604.0   604.0
 C   77  78  99  0    89      459.9  592.0   616.0
 C   77  78  99  0    73      336.6  104.0   620.0
 D  102 100  97  0    44      443.3  240.0  1360.0
 D  102 100  97  0    48      457.8  284.0   432.0
 D  102 100  97  0    45      495.6  172.0  1196.0
 D  102 100  97  0    45      434.7  260.0  1264.0
 D  102 100  97  0    41      432.3  240.0  1252.0
 D  102 100  97  0    52      270.5  100.0   392.0
 D  102 100  97  0    52      385.3  272.0  1292.0
 D  102 100  97  0    48      400.3  244.0  1336.0
 D  102 100  97  0    43      363.1  172.0   760.0
 D  102 100  97  0    57      278.2  292.0   660.0
 D  102 100  97  0    57      259.8  172.0   596.0
 D  102 100  97  0    56      276.4  240.0   600.0
 D  102 100  97  0    50      236.2  172.0   600.0
 D  102 100  97  0    47      288.9  160.0   612.0
 D  102 100  97  0    48      328.4  228.0   108.0
 D  102 100  97  0    45      311.0  236.0   632.0
 E   90  72  81  0    34      257.9   68.0   564.0
 E   90  72  81  0    40      305.8   96.0   604.0
 E   90  72  81  0    38      345.9  596.0   612.0
 E   90  72  81  0    37      129.5  104.0   128.0
 E   90  72  81  0    35      162.1  104.0   148.0
```

78.	E	90	72	81	0	.29	152.7	96.0	196.0	
79	E	90	72	81	0	.30	305.4	96.0	720.0	
80	E	90	72	81	0	.26	379.0	140.0	676.0	
81.	E	90	72	81	0	.28	473.2	676.0	692.0	
82.	E	90	72	81	0	290	558.7	676.0	724.0	
83.	E	90	72	81	0	.29	194.8	100.0	144.0	
84.	E	90	72	81	0	.31	215.9	112.0	496.0	
85.	E	90	72	81	0	.35	206.4	108.0	536.0	
86.	E	90	72	81	0	.30	184.5	92.0	184.0	
87.	E	90	72	81	0	.41	262.7	104.0	612.0	
88.	E	90	72	81	0	.46	223.6	212.0	548.0	
89.	E	90	72	81	0	.55	319.2	204.0	608.0	
90.	E	90	72	81	0	.51	285.5	192.0	604.0	
91.	E	90	72	81	0	.48	331.3	196.0	616.0	
92.	E	90	72	81	0	.28	154.4	92.0	176.0	
93	E	90	72	81	0	.43	296.4	108.0	608.0	
94	E	90	72	81	0	.43	206.0	104.0	608.0	
95.	E	90	72	81	0	.50	286.4	184.0	624.0	
96.	E	90	72	81	0	.52	289.2	208.0	620.0	
97	E	90	72	81	0	52	271.2	204.0	604.0	
98	E	90	72	81	0	.46	253.4	220.0	616.0	
99.	F	146	141	97	1	.47	150.0	100.0	168.0	
100.	F	146	141	97	1	.62	246.1	112.0	588.0	
101	F	146	141	97	1	53	211.2	100.0	576.0	
102.	F	146	141	97	1	54	129.4	100.0	148.0	
103.	F	146	141	97	1	.56	197.2	92.0	200.0	
104.	F	146	141	97	1	.52	203.8	104.0	492.0	
105.	F	146	141	97	1	.48	135.4	112.0	196.0	
106.	F	146	141	97	1	.73	181.1	120.0	236.0	
107.	F	146	141	97	1	.73	210.4	176.0	248.0	
108.	F	146	141	97	1	.68	181.6	160.0	220.0	
109.	F	146	141	97	1	.66	180.8	164.0	240.0	
110.	F	146	141	97	1	70	210.7	168.0	592.0	
111.	F	146	141	97	1	.75	189.8	156.0	444.0	
112.	F	146	141	97	1	.71	207.5	160.0	600.0	
113.	F	146	141	97	1	.58	149.9	88.0	456.0	
114.	F	146	141	97	1	52	164.2	152.0	476.0	
115.	F	146	141	97	1	45	192.2	100.0	284.0	
116.	F	146	141	97	1	.38	226.2	148.0	576.0	
117.	F	146	141	97	1	.31	216.6	176.0	604.0	
118.	F	146	141	97	1	.27	200.8	108.0	532.0	
119.	F	146	141	97	1	.31	238.5	116.0	632.0	
120.	F	146	141	97	1	.31	166.3	84.0	548.0	
121.	F	146	141	97	1	41	145.6	80.0	184.0	
122.	F	146	141	97	1	.44	151.3	108.0	240.0	
123.	F	146	141	97	1	.58	156.4	100.0	180.0	
124.	F	146	141	97	1	.64	175.0	112.0	188.0	
125.	F	146	141	97	1	.63	189.0	128.0	176.0	
126.	F	146	141	97	1	.66	203.2	136.0	464.0	
127.	F	146	141	97	1	.43	173.0	92.0	172.0	
128.	F	146	141	97	1	.47	175.4	88.0	168.0	
129.	G	91	78	118	0	63	180.8	132.0	264.0	
130.	G	91	78	118	0	.77	286.5	224.0	780.0	
131	G	91	78	118	0	.87	249.5	176.0	696.0	
132.	G	91	78	118	0	.85	253.5	156.0	720.0	
133.	G	91	78	118	0	.77	201.3	84.0	252.0	
134.	G	91	78	118	0	.52	117.7	80.0	124.0	
135.	G	91	78	118	0	.89	324.4	204.0	608.0	
136.	G	91	78	118	0	1.05	338.3	216.0	788.0	
137	G	91	78	118	0	.97	341.4	176.0	620.0	
138.	G	91	78	118	0	.74	356.9	212.0	668.0	
139.	G	91	78	118	0	.60	405.2	168.0	760.0	
140.	G	91	78	118	0	.45	318.7	108.0	720.0	
141	G	91	78	118	0	.48	330.2	204.0	772.0	
142.	G	91	78	118	0	.69	330.9	200.0	768.0	
143	G	91	78	118	0	64	370.0	172.0	708.0	
144	G	91	78	118	0	50	370.4	168.0	752.0	
145	G	91	78	118	0	19	338.3	196.0	728.0	
146	G	91	78	118	0	19	320.6	188.0	716.0	
147	G	91	78	118	0	48	309.3	164.0	696.0	
148	G	91	78	118	0	69	190.7	108.0	176.0	
149	G	91	78	118	0	64	179.2	100.0	184.0	

150	M	114	110	96	1	75	446.9	172.0	260.0	
151	M	114	110	96	1	85	452.7	108.0	260.0	
152	M	114	110	96	1	78	460.5	172.0	260.0	
153	M	114	110	96	1	63	364.5	112.0	260.0	
154	M	114	110	96	1	46	477.9	172.0	500.0	
155	M	114	110	96	1	35	444.0	112.0	776.0	
156	M	114	110	96	1	.21	442.5	260.0	1360.0	
157	M	114	110	96	1	.55	440.8	108.0	260.0	
158	M	114	110	96	1	60	482.0	124.0	1268.0	
159	M	114	110	96	1	.67	338.1	172.0	256.0	
160	M	114	110	96	1	.55	425.3	112.0	300.0	
161	M	114	110	96	1	.41	439.4	108.0	260.0	
162	M	114	110	96	1	.31	414.1	112.0	260.0	
163	M	114	110	96	1	.39	466.2	172.0	260.0	
164	M	114	110	96	1	.41	432.3	172.0	260.0	
165	M	114	110	96	1	41	415.7	112.0	260.0	
166	M	114	110	96	1	42	382.7	260.0	1400.0	
167	M	114	110	96	1	39	410.2	172.0	348.0	
168	M	114	110	96	1	52	316.9	172.0	260.0	
169	M	114	110	96	1	53	357.*	112.0	260.0	
170	M	114	110	96	1	59	429.2	172.0	260.0	
171	M	114	110	96	1	61	246.8	112.0	260.0	
172	M	114	110	96	1	61	367.8	172.0	260.0	
173	M	114	110	96	1	58	296.9	92.0	260.0	
174	I	112	118	105	1	.78	429.8	636.0	744.0	
175	I	112	118	105	1	.80	396.3	144.0	744.0	
176	I	112	118	105	1	.67	421.8	608.0	624.0	
177	I	112	118	105	1	.58	425.1	160.0	708.0	
178	I	112	118	105	1	.55	433.7	604.0	672.0	
179	I	112	118	105	1	42	431.1	604.0	736.0	
180	I	112	118	105	1	86	441.9	192.0	776.0	
181	I	112	118	105	1	80	446.2	604.0	712.0	
182	I	112	118	105	1	70	452.9	608.0	692.0	
183	I	112	118	105	1	67	458.3	628.0	704.0	
184	I	112	118	105	1	61	445.0	608.0	668.0	
185	I	112	118	105	1	51	316.2	112.0	628.0	
186	I	112	118	105	1	.29	397.1	112.0	772.0	
187	I	112	118	105	1	.56	379.1	84.0	744.0	
188	I	112	118	105	1	.61	431.9	612.0	708.0	
189	I	112	118	105	1	.62	451.4	608.0	748.0	
190	I	112	118	105	1	52	488.7	612.0	664.0	
191	I	112	118	105	1	46	386.8	96.0	748.0	
192	I	112	118	105	1	73	345.6	112.0	776.0	
193	I	112	118	105	1	81	514.6	668.0	784.0	
194	I	112	118	105	1	76	486.9	664.0	788.0	
195	I	112	118	105	1	.86	298.3	112.0	784.0	
196	I	112	118	105	1	.77	378.0	124.0	728.0	
197	I	112	118	105	1	.81	431.2	588.0	724.0	
198	K	102	105	104	1	47	331.5	188.0	608.0	
199	K	102	105	104	1	67	322.0	176.0	600.0	
200	K	102	105	104	1	71	365.2	496.0	608.0	
201	K	102	105	104	1	68	377.4	180.0	604.0	
202	K	102	105	104	1	55	288.9	172.0	600.0	
203	K	102	105	104	1	55	407.3	596.0	608.0	
204	K	102	105	104	1	62	363.6	588.0	616.0	
205	K	102	105	104	1	62	361.2	160.0	604.0	
206	K	102	105	104	1	52	319.8	596.0	612.0	
207	K	102	105	104	1	48	348.7	596.0	604.0	
208	K	102	105	104	1	58	412.0	476.0	596.0	
209	K	102	105	104	1	61	377.7	588.0	592.0	
210	K	102	105	104	1	58	379.6	588.0	612.0	
211	K	102	105	104	1	48	360.8	192.0	612.0	
212	K	102	105	104	1	30	354.1	472.0	616.0	
213	K	102	105	104	1	50	366.1	460.0	604.0	
214	K	102	105	104	1	51	350.8	168.0	604.0	
215	K	102	105	104	1	49	402.7	588.0	608.0	
216	K	102	105	104	1	48	409.1	592.0	600.0	
217	K	102	105	104	1	37	332.3	148.0	596.0	
218	L	110	102	92	1	72	366.3	464.0	592.0	
219	L	110	102	92	1	68	416.5	476.0	608.0	
220	L	110	102	92	1	63	421.8	524.0	600.0	
221	L	110	102	92	1	58	420.4	452.0	588.0	
222	L	110	102	92	1	62	440.6	500.0	604.0	

223	L	110	102	92	1	64	439 3	532 0	576 0	
224	L	110	102	92	1	64	41[illegible] 6	468 0	612 0	
225	L	110	102	92	1	57	39[illegible] 1	516 0	588 0	
226	L	110	102	92	1	56	439 6	516 0	572 0	
227	L	110	102	92	1	94	399 2	500 0	620 0	
228	L	110	102	92	1	90	376 8	488 0	596 0	
229	L	110	102	92	1	85	405 3	484 0	616 0	
230	L	110	102	92	1	79	40[illegible] 9	492 0	624 0	
231	L	110	102	92	1	75	409 9	[illegible]52 0	620 0	
232	L	110	102	92	1	74	385 3	496 0	560 0	
233	L	110	102	92	1	78	418 8	492 0	60[illegible] 0	
234	L	110	102	92	1	83	403 3	484 0	612 0	
235	L	110	102	92	1	76	407 7	460 0	600 0	
236	L	110	102	92	1	71	401 9	476 0	580 0	
237	L	110	102	92	1	67	421 3	492 0	608 0	
238	M	53	38	68	0	86	144 6	88 0	60[illegible] 0	
239	M	53	38	68	0	92	234 8	68 0	6[illegible]2 0	
240	M	53	38	68	0	94	216 5	108 0	604 0	
241	M	53	38	68	0	91	219 7	[illegible]2 0	608 0	
242	M	53	38	68	0	87	29[illegible] 7	92 0	604 0	
243	M	53	38	68	0	81	[illegible]98 7	[illegible]12 0	5[illegible]2 0	
244	M	53	38	68	0	74	214 5	96 0	432 0	
245	M	53	38	68	0	70	[illegible]60 4	[illegible]08 0	[illegible]36 0	
246	M	53	38	68	0	76	[illegible]73 3	80 0	596 0	
247	M	53	38	68	0	82	198 8	92 0	600 0	
248	M	53	38	68	0	81	165 2	72 0	116 0	
249	M	53	38	68	0	82	226 2	124 0	596 0	
250	M	53	38	68	0	84	[illegible]93 8	72 0	604 0	
251	M	53	38	68	0	84	238 5	108 0	596 0	
252	M	53	38	68	0	74	212 8	104 0	600 0	
253	M	53	38	68	0	46	[illegible]17 9	108 0	140 0	
254	M	53	38	68	0	86	228 0	88 0	604 0	
255	M	53	38	68	0	88	228 8	68 0	592 0	
256	M	53	38	68	0	1 12	35[illegible] 6	576 0	616 0	
257	M	53	38	68	0	1 14	287 8	84 0	616 0	
258	M	53	38	68	0	97	336 0	464 0	608 0	
259	M	53	38	68	0	91	265 8	100 0	596 0	
260	M	53	38	68	0	82	[illegible]71 2	92 0	140 0	
261	M	53	38	68	0	90	216 0	96 0	580 0	
262	M	53	38	68	0	86	279 3	88 0	596 0	
263	M	53	38	68	0	84	237 4	84 0	600 0	
264	M	53	38	68	0	81	[illegible]77 6	[illegible]00 0	6[illegible]2 0	
265	M	53	38	68	0	75	243 2	76 0	604 0	
266	N	91	97	107	1	39	325 1	172 0	608 0	
267	N	91	97	107	1	49	316 8	200 0	596 0	
268	N	91	97	107	1	54	306 7	212 0	616 0	
269	N	91	97	107	1	53	328 1	200 0	628 0	
270	N	91	97	107	1	50	382 6	596 0	612 0	
271	N	91	97	107	1	50	258 5	116 0	608 0	
272	N	91	97	107	1	50	354 4	596 0	616 0	
273	N	91	97	107	1	49	326 1	604 0	604 0	
274	N	91	97	107	1	44	348 7	172 0	612 0	
275	N	91	97	107	1	54	359 8	456 0	616 0	
276	N	91	97	107	1	57	340 9	[illegible]32 0	620 0	
277	N	91	97	107	1	56	346 0	[illegible]32 0	608 0	
278	N	91	97	107	1	50	39[illegible] 0	488 0	596 0	
279	N	91	97	107	1	45	498 2	608 0	[illegible]36 0	
280	N	91	97	107	1	56	339 2	280 0	616 0	
281	N	91	97	107	1	73	339 1	240 0	596 0	
282	N	91	97	107	1	76	35[illegible] 5	312 0	604 0	
283	N	91	97	107	1	71	344 4	[illegible]32 0	624 0	
284	N	91	97	107	1	70	352 5	264 0	68[illegible] 0	
285	N	91	97	107	1	65	297 4	468 0	564 0	
286	N	91	97	107	1	59	316 4	[illegible]20 0	596 0	
287	N	91	97	107	1	53	314 5	[illegible]12 0	608 0	
288	N	91	97	107	1	60	393 8	456 0	580 0	
289	N	91	97	107	1	81	375 1	528 0	624 0	
290	N	91	97	107	1	87	392 7	492 0	6[illegible]2 0	
291	N	91	97	107	1	91	372 8	440 0	628 0	
292	N	91	97	107	1	93	373	416 0	636 0	
293	N	91	97	107	1	87	373 1	468 0	620 0	

```
303.    INPUT ID $ FVC FEV1 FEV1P STATE FLOW MEF FPK FMAX.
304.    CARDS:
305.        P   73  32  44  0    1.14    247.6    96.0    280.0
306.        P   73  32  44  0    1.57    275.6   104.0    248.0
307.        P   73  32  44  0    1.61    192.4    80.0    272.0
308.        P   73  32  44  0    1.51    229.5    80.0    260.0
309.        P   73  32  44  0    1.31    300.5   100.0    324.0
310.        P   73  32  44  0    1.30    180.6   108.0    260.0
311.        P   73  32  44  0    1.13    154.1    80.0    172.0
312.        P   73  32  44  0    1.11    352.8    64.0    260.0
313.        P   73  32  44  0    1.05    236.4    60.0    172.0
314.        P   73  32  44  0    1.0     365.4   108.0    264.0
315.        P   73  32  44  0    1.17    436.5   172.0    260.0
316.        P   73  32  44  0    1.79    341.7   128.0   1016.0
317.        P   73  32  44  0    1.97    367.9   172.0    620.0
318.        P   73  32  44  0    1.91    351.6   148.0    592.0
319.        P   73  32  44  0    1.74    365.4    96.0   1316.0
320.        P   73  32  44  0    1.54    286.6   108.0    560.0
321.        P   73  32  44  0    1.31    312.0   104.0    580.0
322.        P   73  32  44  0    1.16    450.3   172.0   1376.0
323.        P   73  32  44  0    1.03    367.6   100.0    420.0
324.        P   73  32  44  0    0.95    336.5   172.0    600.0
325.        P   73  32  44  0    0.68    484.6   172.0   1164.0
326.        P   73  32  44  0    1.21    527.1   172.0   1376.0
327.        P   73  32  44  0    1.54    514.9   160.0   1416.0
328.        P   73  32  44  0    1.60    625.3   156.0   1376.0
329.        P   73  32  44  0    1.64    475.8   208.0   1360.0
330.        P   73  32  44  0    1.57    383.5   148.0    612.0
331.        P   73  32  44  0    1.40    397.5   172.0   1256.0
332.        P   73  32  44  0    1.32    459.0   160.0   1332.0
333.        P   73  32  44  0    1.12    490.7   172.0   1288.0
334.        P   73  32  44  0    1.08    439.7   172.0   1336.0
335.        P   73  32  44  0    0.65    581.9   172.0   1276.0
336.        P   73  32  44  0    1.44    554.5   180.0   1440.0
337.        P   73  32  44  0    1.88    604.6   120.0   1388.0
338.        P   73  32  44  0    1.72    478.9   196.0   1372.0
339.        P   73  32  44  0    1.57    364.1   108.0    532.0
340.        P   73  32  44  0    1.42    271.9   100.0    636.0
341.        P   73  32  44  0    1.34    473.0   172.0   1452.0
342.        P   73  32  44  0    1.21    436.6   172.0   1360.0
343.        P   73  32  44  0    1.10    379.1    80.0   1056.0
344.        P   73  32  44  0    1.05    565.2   292.0   1372.0
345.        *   72  58 124  0    1.12    140.2    92.0    120.0
346.        *   72  58 124  0    1.37     90.4    92.0    112.0
347.        *   72  58 124  0    1.23    241.7   100.0    140.0
348.        *   72  58 124  0    1.19    186.1    80.0    124.0
349.        *   72  58 124  0    1.29    152.6   112.0    180.0
350.        *   72  58 124  0    1.08    209.7   108.0    148.0
351.        *   72  58 124  0    0.80    190.6    72.0    140.0
352.        *   72  58 124  0    0.78    129.3    72.0    180.0
353.        *   72  58 124  0    0.62    116.4    64.0    128.0
354.        *   72  58 124  0    0.99    121.2   108.0    188.0
355.        *   72  58 124  0    1.46    133.1    88.0    128.0
356.        *   72  58 124  0    1.52    135.6   104.0    188.0
357.        *   72  58 124  0    1.35    138.4   120.0    164.0
358.        *   72  58 124  0    1.38    114.4   104.0    152.0
359.        *   72  58 124  0    1.23    133.0    88.0    192.0
360.        *   72  58 124  0    0.84    124.6   112.0    156.0
361.        *   72  58 124  0    0.92    127.7    88.0    148.0
362.        *   72  58 124  0    1.55    110.4    96.0    136.0
363.        *   72  58 124  0    1.42    113.4    96.0    140.0
364.        *   72  58 124  0    1.65    132.6    96.0    164.0
365.        *   72  58 124  0    1.74    112.4    96.0    172.0
366.        *   72  58 124  0    1.31    103.0   104.0    120.0
367.        *   72  58 124  0    1.03    144.9   104.0    144.0
368.        *   72  58 124  0    0.91    123.1    68.0    176.0
369.        *   72  58 124  0    0.64    106.4    80.0    112.0
```

370.	•	72	58	124	0	0 71	44 4	88 0	136 0
371.	•	72	58	124	0	0 85	110 2	84 0	132 0
372.	•	72	58	124	0	0 90	109 5	84 0	144 0
373.	•	72	58	124	0	0 94	109 5	92 0	144 0
374.	•	72	58	124	0	1 01	103 9	104 0	160 0
375.	•	72	58	124	0	1 07	127 6	112 0	160 0
376.	•	72	58	124	0	1 11	118 5	96 0	168 0
377.	•	72	58	124	0	1 04	117 8	84 0	140.0
378.	•	99	105	105	1	0 69	431 7	112.0	260.0
379.	•	99	105	105	1	1 06	413 2	112.0	124 0
380.	•	99	105	105	1	1.22	592 8	260.0	1408 0
381.	•	99	105	105	1	1.22	421 0	112.0	260.0
382.	•	99	105	105	1	1 14	473 2	108 0	484 0
383.	•	99	105	105	1	1.14	373 5	112.0	172.0
384.	•	99	105	105	1	1 13	534 5	112 0	1316 0
385.	•	99	105	105	1	1 15	519 9	112.0	260 0
386.	•	99	105	105	1	1 18	531 5	112 0	1036 0
387.	•	99	105	105	1	1 29	603 6	108 0	1476 0
388.	•	99	105	105	1	1 29	394 7	112 0	124 0
389.	•	99	105	105	1	1 28	476 2	112 0	776 0
390.	•	99	105	105	1	1 26	478 9	112.0	560 0
391.	•	99	105	105	1	1 20	471 8	112 0	1280 0
392.	•	99	105	105	1	1 18	342 4	108 0	260 0
393.	•	99	105	105	1	1 04	536 3	260 0	1376 0
394.	•	99	105	105	1	1.27	459 5	108.0	256.0
395.	•	99	105	105	1	1 24	562.2	108.0	1312.0
396.	•	99	105	105	1	1 27	535.5	112.0	1332.0
397.	•	99	105	105	1	1.21	543.2	172.0	1372.0
398.	•	99	105	105	1	1 15	560.3	172.0	1344.0
399.	•	99	105	105	1	1.08	389.9	108.0	260.0
400.	•	99	105	105	1	1.07	538 4	172.0	512.0
401.	•	99	105	105	1	0 75	575 6	108.0	1280.0
402.	•	99	105	105	1	1.05	523.8	112.0	260.0
403.	•	99	105	105	1	1.05	484.6	172.0	1316.0
404.	•	99	105	105	1	1.08	361.0	112.0	172.0
405.	•	99	105	105	1	1.13	419.3	108.0	172.0
406.	•	99	105	105	1	1.16	463.6	112.0	260.0
407.	•	99	105	105	1	1.07	524 8	112.0	500.0
408.	#	70	74	106	0	0.46	386.5	116.0	1372.0
409.	#	70	74	106	0	0.64	414 9	112.0	588.0
410.	#	70	74	106	0	0.71	404.2	176.0	652.0
411.	#	70	74	106	0	0 80	400.1	92.0	632.0
412.	#	70	74	106	0	0.89	378.8	156.0	724.0
413.	#	70	74	106	0	0.95	401.1	132.0	672.0
414.	#	70	74	106	0	0.92	391.3	144.0	1180.0
415.	#	70	74	106	0	0.98	170.1	80.0	152.0
416.	#	70	74	106	0	0.97	291.1	116.0	260.0
417.	#	70	74	106	0	0.59	188.0	72.0	260.0
418.	#	70	74	106	0	0.74	127.6	84.0	172.0
419.	#	70	74	106	0	0.92	244.9	152.0	568.0
420.	#	70	74	106	0	0.97	202.7	92.0	260.0
421.	#	70	74	106	0	0.99	219.4	148.0	572.0
422.	#	70	74	106	0	0.96	254.2	92.0	568.0
423.	#	70	74	106	0	0.88	286.4	136.0	604.0
424.	#	70	74	106	0	0.84	249.1	72.0	556.0
425.	#	70	74	106	0	0.94	163.5	124.0	168.0
426.	#	70	74	106	0	0.70	417.1	112.0	640.0
427.	#	70	74	106	0	0.92	289 0	116.0	372 0
428.	#	70	74	106	0	1.05	368.5	116.0	596.0
429.	#	70	74	106	0	1.22	451 9	116.0	676.0
430.	#	70	74	106	0	1 20	438.5	108.0	652 0
431.	#	70	74	106	0	1 18	497.3	556.0	676.0
432.	#	70	74	106	0	1.02	459 5	576.0	644.0
433.	#	70	74	106	0	0.97	465 0	88.0	1136 0
434.	#	70	74	106	0	1 14	357 5	112 0	568.0
435.	#	70	74	106	0	0.27	361 7	108 0	260 0
436.	#	70	74	106	0	0 38	360 9	92.0	1144.0
437.	#	70	74	106	0	0 68	451 5	108 0	676 0
438.	#	70	74	106	0	0 85	414 2	100 0	1352 0
439.	#	70	74	106	0	1 05	435 2	108 0	1144 0
440.	#	70	74	106	0	1 27	359 3	148 0	568 0
441.	#	70	74	106	0	1 19	402 4	144 0	632 0
442.	#	70	74	106	0	1 13	417 8	492 0	1148 0
443.	#	70	74	106	0	1 08	388 0	112 0	632 0

444.	Q	102	83	81	0	1.10	279.3	80.0	600.0
445.	Q	102	83	81	0	1.70	417.0	600.0	608.0
446.	Q	102	83	81	0	1.65	337.0	584.0	616.0
447.	Q	102	83	81	0	1.40	246.2	92.0	600.0
448.	Q	102	83	81	0	1.10	142.2	88.0	600.0
449.	Q	102	83	81	0	0.82	217.7	96.0	600.0
450.	Q	102	83	81	0	0.60	146.9	116.0	600.0
451.	Q	102	83	81	0	0.43	95.2	64.0	600.0
452.	Q	102	83	81	0	0.23	131.0	124.0	600.0
453.	Q	102	83	81	0	1.03	147.8	68.0	600.0
454.	Q	102	83	81	0	1.53	288.4	600.0	600.0
455.	Q	102	83	81	0	1.63	306.3	92.0	612.0
456.	Q	102	83	81	0	1.39	195.7	80.0	604.0
457.	Q	102	83	81	0	1.11	249.5	96.0	608.0
458.	Q	102	83	81	0	0.84	107.0	76.0	104.0
459.	Q	102	83	81	0	0.61	244.1	84.0	600.0
460.	Q	102	83	81	0	0.41	148.4	112.0	600.0
461.	Q	102	83	81	0	0.33	97.5	60.0	108.0
462.	Q	102	83	81	0	1.01	161.5	84.0	600.0
463.	Q	102	83	81	0	1.69	319.7	88.0	620.0
464.	Q	102	83	81	0	1.79	315.3	96.0	612.0
465.	Q	102	83	81	0	1.52	177.3	72.0	604.0
466.	Q	102	83	81	0	1.16	217.4	92.0	600.0
467.	Q	102	83	81	0	0.91	118.0	64.0	164.0
468.	Q	102	83	81	0	0.68	281.1	600.0	600.0
469.	Q	102	83	81	0	0.48	171.9	128.0	600.0
470.	Q	102	83	81	0	0.32	101.1	72.0	600.0
471.	Q	102	83	81	0	0.77	112.9	64.0	132.0
472.	Q	102	83	81	0	1.52	311.3	104.0	628.0
473.	Q	102	83	81	0	1.65	272.1	76.0	612.0
474.	Q	102	83	81	0	1.57	350.1	204.0	616.0
475.	Q	102	83	81	0	1.32	273.9	92.0	604.0
476.	Q	102	83	81	0	1.06	153.8	108.0	600.0
477.	Q	102	83	81	0	0.73	249.1	88.0	600.0
478.	Q	102	83	81	0	0.49	190.1	600.0	600.0
479.	Q	102	83	81	0	0.36	98.0	64.0	600.0
480.	X	93	78	85	0	1.11	290.3	160.0	732.0
481.	X	93	78	85	0	1.34	356.5	196.0	772.0
482.	X	93	78	85	0	1.05	272.3	120.0	624.0
483.	X	93	78	85	0	0.92	323.5	96.0	688.0
484.	X	93	78	85	0	0.79	268.1	156.0	636.0
485.	X	93	78	85	0	0.57	328.5	188.0	648.0
486.	X	93	78	85	0	1.00	240.0	104.0	604.0
487.	X	93	78	85	0	0.88	262.1	116.0	560.0
488.	X	93	78	85	0	0.78	199.0	96.0	180.0
489.	X	93	78	85	0	0.61	174.6	80.0	120.0
490.	X	93	78	85	0	0.87	235.5	136.0	600.0
491.	X	93	78	85	0	0.78	230.5	108.0	260.0
492.	X	93	78	85	0	0.74	222.9	96.0	416.0
493.	X	93	78	85	0	0.65	141.0	112.0	164.0
494.	X	93	78	85	0	0.52	206.0	100.0	260.0
495.	X	93	78	85	0	0.41	277.2	104.0	448.0
496.	X	93	78	85	0	0.85	248.5	112.0	520.0
497.	X	93	78	85	0	0.89	217.2	100.0	496.0
498.	X	93	78	85	0	0.83	271.2	88.0	596.0
499.	X	93	78	85	0	0.72	182.6	96.0	172.0
500.	V	101	106	104	1	1.11	132.2	88.0	144.0
501.	V	101	106	104	1	1.73	208.8	108.0	396.0
502.	V	101	106	104	1	1.74	203.8	116.0	180.0
503.	V	101	106	104	1	1.57	206.1	104.0	160.0
504.	V	101	106	104	1	1.42	223.9	96.0	348.0
505.	V	101	106	104	1	1.27	146.7	100.0	144.0
506.	V	101	106	104	1	1.06	162.8	112.0	160.0
507.	V	101	106	104	1	0.87	150.2	104.0	164.0
508.	V	101	106	104	1	1.51	434.6	628.0	648.0
509.	V	101	106	104	1	1.61	336.6	628.0	644.0
510.	V	101	106	104	1	1.43	343.6	620.0	636.0
511.	V	101	106	104	1	1.23	387.7	628.0	632.0
512.	V	101	106	104	1	1.03	298.0	620.0	640.0
513.	V	101	106	104	1	0.83	237.9	116.0	628.0
514.	V	101	106	104	1	1.92	353.9	104.0	740.0
515.	V	101	106	104	1	2.07	362.8	120.0	636.0

516.	V	101	106	104	1	1 35	328 1	116 0	636 0
517.	V	101	106	104	1	0 99	283 4	116 0	636.0
518.	V	101	106	104	1	0.66	225 5	104 0	628.0
519.	V	101	106	104	1	1 66	426.3	620 0	640.0
520.	V	101	106	104	1	1 61	396.7	616 0	628 0
521.	V	101	106	104	1	1 04	369 1	620.0	628.0
522.	V	101	106	104	1	0 69	271.8	616.0	624 0
523.	V	101	106	104	1	0.51	238 4	108.0	624.0
524.	W	107	114	106	1	0 26	343.3	108.0	260.0
525.	W	107	114	106	1	0.41	300.1	112.0	260.0
526.	W	107	114	106	1	0 48	352.4	108.0	260.0
527.	W	107	114	106	1	0.46	341 7	128.0	520.0
528.	W	107	114	106	1	0.37	295.5	108.0	260.0
529.	W	107	114	106	1	0.29	313.5	112.0	260.0
530.	W	107	114	106	1	0.63	475.7	260.0	1404
531.	W	107	114	106	1	0.55	430.0	180.0	1212.0
532.	W	107	114	106	1	0.78	395.1	260.0	1056.0
533.	W	107	114	106	1	0 78	231 6	124.0	288.0
534.	W	107	114	106	1	0.56	348.2	176.0	528.0
535.	W	107	114	106	1	0.35	148.9	84.0	192.0
536.	W	107	114	106	1	0.53	211 3	124 0	320.0
537.	W	107	114	106	1	0.49	205.4	120.0	260.0
538.	W	107	114	106	1	0.49	270 6	172.0	384.0
539.	W	107	114	106	1	0.43	381.6	172.0	388 0
540.	W	107	114	106	1	0.34	323 4	84.0	260.0
541.	W	107	114	106	1	0.34	244 8	148.0	348.0
542.	W	107	114	106	1	0.54	250.4	88.0	600.0
543.	W	107	114	106	1	0.55	297.9	140.0	632.0
544.	W	107	114	106	1	0.47	232.4	116.0	364.0
545.	W	107	114	106	1	0.36	288.8	108.0	628.0
546.	S	92	95	103	0	1.05	227.4	96.0	260.0
547.	S	92	95	103	0	1.35	238.8	92.0	260.0
548.	S	92	95	103	0	1.38	267.9	120.0	260.0
549.	S	92	95	103	0	1.25	262.9	100.0	536.0
550.	S	92	95	103	0	1.03	316.6	56.0	1328.0
551.	S	92	95	103	0	0.83	593.5	120.0	1356.0
552.	S	92	95	103	0	0.88	354 1	120.0	1340.0
553.	S	92	95	103	0	0.88	129.6	100.0	168.0
554.	S	92	95	103	0	1.14	516.1	92.0	976.0
555.	S	92	95	103	0	1 04	329.7	76.0	772.0
556.	S	92	95	103	0	0.86	221.3	112.0	496.0
557.	S	92	95	103	0	0.80	543.7	600.0	952.0
558.	S	92	95	103	0	0.74	284.8	80.0	776.0
559.	S	92	95	103	0	0.61	202.3	120.0	260.0
560.	S	92	95	103	0	1.17	361.8	120.0	260.0
561.	S	92	95	103	0	1.58	291.7	120.0	604.0
562.	S	92	95	103	0	1.68	360.3	108.0	760.0
563.	S	92	95	103	0	1.58	423.3	580.0	836.0
564.	S	92	95	103	0	1.49	400.2	120.0	660.0
565.	S	92	95	103	0	1.25	351.5	120.0	260.0
566.	S	92	95	103	0	0.80	384.7	120.0	260.0
567.	S	92	95	103	0	1.68	695.6	120.0	1392.0
568.	S	92	95	103	0	1.80	636.0	120.0	1428.0
569.	S	92	95	103	0	1.50	581.1	120.0	260.0
570.	S	92	95	103	0	1.22	362.8	120.0	612.0
571.	S	92	95	103	0	1.00	266.2	120.0	260.0
572.	S	92	95	103	0	0.94	292.6	88.0	260.0
573.	T	83	76	91	0	0.64	225.1	104.0	560.0
574.	T	83	76	91	0	0.99	127 3	96.0	120.0
575.	T	83	76	91	0	1.12	389.4	588.0	616.0
576.	T	83	76	91	0	1.30	402.6	584.0	612.0
577.	T	83	76	91	0	1.26	158.4	92.0	588.0
578.	T	83	76	91	0	1.05	413.6	588.0	608.0
579.	T	83	76	91	0	1.05	241.0	80.0	588.0
580.	T	83	76	91	0	0.89	328.8	592.0	592.0
581.	T	83	76	91	0	0.66	257.3	76.0	596.0
582.	T	83	76	91	0	0.22	94.6	84.0	112.0
583.	T	83	76	91	0	0.94	354.8	588.0	596.0
584.	T	83	76	91	0	1.20	323.0	592.0	608.0
585.	T	83	76	91	0	1.48	399.8	584.0	612.0
586.	T	83	76	91	0	1.48	234.2	84.0	600.0
587.	T	83	76	91	0	1.25	414.6	588.0	600.0
588.	T	83	76	91	0	0.99	193.6	112.0	584.0
589	T	83	76	91	0	0.96	114.4	80.0	592.0
590	T	83	76	91	0	0.69	393.4	592.0	604.0

591	T	83	76	91	C	0.84	128.8	100.0	112.0
592	T	83	76	91	0	1.05	357.2	584.0	604.0
593	T	83	76	91	0	1.29	317.9	228.0	608.0
594	T	83	76	91	0	1.38	155.4	88.0	456.0
595	T	83	76	91	0	1.34	364.3	584.0	616.0
596	T	83	76	91	0	1.08	235.7	92.0	592.0
597	T	83	76	91	0	0.83	368.1	592.0	608.0
598	T	83	76	91	0	0.67	318.9	76.0	600.0
599	T	83	76	91	0	0.28	121.5	76.0	148.0
600	T	83	76	91	0	0.85	390.3	592.0	592.0
601	T	83	76	91	0	1.12	360.3	584.0	592.0
602	T	83	76	91	0	1.32	305.8	124.0	600.0
603	T	83	76	91	0	1.26	379.4	584.0	596.0
604	T	83	76	91	0	1.15	249.2	96.0	596.0
605	T	83	76	91	0	1.08	198.9	116.0	588.0
606	T	83	76	91	0	1.02	397.2	588.0	600.0
607	T	83	76	91	0	0.95	253.2	100.0	592.0
608	T	83	76	91	0	0.54	165.5	100.0	592.0
609	U	73	66	90	0	0.91	156.0	96.0	260.0
610	U	73	66	90	0	0.88	222.3	172.0	560.0
611	U	73	66	90	0	1.06	234.4	84.0	260.0
612	U	73	66	90	0	1.29	129.7	108.0	148.0
613	U	73	66	90	0	1.32	156.5	88.0	260.0
614	U	73	66	90	0	0.91	262.0	96.0	520.0
615	U	73	66	90	0	0.68	114.7	104.0	172.0
616	U	73	66	90	0	0.96	118.4	92.0	100.0
617	U	73	66	90	0	1.01	158.3	72.0	260.0
618	U	73	66	90	0	1.03	137.5	100.0	160.0
619	U	73	66	90	0	0.99	114.2	80.0	124.0
620	U	73	66	90	0	0.89	102.9	80.0	172.0
621	U	73	66	90	0	0.90	102.1	96.0	136.0
622	U	73	66	90	0	0.99	115.1	92.0	132.0
623	U	73	66	90	0	0.99	134.2	104.0	172.0
624	U	73	66	90	0	0.99	96.9	96.0	112.0
625	U	73	66	90	0	1.07	115.0	96.0	168.0
626	U	73	66	90	0	0.39	173.9	116.0	260.0
627	U	73	66	90	0	0.97	131.5	80.0	260.0
628	U	73	66	90	0	1.24	173.3	96.0	260.0
629	U	73	66	90	0	1.37	106.4	68.0	128.0
630	U	73	66	90	0	1.27	112.8	80.0	120.0
631	U	73	66	90	0	0.90	169.0	96.0	260.0
632	Y	101	113	113	1	0.59	432.5	112.0	172.0
633	Y	101	113	113	1	0.70	442.8	112.0	236.0
634	Y	101	113	113	1	0.78	523.5	108.0	1348.0
635	Y	101	113	113	1	0.78	411.5	108.0	204.0
636	Y	101	113	113	1	0.74	402.5	112.0	228.0
637	Y	101	113	113	1	0.65	428.5	172.0	1364.0
638	Y	101	113	113	1	0.64	484.4	112.0	532.0
639	Y	101	113	113	1	0.58	381.1	108.0	176.0
640	Y	101	113	113	1	0.52	442.1	112.0	172.0
641	Y	101	113	113	1	1.15	170.6	100.0	268.0
642	Y	101	113	113	1	1.55	303.6	252.0	580.0
643	Y	101	113	113	1	1.32	184.5	88.0	380.0
644	Y	101	113	113	1	1.18	246.5	164.0	612.0
645	Y	101	113	113	1	1.01	136.0	104.0	156.0
646	Y	101	113	113	1	0.78	166.9	76.0	196.0
647	Y	101	113	113	1	0.63	130.2	116.0	144.0
648	Y	101	113	113	1	0.48	138.6	80.0	168.0
649	Y	101	113	113	1	1.28	171.0	96.0	152.0
650	Y	101	113	113	1	1.58	278.1	88.0	672.0
651	Y	101	113	113	1	1.47	202.5	92.0	504.0
652	Y	101	113	113	1	1.30	234.7	76.0	508.0
653	Y	101	113	113	1	1.19	166.4	88.0	244.0
654	Y	101	113	113	1	1.03	190.2	92.0	268.0
655	Y	101	113	113	1	0.89	143.5	120.0	168.0
656	Y	101	113	113	1	0.75	130.9	92.0	140.0
657	Y	101	113	113	1	1.34	305.2	88.0	736.0
658	Y	101	113	113	1	1.57	245.7	112.0	616.0
659	Y	101	113	113	1	1.28	229.2	160.0	328.0
660	Y	101	113	113	1	1.11	144.7	108.0	280.0
661	Y	101	113	113	1	0.95	171.3	88.0	260.0
662	Y	101	113	113	1	0.86	111.5	104.0	148.0
663	Y	101	113	113	1	0.74	107.6	84.0	160.0
664	Y	101	113	113	1	0.61	111.0	76.0	152.0

Inspiration:

```
COMMENT STATE NORMAL=1, ABNORMAL=0;
TITLE POWER SPECTRA DATA OF INSPIRATORY SOUND;
INPUT ID $ FVC FEV1 FEV1P STATE FLOW MPF FPK FMAX;
CARDS;
B  82  70  85  0  1.41   902.7  1492  1496
B  82  70  85  0  1.41   704.2   256  1496
B  82  70  85  0  1.08   842     404  1488
B  82  70  85  0   .84   949.1   424  1464
B  82  70  85  0  1.37   784.5  1472  1488
B  82  70  85  0  1.42   963    1476  1480
B  82  70  85  0  1.32   853.9  1436  1496
B  82  70  85  0  1.08   970     172  1496
B  82  70  85  0   .77  1017    1460  1492
B  82  70  85  0  1.20   727.4   260  1464
B  82  70  85  0  1.41   847.5   172  1496
B  82  70  85  0  1.30   951.5   240  1488
B  82  70  85  0  1.08  1129    1468  1496
B  82  70  85  0  1.06   937.7   260  1496
B  82  70  85  0  1.38   870.1   112  1496
B  82  70  85  0  1.21   909.2  1320  1492
B  82  70  85  0  1.00   869.2   172  1496
C  77  78  99  0  1.34   402.7   452   664
C  77  78  99  0  1.34   369.7   464   592
C  77  78  99  0  1.30   329.3   104   588
C  77  78  99  0  1.20   399.4   444   716.0
C  77  78  99  0  1.12   430.7   696   736.0
C  77  78  99  0  1.09   454.2   688   732.0
C  77  78  99  0  0.99   455.4   600.0 608.0
C  77  78  99  0  0.98   442.0   568.0 648.0
C  77  78  99  0  1.40   444.8   588.0 788.0
C  77  78  99  0  1.40   419.4   436.0 636.0
C  77  78  99  0  1.29   395.2   472.0 620.0
C  77  78  99  0  1.24   421.7   160.0 744.0
C  77  78  99  0  1.13   427.9   680.0 684.0
D 102 100  97  0  1.00   371.7   108.0  180.0
D 102 100  97  0  1.27   499.1   100.0 1468.0
D 102 100  97  0  1.15   423.3   104.0 1336.0
D 102 100  97  0  1.02   672.0   172.0 1488.0
D 102 100  97  0   .74   500.2   120.0 1432.0
D 102 100  97  0  1.19   470.6   100.0 1432.0
D 102 100  97  0  1.36   579.0   100.0 1452.0
D 102 100  97  0  1.27   396.0   104.0  432.0
D 102 100  97  0  1.04   340.7   104.0  260.0
D 102 100  97  0   .99   614.9   740.0 1360.0
D 102 100  97  0  1.44   560.7   712.0  904.0
D 102 100  97  0  1.41   458.1   112.0  896.0
D 102 100  97  0  1.19   413.3   104.0  212.0
D 102 100  97  0   .75   643.1   124.0 1460.0
D 102 100  97  0  1.25   394.9   604.0  796.0
D 102 100  97  0  1.54   258.8   180.0  600.0
D 102 100  97  0  1.39   223.6   104.0  608.0
D 102 100  97  0  1.19   255.3   108.0  704.0
D 102 100  97  0   .84   372.9   604.0  612.0
E  90  72  81  0  1.00   364.6   104.0  648.0
E  90  72  81  0  1.07   390.1   616.0  708.0
E  90  72  81  0  1.08   368.1   216.0  704.0
E  90  72  81  0   .84   356.1   116.0  700.0
E  90  72  81  0   .80   323.5   104.0  612.0
E  90  72  81  0  1.18   354.1   200.0  624.0
E  90  72  81  0  1.21   351.9   508.0  624.0
E  90  72  81  0  1.16   318.7   208.0  624.0
E  90  72  81  0  1.10   302.5   100.0  600.0
E  90  72  81  0   .97   414.2   612.0  724.0
E  90  72  81  0  1.15   430.0   608.0  748.0
E  90  72  81  0  1.14   412.7   192.0  744.0
E  90  72  81  0  1.13   383.7   104.0  724.0
E  90  72  81  0  1.05   405.1   108.0  700.0
E  90  72  81  0  1.01   378.0   208.0  716.0
E  90  72  81  0  1.25   372.0   100.0  692.0
E  90  72  81  0  1.33   404.3   224.0  708.0
E  90  72  81  0  1.29   419.1   228.0  740.0
E  90  72  81  0  1.09   365.7   200.0  628.0
```

78	F	146	141	97	1	.50	315.4	100.0	512.0
79	F	146	141	97	1	.82	242.8	120.0	192.0
80	F	146	141	97	1	1.12	288.2	104.0	568.0
81	F	146	141	97	1	1.51	274.0	104.0	588.0
82	F	146	141	97	1	1.60	277.2	108.0	520.0
83	F	146	141	97	1	1.74	400.0	100.0	1032.0
84	F	146	141	97	1	0.64	310.3	112.0	172.0
85	F	146	141	97	1	1.28	314.0	104.0	556.0
86	F	146	141	97	1	1.66	263.6	100.0	516.0
87	F	146	141	97	1	1.87	404.1	120.0	1048.0
88	F	146	141	97	1	1.88	620.1	1028.0	1036.0
89	F	146	141	97	1	1.88	624.7	1028.0	1036.0
90	F	146	141	97	1	1.80	216.2	104.0	176.0
91	F	146	141	97	1	.45	380.4	100.0	692.0
92	F	146	141	97	1	.72	302.5	100.0	628.0
93	F	146	141	97	1	.83	259.9	100.0	612.0
94	F	146	141	97	1	1.07	291.9	100.0	600.0
95	F	146	141	97	1	1.42	361.5	168.0	1228.0
96	F	146	141	97	1	1.66	303.7	104.0	592.0
97	F	146	141	97	1	1.65	314.4	136.0	604.0
98	F	146	141	97	1	1.58	172.6	100.0	172.0
99	F	146	141	97	1	1.48	224.4	120.0	492.0
100	F	146	141	97	1	.66	308.5	100.0	256.0
101	F	146	141	97	1	.98	264.7	100.0	456.0
102	F	146	141	97	1	1.1	300.8	104.0	584.0
103	F	146	141	97	1	1.27	302.0	100.0	580.0
104	F	146	141	97	1	1.40	258.8	120.0	604.0
105	F	146	141	97	1	1.70	287.1	104.0	600.0
106	G	91	78	118	0	.15	434.5	612.0	736.0
107	G	91	78	118	0	.46	343.8	104.0	728.0
108	G	91	78	118	0	1.1	482.2	160.0	1020.0
109	G	91	78	118	0	1.2	427.7	228.0	716.0
110	G	91	78	118	0	1.27	404.6	192.0	716.0
111	G	91	78	118	0	1.46	343.7	208.0	712.0
112	G	91	78	118	0	1.50	484.0	236.0	1024.0
113	G	91	78	118	0	1.50	419.0	188.0	1016.0
114	G	91	78	118	0	1.48	368.8	172.0	760.0
115	G	91	78	118	0	1.25	425.4	708.0	764.0
116	G	91	78	118	0	1.45	457.0	180.0	780.0
117	G	91	78	118	0	1.36	497.3	688.0	740.0
118	G	91	78	118	0	1.21	406.2	100.0	748.0
119	G	91	78	118	0	0.72	513.2	180.0	844.0
120	G	91	78	118	0	1.16	436.4	176.0	756.0
121	G	91	78	118	0	1.04	381.1	208.0	772.0
122	G	91	78	118	0	1.17	427.7	244.0	744.0
123	H	114	110	96	1	1.20	577.1	260.0	1372.0
124	H	114	110	96	1	1.10	569.9	260.0	1400.0
125	H	114	110	96	1	1.00	657.1	260.0	1472.0
126	H	114	110	96	1	.78	622.2	260.0	1228.0
127	H	114	110	96	1	.94	640.3	204.0	1348.0
128	H	114	110	96	1	0.91	541.0	196.0	1472.0
129	H	114	110	96	1	0.87	656.3	260.0	1268.0
130	H	114	110	96	1	0.86	618.9	172.0	1360.0
131	H	114	110	96	1	.86	686.1	260.0	1364.0
132	H	114	110	96	1	.79	689.2	260.0	1380.0
133	H	114	110	96	1	1.3	610.7	204.0	1340.0
134	H	114	110	96	1	1.2	604.8	260.0	1468.0
135	H	114	110	96	1	.90	685.1	260.0	1460.0
136	H	114	110	96	1	.70	673.0	260.0	1424.0
137	H	114	110	96	1	.94	623.9	172.0	1432.0
138	H	114	110	96	1	.93	555.0	172.0	1404.0
139	H	114	110	96	1	.87	620.0	172.0	1348.0
140	H	114	110	96	1	.77	513.1	172.0	260.0
141	I	112	118	105	1	1.06	533.6	584.0	768.0
142	I	112	118	105	1	1.26	478.0	616.0	768.0
143	I	112	118	105	1	1.34	518.1	588.0	740.0
144	I	112	118	105	1	1.31	521.9	608.0	716.0
145	I	112	118	105	1	1.48	486.6	632.0	788.0
146	I	112	118	105	1	1.57	509.1	448.0	780.0
147	I	112	118	105	1	1.59	467.5	452.0	752.0

148.	I	112	118	105	1	1.67	474.6	680.0	740.0	
149.	I	112	118	105	1	1.30	465.9	600.0	780.0	
150.	I	112	118	105	1	1.70	489.1	456.0	780.0	
151.	I	112	118	105	1	1.66	482.4	592.0	632.0	
152.	I	112	118	105	1	1.71	441.6	476.0	788.0	
153.	I	112	118	105	1	1.83	471.0	456.0	780.0	
154.	I	112	118	105	1	1.90	496.9	536.0	760.0	
155.	I	112	118	105	1	.64	565.9	808.0	1328.0	
156.	I	112	118	105	1	1.02	619.3	172.0	1260.0	
157.	I	112	118	105	1	1.24	664.8	256.0	1400.0	
158.	I	112	118	105	1	1.44	653.7	780.0	1136.0	
159.	I	112	118	105	1	1.34	689.7	228.0	1444.0	
160.	I	112	118	105	1	1.32	705.2	288.0	1448.0	
161.	I	112	118	105	1	1.18	695.3	260.0	1392.0	
162.	I	112	118	105	1	1.15	828.8	1364.0	1476.0	
163.	I	112	118	105	1	.99	757.1	260.0	1484.0	
164.	I	112	118	105	1	1.70	458.2	456.0	776.0	
165.	I	112	118	105	1	2.2	368.3	152.0	776.0	
166.	I	112	118	105	1	2.3	477.1	492.0	772.0	
167.	I	112	118	105	1	2.4	442.9	508.0	780.0	
168.	I	112	118	105	1	2.42	439.4	472.0	1460.0	
169.	I	112	118	105	1	2.17	517.1	300.0	1464	
195.	K	102	105	104	1	.95	393.3	496.0	600.0	
196.	K	102	105	104	1	1.27	364.0	484.0	608.0	
197.	K	102	105	104	1	1.21	356.3	452.0	604.0	
198.	K	102	105	104	1	1.16	399.4	472.0	608.0	
199.	K	102	105	104	1	1.01	310.3	152.0	592.0	
200.	K	102	105	104	1	.73	269.2	128.0	592.0	
201.	K	102	105	104	1	.69	352.4	508.0	596.0	
202.	K	102	105	104	1	1.12	381.5	188.0	612.0	
203.	K	102	105	104	1	1.17	398.6	500.0	612.0	
204.	K	102	105	104	1	1.10	220.2	108.0	580.0	
205.	K	102	105	104	1	0.84	339.5	192.0	612.0	
206.	K	102	105	104	1	.89	295.5	108.0	600.0	
207.	K	102	105	104	1	1.35	431.3	464.0	580.0	
208.	K	102	105	104	1	1.30	432.1	448.0	596.0	
209.	K	102	105	104	1	1.25	373.7	532.0	604.0	
210.	K	102	105	104	1	1.06	364.6	484.0	600.0	
211.	K	102	105	104	1	.90	220.2	88.0	584.0	
212.	K	102	105	104	1	.85	400.9	484.0	596.0	
213.	K	102	105	104	1	1.37	445.6	476.0	600.0	
214.	K	102	105	104	1	1.34	405.3	460.0	600.0	
215.	K	102	105	104	1	1.22	403.4	488.0	588.0	
216.	K	102	105	104	1	0.95	319.0	468.0	592.0	
217.	L	110	102	92	1	.70	395.5	472.0	536.0	
218.	L	110	102	92	1	0.87	397.9	480.0	644.0	
219.	L	110	102	92	1	0.87	379.7	488.0	552.0	
220.	L	110	102	92	1	0.87	424.1	488.0	608.0	
221.	L	110	102	92	1	0.74	395.4	460.0	604.0	
222.	L	110	102	92	1	1.38	302.5	464.0	628.0	
223.	L	110	102	92	1	1.18	373.9	472.0	572.0	
224.	L	110	102	92	1	1.10	395.7	520.0	540.0	
225.	L	110	102	92	1	0.99	402.4	512.0	600.0	
226.	L	110	102	92	1	.92	395.6	492.0	580.0	
227.	L	110	102	92	1	.93	304.0	500.0	580.0	
228.	L	110	102	92	1	.98	428.7	500.0	568.0	
229.	L	110	102	92	1	1.12	421.5	504.0	636.0	
230.	L	110	102	92	1	.93	429.6	496.0	620.0	
231.	L	110	102	92	1	.77	435.8	476.0	544.0	
232.	L	110	102	92	1	1.03	332.1	504.0	596.0	
233.	L	110	102	92	1	1.12	371.5	508.0	540.0	
234.	L	110	102	92	1	1.05	361.9	488.0	580.0	
235.	L	110	102	92	1	1.04	394.3	472.0	596.0	
236.	L	110	102	92	1	1.11	353.8	464.0	616.0	
237.	M	53	38	68	0	1.17	243.8	84.0	596.0	
238.	M	53	38	68	0	1.91	279.4	532.0	580.0	
239.	M	53	38	68	0	2.0	205.2	84.0	560.0	
240.	M	53	38	68	0	2.3	241.1	108.0	576.0	

241	M	53	38	68	0	1 91	240 0	72 0	592 0
242	M	53	38	68	0	1 57	292 5	100 0	596 0
243	M	53	38	68	0	0 89	198 3	84 0	448 0
244	M	53	38	68	0	1 16	184 3	104 0	140 0
245	M	53	38	68	0	1 25	299 3	536 0	600 0
246	M	53	38	68	0	1 17	251 9	84 0	604 0
247	M	53	38	68	0	1 08	209 8	96 0	544 0
248	M	53	38	68	0	1 28	154 8	76 0	148 0
249	M	53	38	68	0	0 83	235 3	144 0	596 0
250	M	53	38	68	0	1 42	366 8	588 0	608 0
251	M	53	38	68	0	1 46	396 3	452 0	592 0
252	M	53	38	68	0	1 49	354 6	588 0	596 0
253	M	53	38	68	0	1 56	377 1	540 0	604 0
254	M	53	38	68	0	1 48	356 9	588 0	604 0
255	M	53	38	68	0	0 86	322 6	120 0	624 0
256	M	53	38	68	0	1 19	322 5	80 0	604 0
257	M	53	38	68	0	1 21	287 [illegible]	104 0	588 0
258	M	53	38	68	0	1 12	290 5	96 0	600 0
259	M	53	38	68	0	1 03	165 [illegible]	120 0	596 0
260	M	53	38	68	0	1 14	241 [illegible]	84 0	588 0
261	N	91	97	107	1	45	319 7	188 0	588 0
262	N	91	97	107	1	61	353 5	596 0	620 0
263	N	91	97	107	1	95	401 1	576 0	616 0
264	N	91	97	107	1	93	388 2	592 0	620 0
265	N	91	97	107	1	83	384 8	592 0	612 0
266	N	91	97	107	1	67	411 0	600 0	608 0
267	N	91	97	107	1	53	296 4	100 0	624 0
268	N	91	97	107	1	55	435 6	444 0	688 0
269	N	91	97	107	1	70	383 5	600 0	644 0
270	N	91	97	107	1	78	366 5	452 0	636 0
271	N	91	97	107	1	77	424 2	604 0	628 0
272	N	91	97	107	1	71	367 6	452 0	664 0
273	N	91	97	107	1	61	391 3	616 0	636 0
274	N	91	97	107	1	84	403 3	452 0	628 0
275	N	91	97	107	1	1 07	404 1	444 0	616 0
276	N	91	97	107	1	1 15	396 1	448 0	648 0
277	N	91	97	107	1	1 09	416 8	452 0	624 0
278	N	91	97	107	1	1 07	401 3	424 0	620 0
279	N	91	97	107	1	1 01	341 8	428 0	652 0
280	N	91	97	107	1	60	348 2	116 0	648 0
281	N	91	97	107	1	86	406 1	260 0	664 0
282	N	91	97	107	1	89	405 9	464 0	628 0
283	N	91	97	107	1	92	404 4	424 0	660 0
284	N	91	97	107	1	84	404 6	204 0	684 0
285	N	91	97	107	1	74	413 4	484 0	636 0

```
INPUT ID S PVC FEV1 FEV1R STATE FLOW MPF FPK FMAX
CARDS
    P   73  32  40  0    1 28    295 5     84 0    280 0
    P   73  32  40  0    2 19    416 2     92 0    260 0
    P   73  32  40  0    2 29    539 4    172 0   1416 0
    P   73  32  40  0    2 47    822 6   1316 0   1448 0
    P   73  32  40  0    2 59    475 0    180 0   1348 0
    P   73  32  40  0    2 76    350 2    172 0   1404 0
    P   73  32  40  0    2 76    361 6    176 0    528 0
    P   73  32  40  0    1 65    505 5    172 0   1296 0
    P   73  32  40  0    2 40    407 9    152 0   1276 0
    P   73  32  40  0    2 55    427 7    172 0   1344 0
    P   73  32  40  0    2 64    442 8    168 0   1356 0
    P   73  32  40  0    2 64    301 0     96 0    260 0
    P   73  32  40  0    2 21    275 8    172 0    260 0
    P   73  32  40  0    1 17    748 0    116 0   1416 0
    P   73  32  40  0    2 15    775 1     80 0   1484 0
    P   73  32  40  0    2 54    334 0    172 0    408 0
    P   73  32  40  0    2 89    291 2    172 0    268 0
    P   73  32  40  0    2 98    314 9    172 0    240 0
    P   73  32  40  0    2 44    301 0    116 0    504 0
    P   73  32  40  0    1 64    380 2    104 0   1340 0
    P   73  32  40  0    2 03    585 7    172 0   1332 0
    P   73  32  40  0    2 33    547 1    172 0   1252 0
    P   73  32  40  0    2 52    434 5    164 0   1316 0
    P   73  32  40  0    2 61    633 2    164 0   1464 0
    P   73  32  40  0    2 48    452 0    156 0    624 0
    C  102  83  81  0      56    103 5     64 0    144 0
    C  102  83  81  0    1 13    328 0    112 0    600 0
    C  102  83  81  0    1 39    235 0     80 0    616 0
    C  102  83  81  0    1 37    175 1     60 0    604 0
    C  102  83  81  0    1 22    235 3    100 0    612 0
    C  102  83  81  0    1 07    137 8     68 0    612 0
    C  102  83  81  0      99    276 4    112 0    604 0
    C  102  83  81  0      86    125 7    104 0    600 0
    C  102  83  81  0      71     94 5     68 0    600 0
    C  102  83  81  0      73    141 9    100 0    600 0
    C  102  83  81  0    1 18    343 2    600 0    624 0
    C  102  83  81  0    1 47    247 0     88 0    632 0
    C  102  83  81  0    1 43    173 2     64 0    604 0
    C  102  83  81  0    1 29    315 8    104 0    680 0
    C  102  83  81  0    1 09    140 5     60 0    140 0
    C  102  83  81  0    1 11    269 7     88 0    608 0
    C  102  83  81  0    1 07    118 3     96 0    116 0
    C  102  83  81  0      68     99 5     84 0    600 0
    C  102  83  81  0      88    156 0    120 0    600 0
    C  102  83  81  0    1 35    324 3    100 0    632 0
    C  102  83  81  0    1 57    224 3    100 0    624 0
    C  102  83  81  0    1 60    220 6     64 0    628 0
    C  102  83  81  0    1 62    453 0    604 0    620 0
    C  102  83  81  0    1 43    161 9     92 0    608 0
    C  102  83  81  0    1 11    158 1     60 0    608 0
    C  102  83  81  0      95    126 8    100 0    108 0
    C  102  83  81  0      70    101 5     64 0    600 0
    C  102  83  81  0        68      144 1      88 0    156 0
    C  102  83  81  0    1 31    229 0     56 0    620 0
    C  102  83  81  0    1 55    338 3    600 0    640 0
    C  102  83  81  0    1 70    197 3    100 0    620 0
    C  102  83  81  0    1 61    209 2     64 0    620 0
    C  102  83  81  0    1 58    376 7    608 0    608 0
    C  102  83  81  0    1 48    194 3     80 0    612 0
    C  102  83  81  0    1 14    199 7    116 0    624 0
    C  102  83  81  0    1 03    110 2     96 0    108 0
    C  102  83  81  0      91    124 9     60 0    608 0
    S   92  99 103  0    1 60    278 5    228 0    676 0
    S   92  99 103  0    1 52    208 4    172 0    304 0
    S   92  99 103  0    1 38    183 6    112 0    260 0
    S   92  99 103  0    1 19    220 7    120 0    284 0
    S   92  99 103  0    1 97    785 3    928 0    932 0
    S   92  99 103  0    2 22    311 2    104 0    144 0
```

440	S	92	95	103	0	2.08	505.4	172.0	1376.0
441	S	92	95	103	0	1.87	318.9	92.0	636.0
442	S	92	95	103	0	1.29	187.7	76.0	156.0
443	S	92	95	103	0	1.82	689.9	120.0	1436.0
444	S	92	95	103	0	2.18	589.0	120.0	1412.0
445	S	92	95	103	0	2.04	562.5	120.0	1332.0
446	S	92	95	103	0	1.63	572.4	120.0	1224.0
447	S	92	95	103	0	.62	575.7	120.0	260.0
448	S	92	95	103	0	1.15	334.4	120.0	608.0
449	S	92	95	103	0	1.80	361.6	204.0	668.0
450	S	92	95	103	0	1.80	379.0	160.0	776.0
451	S	92	95	103	0	1.60	417.4	120.0	420.0
452	S	92	95	103	0	1.38	386.5	120.0	260.0
453	T	83	76	91	0	.63	419.7	260.0	1224.0
454	T	83	76	91	0	.97	285.1	104.0	592.0
455	T	83	76	91	0	1.02	98.7	92.0	136.0
456	T	83	76	91	0	1.12	303.6	88.0	596.0
457	T	83	76	91	0	1.06	105.1	92.0	132.0
458	T	83	76	91	0	1.17	271.4	100.0	592.0
459	T	83	76	91	0	1.08	299.5	588.0	596.0
460	T	83	76	91	0	.96	100.4	92.0	124.0
461	T	83	76	91	0	.73	134.1	76.0	592.0
462	T	83	76	91	0	.98	403.1	592.0	604.0
463	T	83	76	91	0	1.09	147.2	104.0	592.0
464	T	83	76	91	0	1.18	347.1	592.0	600.0
465	T	83	76	91	0	1.20	179.5	96.0	588.0
466	T	83	76	91	0	1.15	122.6	100.0	144.0
467	T	83	76	91	0	1.08	357.4	588.0	592.0
468	T	83	76	91	0	.57	256.7	128.0	600.0
469	T	83	76	91	0	.82	164.7	128.0	208.0
470	T	83	76	91	0	.83	160.3	120.0	588.0
471	T	83	76	91	0	.94	415.8	584.0	600.0
472	T	83	76	91	0	.99	245.8	108.0	600.0
473	T	83	76	91	0	1.08	149.9	104.0	588.0
474	T	83	76	91	0	1.23	344.0	128.0	592.0
475	T	83	76	91	0	.88	308.5	116.0	600.0
476	T	83	76	91	0	.86	209.8	116.0	592.0
477	T	83	76	91	0	.96	347.3	96.0	600.0
478	T	83	76	91	0	1.05	193.3	112.0	584.0
479	T	83	76	91	0	1.09	413.4	240.0	1224.0
480	T	83	76	91	0	1.09	317.6	100.0	1224.0
481	T	83	76	91	0	1.052	170.0	108.0	584.0
482	T	83	76	91	0	1.09	399.2	252.0	608.0
483	T	83	76	91	0	.69	364.1	116.0	1224.0
484	U	73	66	90	0	.85	208.9	84.0	644.0
485	U	73	66	90	0	.90	350.3	88.0	1352.0
486	U	73	66	90	0	.80	160.6	100.0	172.0
487	U	73	66	90	0	.75	226.8	84.0	588.0
488	U	73	66	90	0	.36	225.2	100.0	260.0
489	U	73	66	90	0	.60	102.5	88.0	116.0
490	U	73	66	90	0	1.10	98.6	96.0	104.0
491	U	73	66	90	0	1.17	177.7	108.0	220.0
492	U	73	66	90	0	1.00	99.6	100.0	108.0
493	U	73	66	90	0	.88	146.4	52.0	260.0
494	U	73	66	90	0	.82	207.5	96.0	260.0
495	U	73	66	90	0	.96	100.7	96.0	140.0
496	U	73	66	90	0	.98	140.6	96.0	208.0
497	U	73	66	90	0	.98	190.0	88.0	260.0
498	U	73	66	90	0	.73	97.1	92.0	132.0
499	U	73	66	90	0	.31	123.2	96.0	204.0
500	U	73	66	90	0	.89	164.1	80.0	264.0
501	U	73	66	90	0	1.06	97.5	52.0	144.0
502	U	73	66	90	0	.98	115.3	88.0	124.0
503	U	73	66	90	0	.91	165.5	96.0	260.0
504	U	73	66	90	0	.81	93.8	96.0	116.0
505	U	73	66	90	0	.43	110.5	92.0	172.0
506	V	101	106	104	1	.90	206.6	76.0	604.0
507	V	101	106	104	1	1.32	240.5	100.0	612.0
508	V	101	106	104	1	1.56	303.0	100.0	620.0

509	V	101	106	104	1	1 70	266 3	124 0	628 0
510	V	101	106	104	1	1 63	300 1	100 0	624 0
511	V	101	106	104	1	1 46	392 6	600 0	652 0
512	V	101	106	104	1	1 20	214 3	96 0	620 0
513	V	101	106	104	1	72	175 0	120 0	260 0
514	V	101	106	104	1	1 38	440 7	624 0	652 0
515	V	101	106	104	1	1 80	443 6	616 0	652 0
516	V	101	106	104	1	1 89	450 4	624 0	652 0
517	V	101	106	104	1	1 82	351 2	116 0	684 0
518	V	101	106	104	1	1 61	481 2	632 0	656 0
519	V	101	106	104	1	1 10	247 2	104 0	172 0
520	V	101	106	104	1	80	162 8	132 0	156 0
521	V	101	106	104	1	1 46	197 4	140 0	284 0
522	V	101	106	104	1	2 06	315 0	104 0	692 0
523	V	101	106	104	1	2 35	315 2	156 0	656 0
524	V	101	106	104	1	2 18	262 3	104 0	176 0
525	V	101	106	104	1	1 70	228 5	92 0	668 0
526	V	101	106	104	1	70	157 1	104 0	208 0
527	V	101	106	104	1	97	272 4	88 0	632 0
528	V	101	106	104	1	1 77	494 9	628 0	640 0
529	V	101	106	104	1	2 17	433 5	644 0	644 0
530	V	101	106	104	1	2 08	366 9	628 0	676 0
531	V	101	106	104	1	1 60	295 6	112 0	684 0
532	V	101	106	104	1	62	170 2	120 0	184 0
533	W	107	114	106	1	78	395 2	260 0	548 0
534	W	107	114	106	1	1 23	358 0	112 0	552 0
535	W	107	114	106	1	1 10	453 4	128 0	348 0
536	W	107	114	106	1	1 01	242 9	136 0	412 0
537	W	107	114	106	1	80	295 6	104 0	404 0
538	W	107	114	106	1	56	154 5	76 0	260 0
539	W	107	114	106	1	52	415 0	124 0	304 0
540	W	107	114	106	1	88	392 3	128 0	536 0
541	W	107	114	106	1	97	331 7	104 0	588 0
542	W	107	114	106	1	91	270 0	152 0	600 0
543	W	107	114	106	1	65	257 5	140 0	284 0
544	W	107	114	106	1	73	338 1	96 0	660 0
545	W	107	114	106	1	94	288 4	100 0	592 0
546	W	107	114	106	1	1 04	289 7	124 0	400 0
547	W	107	114	106	1	92	196 7	124 0	328 0
548	W	107	114	106	1	66	199 5	156 0	204 0
549	W	107	114	106	1	79	134 9	124 0	172 0
550	W	107	114	106	1	1 10	211 8	124 0	380 0
551	W	107	114	106	1	1 18	229 6	112 0	328 0
552	W	107	114	106	1	1 11	243 0	132 0	616 0
553	W	107	114	106	1	94	183 0	84 0	384 0
554	X	93	78	85	0	73	146 7	116 0	164 0
555	X	93	78	85	0	98	219 1	104 0	200 0
556	X	93	78	85	0	93	197 8	104 0	156 0
557	X	93	78	85	0	97	181 3	92 0	208 0
558	X	93	78	85	0	59	124 5	96 0	164 0
559	X	93	78	85	0	84	148 7	104 0	172 0
560	X	93	78	85	0	1 01	221 9	136 0	288 0
561	X	93	78	85	0	96	203 6	100 0	152 0
562	X	93	78	85	0	85	148 4	64 0	172 0
563	X	93	78	85	0	77	246 6	108 0	260 0
564	X	93	78	85	0	53	365 8	132 0	568 0
565	X	93	78	85	0	67	139 5	88 0	260 0
566	X	93	78	85	0	1 01	238 0	108 0	492 0
567	X	93	78	85	0	1 03	184 5	84 0	260 0
568	X	93	78	85	0	95	287 5	116 0	356 0
569	X	93	78	85	0	84	283 6	104 0	468 0
570	X	93	78	85	0	72	175 7	108 0	172 0
571	X	93	78	85	0	33	120 1	80 0	136 0
572	X	93	78	85	0	87	229 1	108 0	260 0
573	X	93	78	85	0	1 48	237 9	164 0	492 0
574	X	93	78	85	0	1 41	140 2	120 0	200 0
575	X	93	78	85	0	1 42	140 1	104 0	172 0
576	X	93	78	85	0	1 32	141 7	116 0	136 0
577	X	93	78	85	0	96	131 6	108 0	192 0
578	X	93	78	85	0	82	109 9	84 0	168 0
579	Y	101	113	113	1	69	447 4	116 0	1224 0
580	Y	101	113	113	1	1 05	322 0	112 0	172 0
581	Y	101	113	113	1	1 18	367 9	108 0	268 0

582	Y	101	113	113	1	1.21	481.2	112.0	260.0
583	Y	101	113	113	1	1.23	395.1	116.0	336.0
584	Y	101	113	113	1	.97	324.6	112.0	184.0
585	Y	101	113	113	1	1.06	175.1	112.0	248.0
586	Y	101	113	113	1	1.30	131.0	88.0	168.0
587	Y	101	113	113	1	1.45	183.0	124.0	276.0
588	Y	101	113	113	1	1.57	170.5	84.0	260.0
589	Y	101	113	113	1	1.39	150.6	96.0	188.0
590	Y	101	113	113	1	.87	144.9	92.0	136.0
591	Y	101	113	113	1	1.17	146.6	104.0	192.0
592	Y	101	113	113	1	1.49	188.2	112.0	260.0
593	Y	101	113	113	1	1.53	141.5	92.0	124.0
594	Y	101	113	113	1	1.48	161.2	84.0	428.0
595	Y	101	113	113	1	1.29	136.2	100.0	156.0
596	Y	101	113	113	1	1.09	179.3	96.0	180.0
597	Y	101	113	113	1	1.32	125.0	84.0	132.0
598	Y	101	113	113	1	1.47	185.9	112.0	152.0
599	Y	101	113	113	1	1.31	114.1	80.0	156.0
600	Y	101	113	113	1	1.29	139.2	116.0	152.0
601	Y	101	113	113	1	1.17	124.0	96.0	152.0
625	*	72	58	124	0	1.54	141.5	108.0	152.0
626	*	72	58	124	0	1.80	170.4	104.0	148.0
627	*	72	58	124	0	1.71	168.8	80.0	204.0
628	*	72	58	124	0	1.35	196.3	68.0	132.0
629	*	72	58	124	0	1.04	128.7	96.0	160.0
630	*	72	58	124	0	1.43	159.5	116.0	72.0
631	*	72	58	124	0	1.92	166.7	104.0	28.0
632	*	72	58	124	0	1.73	124.2	104.0	48.0
633	*	72	58	124	0	1.42	134.7	108.0	180.0
634	*	72	58	124	0	1.19	143.7	84.0	172.0
635	*	72	58	124	0	1.11	123.7	92.0	136.0
636	*	72	58	124	0	1.69	114.6	104.0	160.0
637	*	72	58	124	0	1.61	119.9	120.0	168.0
638	*	72	58	124	0	1.51	131.7	96.0	148.0
639	*	72	58	124	0	.78	178.5	100.0	148.0
640	*	72	58	124	0	1.48	116.4	116.0	160.0
641	*	72	58	124	0	1.62	106.4	84.0	152.0
642	*	72	58	124	0	1.95	134.7	100.0	148.0
643	*	72	58	124	0	1.72	131.2	88.0	156.0
644	*	72	58	124	0	1.35	98.8	88.0	108.0
645	*	99	105	105	1	.71	324.4	108.0	260.0
646	*	99	105	105	1	.74	347.2	128.0	300.0
647	*	99	105	105	1	.88	368.5	108.0	204.0
648	*	99	105	105	1	.95	426.3	120.0	1228.0
649	*	99	105	105	1	.93	341.4	96.0	256.0
650	*	99	105	105	1	.96	325.8	128.0	260.0
651	*	99	105	105	1	.98	353.1	108.0	216.0
652	*	99	105	105	1	.98	344.7	100.0	216.0
653	*	99	105	105	1	.97	383.1	112.0	1224.0
654	*	99	105	105	1	.88	329.6	92.0	468.0
655	*	99	105	105	1	1.08	416.4	172.0	1296.0
656	*	99	105	105	1	1.18	352.1	108.0	1260.0
657	*	99	105	105	1	1.19	343.0	148.0	332.0
658	*	99	105	105	1	1.17	382.2	116.0	396.0
659	*	99	105	105	1	1.21	407.5	124.0	1224.0
660	*	99	105	105	1	1.21	343.5	136.0	1224.0
661	*	99	105	105	1	1.16	335.2	148.0	428.0
662	*	99	105	105	1	1.14	385.1	108.0	204.0
663	*	99	105	105	1	1.03	368.8	100.0	540.0
664	*	99	105	105	1	.95	367.8	108.0	260.0
665	*	99	105	105	1	.66	351.5	108.0	380.0
666	*	99	105	105	1	.93	429.3	120.0	1224.0
667	*	99	105	105	1	1.01	387.3	168.0	492.0
668	*	99	105	105	1	1.03	346.8	108.0	472.0
669	*	99	105	105	1	.99	330.6	108.0	260.0
670	*	99	105	105	1	1.01	410.1	112.0	1224.0
671	*	99	105	105	1	.99	417.0	116.0	1224.0
672	*	99	105	105	1	1.03	418.6	140.0	1272.0

673	•	99	105	105	1	1	08	325	9	108 0	2[illegible] 0
674	•	99	105	105	1		97	292	6	116 0	172 0
675	•	99	105	105	1	1	12	403	0	96 0	500 0
676	•	99	105	105	1	1	12	364	8	148 0	276 0
677	•	99	105	105	1	1	06	382	8	108 0	1224 0
678	•	99	105	105	1	1	10	392	6	108 0	260 0
679	•	99	105	105	1	1	22	349	1	112 0	172 0
680	•	99	105	105	1	1	21	336	1	112 1	288 0
681	•	99	105	105	1	1	21	380	5	116 0	1224 0
682	•	99	105	105	1	1	12	355	2	108 0	260 0
683	•	99	105	105	1		98	278	5	112 0	172 0
684	•	70	58	124	0		75	314	2	152 0	364 0
685	•	70	58	124	0	1	19	288	9	144 0	632 0
686	•	70	58	124	0	1	23	308	3	112 0	292 0
687	•	70	58	124	0		87	303	4	88 0	448 0
688	•	70	58	124	0	0	32	331	4	112 0	1264 0
689	•	70	58	124	0	1	53	144	4	100 0	176 0
30	•	70	58	124	0	1	73	140	8	80 0	152 0
691	•	70	58	124	0	1	58	140	7	96 0	156 0
692	•	70	58	124	0	1	19	151	3	96 0	164 0
693	•	70	58	124	0	1	04	350	9	108 0	628 0
694	•	70	58	124	0	1	43	324	6	144 0	600 0
695	•	70	58	124	0	1	58	287	6	112 0	568 0
696	•	70	58	124	0	1	61	448	5	100 0	700 0
697	•	70	58	124	0	1	34	305	6	140 0	544 0
698	•	70	58	124	0		81	355	5	128 0	1340 0
699	•	70	58	124	0		65	408	1	100 0	1332 0
700	•	70	58	124	0	1	32	301	9	136 0	260 0
701	•	70	58	124	0	1	81	400	9	152 0	676 0
702	•	70	58	124	0	1	86	318	8	112 0	628 0
703	•	70	58	124	0	1	65	346	4	104 0	1224 0
704	•	70	58	124	0	1	17	326	9	112 0	1224 0

END

2-87

DTIC